

**A COMPARATIVE STUDY AND APPLICATION OF  
CONTINUOUSLY VARIABLE TRANSMISSION TO A SINGLE  
MAIN ROTOR HEAVY LIFT HELICOPTER**

A Thesis Dissertation  
Presented to  
The Academic Faculty

by

Sameer Hameer

In Partial Fulfillment  
of the Requirements for the Degree  
Doctor of Philosophy in the  
School of Aerospace Engineering

Georgia Institute of Technology  
December 2009

**A COMPARATIVE STUDY AND APPLICATION OF  
CONTINUOUSLY VARIABLE TRANSMISSION TO A SINGLE  
MAIN ROTOR HEAVY LIFT HELICOPTER**

Approved by:

Dr. Daniel Schrage, Advisor  
School of Aerospace Engineering  
*Georgia Institute of Technology*

Dr. Olivier Bauchau  
School of Aerospace Engineering  
*Georgia Institute of Technology*

Dr. Mark Costello  
School of Aerospace Engineering  
*Georgia Institute of Technology*

Dr. Robert Loewy  
School of Aerospace Engineering  
*Georgia Institute of Technology*

Mr. Charles Crawford  
Georgia Tech Research Institute  
*Georgia Institute of Technology*

Date Approved: 10/09/2009

This thesis is dedicated to my family, my advisor, and the faculty of the school of Aerospace Engineering for their outstanding support of my pursuit of the ph.D. program in Aerospace Engineering.

## **ACKNOWLEDGEMENTS**

I would like to thank Dr. Schrage, Mr. Saribay, Tina Rezvani, Dr. Loewy, Dr. Costello, Dr. Bauchau, and Mr. Crawford for their invaluable assistance and guidance which motivated the write up of this thesis dissertation.

# TABLE OF CONTENTS

	Page
ACKNOWLEDGEMENTS	iv
LIST OF TABLES	vii
LIST OF FIGURES	viii
SUMMARY	xi
<u>CHAPTER</u>	
1 INTRODUCTION	1
1.1 Motivation	3
1.2 Research Objectives	6
1.3 Benchmarking	6
2 HYPOTHESIS AND RESEARCH QUESTIONS	9
2.1 Proposed Solutions	10
3 RESEARCH PLAN	12
4 DRIVETRAIN DESIGN CONSTRAINT	15
5 CONTINUOUSLY VARIABLE TRANSMISSION CONCEPTS	21

6	METHODOLOGY AND RESULTS	27
6.1	Weight Analysis	29
6.2	Acoustic Analysis	43
6.3	Safety Analysis	48
6.4	Static Finite Element Analysis	76
6.5	Housing and Lubrication Analysis	103
7	CONCLUDING REMARKS	107
8	RECCOMENDATIONS	114
	APPENDIX A: PLANETARY GEAR ANALYSIS	115
	APPENDIX B: P-CVT ANALYSIS	123
	APPENDIX C: APDL CODES	134
	APPENDIX D: MATHEMATICAL ANALYSIS OF THE P-CVT	147
	REFERENCES	169

## LIST OF TABLES

	Page
Table 1: Design Parameters <sup>20</sup> .	36
Table 2: Design Constraints <sup>20</sup> .	37
Table 3: Weight Breakdown of the Split Torque Type P-CVT.	41
Table 4: Weight Comparison of the Drivetrains.	42
Table 5: Failure types.	52
Table 6: Hazard Levels.	54
Table 7: Risk Matrix.	54
Table 8: System Operational Functional Hazard Assessment.	55
Table 9: Summary of failure rates used in the analysis.	56
Table 10: FTA/RBD analysis summary of results.	57
Table 11: SPN Component Groups & Failure Rates.	59
Table 12: Availability SPN Distributions.	60
Table 13: Mission Success SPN distributions.	61
Table 14: Parts of FAR 29 that are applicable to the P-CVT.	63
Table 15: Parts of MIL-516B that are applicable to the P-CVT.	63
Table 16: 3D Convergence Stress Values.	91
Table 17: 2D Convergence Stress Values.	97

## LIST OF FIGURES

	Page
Figure 3: Gearbox Weight vs. RPM Reduction for JHL.	17
Figure 4: Shaft Weight vs. RPM Reduction for JHL.	18
Figure 5: Transmission Weight vs. RPM Reduction for JHL.	19
Figure 6: Variable Speed Power Turbine.	5
Figure 7: Pulley Type CVT.	22
Figure 8: Toroidal Type CVT.	23
Figure 9: Split Torque P-CVT <sup>5</sup> .	24
Figure 10: JHL Diagram and P-CVT Split Torque Connected in Series <sup>6, 5</sup> .	28
Figure 11: Tensile stress for the four facegears of the first stage P-CVT.	33
Figure 12: Tensile stress for the four face gears of the second stage PVT.	34
Figure 13: SPL vs. Time for 1 <sup>st</sup> stage Planetary Gear System.	43
Figure 14: SPL vs. Time for 2 <sup>nd</sup> Stage Planetary Gear System.	43
Figure 15: Split Torque Transmission <sup>17</sup> .	7
Figure 16: Drive System Weight Trends <sup>29</sup> .	8
Figure 17: Decision Matrix.	13
Figure 18: P-CVT Electromechanical Transmission <sup>5</sup> .	25
Figure 19: Drivetrain Schematic.	29
Figure 20: Drive System Technology Objectives <sup>29</sup> .	14
Figure 21: Design Flow Chart for Weight Analysis <sup>20</sup> .	35
Figure 22: Double Nutator mounted on a Shaft pinned at both ends.	40
Figure 23: Schematic of the Active gear strut technology deployment in a helicopter <sup>22, 46</sup>	

Figure 24: FXLMS Algorithm <sup>21</sup> .	47
Figure 25: Active gear Strut <sup>21</sup> .	47
Figure 26: Component-wise breakdown of the P-CVT.	51
Figure 27: Overall system fault-tree.	56
Figure 28: Typical RBDs derived from the Fault-tree, level I (above) Electrical system (below).	58
Figure 29: Availability SPN.	60
Figure 30: Mission Success SPN.	62
Figure 31: Cross Section View of the PCVT <sup>[20]</sup> .	78
Figure 32: The 3D Geometry Model.	78
Figure 33: The 2D Geometry Model.	79
Figure 34: Zero Displacements are applied to the corners of the shaft.	84
Figure 35: Couple forces are applied to each gear to act as torque.	85
Figure 36: Applying force & displacement boundary conditions to the 2D model.	85
Figure 37: Mesh Density=6.	87
Figure 38: Mesh Density=5.	88
Figure 39: Mesh Density=4.	88
Figure 40: Mesh Density=3.	89
Figure 41: Mesh Density=2.	89
Figure 42: Mesh Density= 1 & .3.	90
Figure 43: 3D Model Convergence.	90
Figure 44: Mesh Model for the selected converged stress value.	91
Figure 45: Displacement Plot.	92
Figure 46: 2D Mesh density = 6.	93

Figure 47: 2D Mesh density = 4.	94
Figure 48: 2D Mesh density = 2.	94
Figure 49: 2D Mesh density=1 & 0.3.	95
Figure 50: Mesh Model for the selected converged stress value.	95
Figure 51: Displacement Plot.	96
Figure 52: 2D Convergence plot.	97
Figure 53: Housing Design Flow Chart <sup>26</sup> .	104
Figure 54: Pure Truss Design <sup>26</sup> .	105
Figure 55: Detailed Layout of the Fabricated Housing looking Aft <sup>26</sup> .	106
Figure 56: Split Torque Type P-CVT Gearbox <sup>5</sup> .	27

## SUMMARY

Rotorcraft transmission design is limited by empirical weight trends that are proportional to the power/torque raised to the two-thirds coupled with the relative inexperience industry has with the employment of variable speed transmission to heavy lift helicopters of the order of 100,000 lbs gross weight and 30,000 installed horsepower. The advanced rotorcraft transmission program objectives are to reduce transmission weight by at least 25%, reduce sound pressure levels by at least 10 dB, have a 5000 hr mean time between removal, and also incorporate the use of split torque technology in rotorcraft drivetrains of the future. The major obstacle that challenges rotorcraft drivetrain design is the selection, design, and optimization of a variable speed transmission in the goal of achieving a 50% reduction in rotor speed and its ability to handle high torque with light weight gears, as opposed to using a two-speed transmission which has inherent structural problems and is highly unreliable due to the embodiment of the traction type transmission, complex clutch and brake system. This thesis selects a nontraction pericyclic continuously variable transmission (P-CVT) as the best approach for a single main rotor heavy lift helicopter. The objective is to target and overcome the above mentioned obstacle for drivetrain design. Overcoming this obstacle provides advancement in the state of the art of drivetrain design over existing planetary and split torque transmissions currently used in helicopters. The goal of the optimization process was to decrease weight, decrease noise, increase efficiency, and increase safety and reliability. The objective function utilized the minimization of the weight and the major constraint is the tooth bending stress of the facegears. The most important parameters of

the optimization process are weight, maintainability, and reliability which are cross-functionally related to each other, and these parameters are related to the torques and operating speeds. The analysis of the split torque type P-CVT achieved a weight reduction of 42.5% and 40.7% over planetary and split torque transmissions respectively. In addition, a 19.5 dB sound pressure level reduction was achieved using active gear struts, and also the use of fabricated steel truss like housing provided a higher maintainability and reliability, low cost, and low weight over cast magnesium housing currently employed in helicopters. The static finite element analysis of the split torque type P-CVT, both 2-D and 3-D, yielded stresses below the allowable bending stress of the material. The goal of the finite element analysis is to see if the designed product has met its functional requirements. The safety assessment of the split torque type P-CVT yielded a 99% probability of mission success based on a Monte Carlo simulation using stochastic- petri net analysis and a failure hazard analysis. This was followed by an FTA/RBD analysis which yielded an overall system failure rate of 140.35 failures per million hours, and a preliminary certification and time line of certification was performed. The use of spherical facegears and pericyclic kinematics has advanced the state of the art in drivetrain design primarily in the reduction of weight and noise coupled with high safety, reliability, and efficiency.

# CHAPTER 1

## INTRODUCTION

Propulsion coupled with drive train design forms the major areas of preliminary design along with structures and aerodynamics. The outputs of propulsion and aerodynamics are thrust to weight ratio and blade loading respectively. These outputs feed into the structures module for determining weight. Ideally the thrust to weight ratio is zero and the blade loading is infinite. Preliminary design involves freezing the configuration that was achieved from conceptual design and begins analysis in the major areas described above. The RF sizing method starts with performance requirements and mission requirements. The output of performance requirements and mission requirements are power loading and gives weight respectively which allows for the determination of installed power. Installed power takes into account process losses, transmission losses, density altitude corrections and so forth. The next step is the selection of the engine/s. The purpose of the transmission system is to deliver power from the engine to the rotor/s. The inputs to transmission design are power and revolutions per minute (RPM) and the outputs are size, efficiency, weight and noise. The major emphasis is to optimize these four outputs in terms of increasing efficiency, decreasing size, reducing weight, and noise. The selection of a drive train is based on the optimization of these outputs. There is a “square-cube law” effect which is inherent in rotorcraft transmission design which causes the weight to be proportional to the

power raised to the two-thirds. The transmission must be sized based on the maximum rotor power required for the critical segment in the mission. This input comes from the aerodynamic analysis including tip speed and rotor radius to determine rotor rpm. The propulsion analysis gives the engine RPM, specific power, and specific fuel consumption. The engine RPM divided by the rotor RPM gives the total gear reduction required. The output of transmission design, which are weight and noise, can be fed into the structures module and the noise module to determine weight and balance and noise analysis respectively.

## 1.1 Motivation

The rotorcraft industry has very little experience with the application of variable speed transmissions to heavy lift helicopters<sup>5</sup>. Most Methodology used in rotorcraft drivetrain design is over 25 years old and needs improvements to reduce vibrations, noise, weight, improving SFC, and so forth<sup>5</sup>. Therefore, a comprehensive analysis of variable speed concepts is essential in designing future drivetrains for rotorcraft.

Variable speed transmission is a promising prospect because of the ability to vary the rotor RPM, so that each section of the rotor can operate at its best lift to drag ratio.

Traditionally, varying the speed is done through the engine; however, the specific fuel consumption deteriorates when the turboshaft speed is changed. The whole basis of a variable speed transmission is to be able to slow down the rotor in cruise, thus minimizing the profile power and also being able to travel at advance ratios greater than 1, as the maximum speed of a rotorcraft is limited by compressibility effects on the advancing side and blade stall on the retreating side. The variation of rotor RPM is the eighth degree of freedom, as the rotorcraft has technically 10 degrees of freedom: velocities in the x, y, and z directions and the angular rates (roll, pitch, yaw) which make the 6 degrees of freedom while flapping is the seventh degree of freedom and then with respect to a stationary rotor, there is the progressive and regressive nodes which makeup the 9<sup>th</sup> and 10<sup>th</sup> degree of freedom. There are several variable speed transmission concepts ranging from varying the speed of the ring gear in a planetary gear system, use of traction through variable diameter pulleys, and split torque planetary differential, where the horsepower from the sun gear is shared between the ring and the pinions. There is a disadvantage of using traction to

generate power, because power is transmitted through friction i.e. the normal force is required to produce the tangential force, which decreases the power capacity and also there is a significant weight addition associated with traction. Two-Speed transmission is recommended over traction, as a planetary gear system is used where either the ring, sun or arm carrier serve as input, output or variable, thus, giving eight different combinations. The next generation of heavy lift rotorcraft is hinged on light weight transmission in order to decrease the installed power. This is a direct result from the square cube law which states that the square of the power is proportional to the transmission weight cubed. Therefore, if you double the power, the weight will be 1.58 times the original weight, and if you triple the power, the weight will be 2.08 times its original weight, and if you quadruple the power, the weight will be 2.52 times its original weight. Therefore, there is a need for light weight gearboxes. The problem with variable speed is that as the speed is decreased, there is high torque for a specified power. Therefore, the drive train should be designed, such that it is able to produce high torque with light weight gears. Light weight gears have lower rotational moment of inertia. This is the main issue that Dr. Robert Handschuh raised in the heavy lift rotorcraft systems investigation review<sup>29</sup>. The other issue is to look into variable speed turboshaft engines where the main shaft from the turbine is connected to a planetary gear system and auxiliary turbine blades are attached to the ring gear and the ring gear speed is varied by the flow entering through the variable guide valves, as shown in Figure 6.

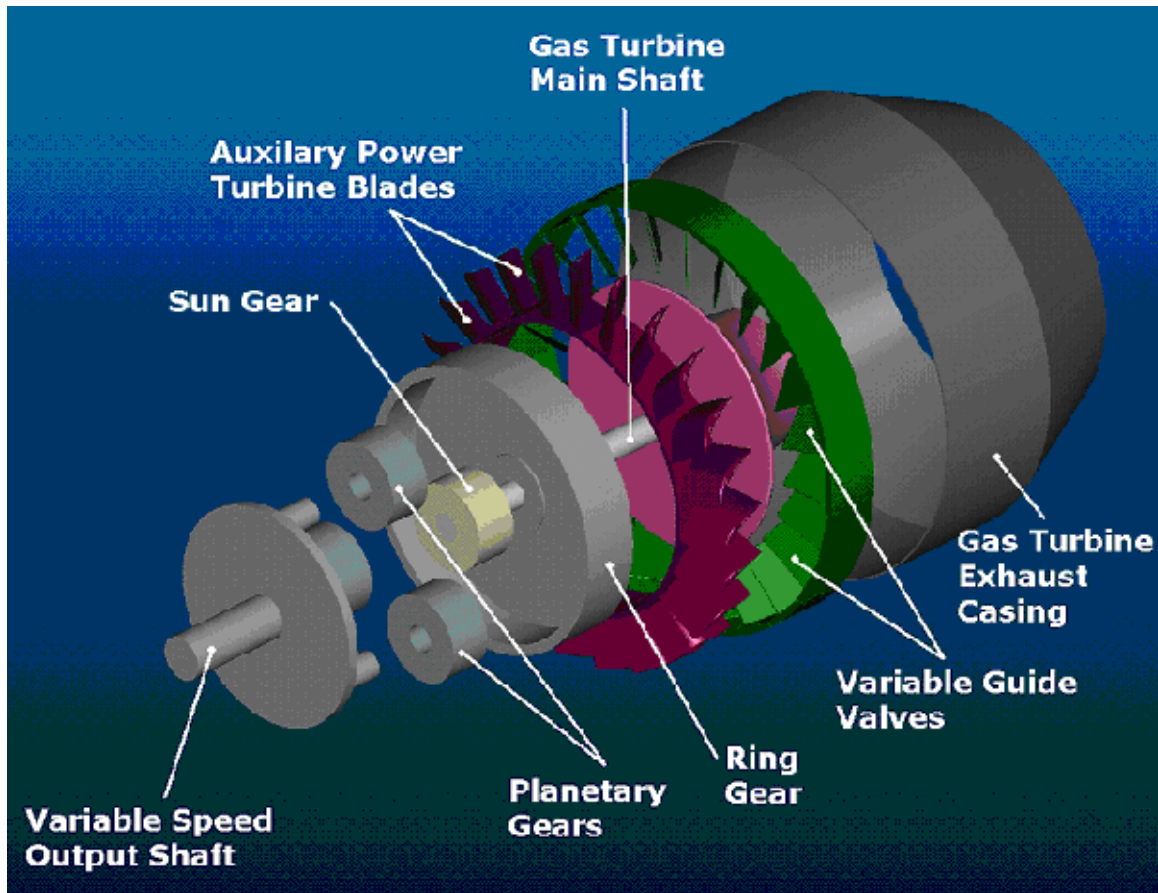


**Figure 6:** Variable Speed Power Turbine.

(<http://www.swri.org/4org/d18/mechflu/planteng/gasturb/varspeed.htm>)

However, the use of a wide range speed turboshaft engine still needs to be investigated and there is a need to establish concrete proof that there isn't any specific fuel consumption penalty associated with the variable speed power turbine. Therefore, more research and development should be targeted at developing a drive/train propulsion system that can handle high torque with light weight gears.

## 1.2 Research Objectives

Research conducted on traction and nontraction based continuously variable transmissions have resulted in the selection of the pericyclic continuously variable transmission (P-CVT) as the best approach for a single main rotor heavy lift helicopter. The main emphasis will be placed on designing and analyzing a P-CVT for heavy lift helicopter. The applicability of the P-CVT as the drivetrain of the future will be compared to existing planetary and split torque transmissions to determine its feasibility in rotorcraft drivetrain design.

## 1.3 Benchmarking

Rotorcraft drivetrain design is centered around planetary and split torque transmissions which has load sharing members that distribute the torque, so that gears can be smaller and light weight. The Mi-26 helicopter employs the split torque transmission while the CH-47D employs planetary gears. The Mi-26 drivetrain design has a final stage reduction ratio of about 8.76 which is higher than planetary gear systems as a higher last stage reduction ratio results in lower weight. The use of facegears in split torque transmissions has reduced gear vibration excitation noise and weight. And it's being currently used in the AH-64D Apache Longbow and has been shown to provide significant weight reduction. The advantages of a split torque transmission over a planetary gear system are high final stage reduction ratio, fewer gear stage count, low energy losses, increased reliability, fewer number of gears and bearings, and low noise<sup>17</sup>. An illustration of a split torque transmission is shown in figure 15.

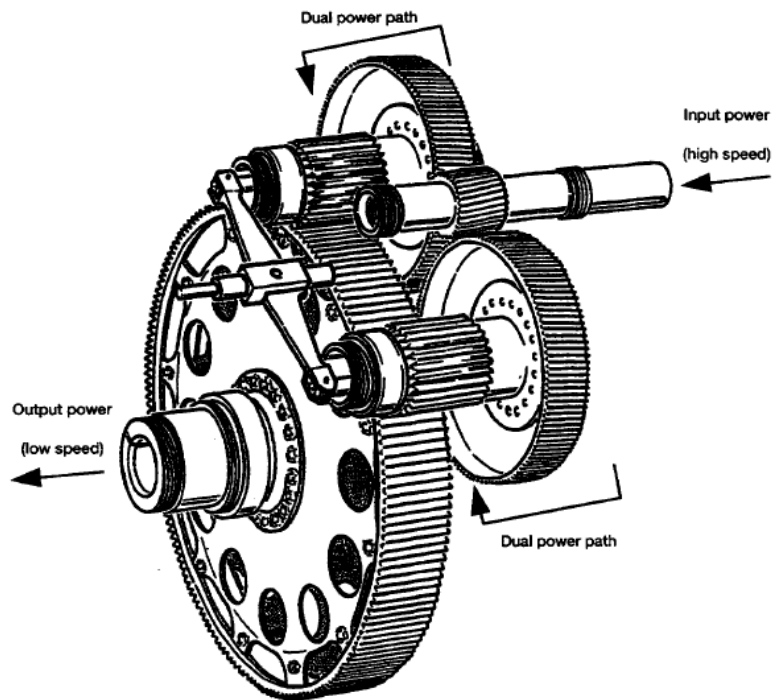
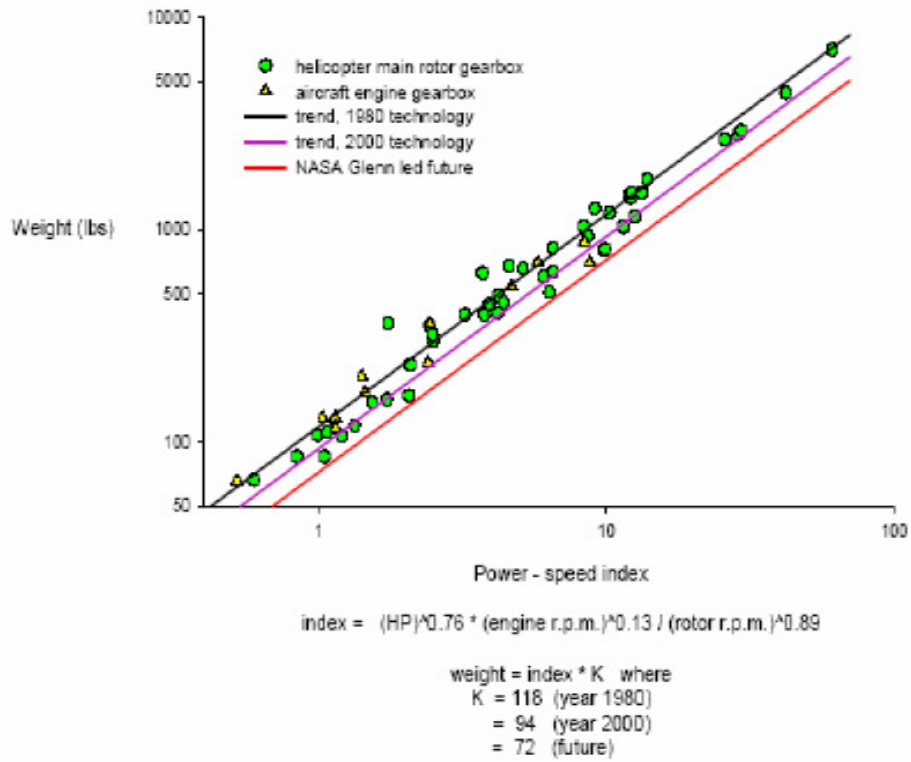


Figure 1.1.—Split torque design for helicopter application.

**Figure 15:** Split Torque Transmission<sup>17</sup>.

Historical and future gearbox weight trends are shown in figure 16.

Historic and future gearbox weight trends  
 (based on 49 single-rotor helicopter and 12 aircraft engine gearboxes)



Tim Krantz, Dec. 2002

**Figure 16: Drive System Weight Trends<sup>29</sup>.**

## CHAPTER 2

### HYPOTHESIS AND RESEARCH QUESTIONS

Is it feasible to design and optimize a split torque pericyclic continuously variable transmission for a single main rotor heavy lift helicopter with the goal of achieving a 50% rotor speed reduction by designing a variator that varies the speed continuously from zero to 50%. This is opposed to using a two speed transmission which has structural problems and is highly unreliable due to the embodiment of the traction type transmission, complex clutch and brake system. The resulting research questions are:

- Two speed transmission versus variable speed transmission?
- Traction versus nontraction CVT ?
- Power handling capabilities of CVT?
- Optimization of Variator at fixed ratios versus infinite ratios?
- Safety, Reliability, and efficiency of CVT?

Rotorcraft drivetrain methodology is based on empirical relationships derived from historical data that is over 25 years old<sup>5</sup>. The Achilles heel of the rotorcraft industry has been its relative inexperience with the application of variable speed transmissions to heavy lift helicopters<sup>5</sup>. The rotorcraft industry has made technological achievements in the use of split torque transmissions in the Mi-26 helicopter, the use of facegears in the improved Apache helicopter, and studies focused on variable rotor speed mechanisms in the US, Europe, and Japan<sup>5</sup>. A study done by NASA shows that all variable speed transmissions that utilize traction based transmissions are inapplicable for helicopters due to low reliability, high weight, and most importantly low efficiency<sup>5</sup>. My research work will focus on performing the design and optimization of a split torque pericyclic

continuously variable transmission by performing weight assessment, safety assessment, noise assessment, efficiency assessment, housing and lubrication assessment, and static finite element analysis assessment.

## 2.1 Proposed Solutions

- Two speed transmission has a disadvantage during upshifting (i.e. cruise to hover). The process of going from a low power setting to a high power setting results in drivetrain shock induced loads. A variator concept is needed to address the upshifting scenario while a clutch is recommended for the downshifting scenario, as outlined by Dr. Robert F. Handschuh<sup>29</sup>.
- Traction based CVTs, including pulley based, that rely on friction to transfer torque are discarded based on low reliability, poor bearing life, high rotating inertias, low power capacity, low power density, high parts count, large weight, high vibration, and most importantly low efficiency.
- The power handling capabilities of the P-CVT are much higher than traction based CVTs due to high power density and high contact ratios.
- The variator needs to be optimized for fixed ratios and then a variator selected that has minimum weight for a fixed ratio. Suppose a 50% rotor speed reduction is desired then a variator would vary the speed from zero to 50% as opposed to using a two speed transmission.

- The safety assessment of the CVTs lean towards the P-CVT, as it has a higher reliability of over 98% since it uses positive engagement (gearing) to transfer the torque as opposed to traction based which are highly unreliable.
- The efficiency of the P-CVT is about 98% and due to a high power density (small size and weight) and the regenerative braking system employed leads to a lower weight heat exchanger which is usually about 10% of the weight of the drivetrain.

## **CHAPTER 3**

### **RESEARCH PLAN**

The research plan will include determining the weight of an optimum P-CVT which is the sum of the gearbox weight and shaft weight, employing active noise control for the optimum P-CVT and delineate the noise tones that are caused by resonances in the gearbox housing and try to suppress these undesirable tones using liner technologies, housing elements shape modification, and other acoustic shielding mechanisms, performing a safety assessment of the optimum P-CVT, calculating the efficiency of the optimum P-CVT, analyze lubrication systems for the optimum P-CVT as the design of the P-CVT conserves oil usage, and finally select and analyze the housing of the P-CVT including the weight. The metrics that will be used are weight, noise, efficiency, and safety. The overall evaluation criteria (OEC) is defined as the product of weight and noise divided by the sum of efficiency and safety. A decision matrix was constructed and it yielded the order of importance of the above metrics and is shown in Figure 17. The OEC can be expressed mathematically as follows:

$$\text{OEC} = [\text{Weight} * \text{Noise}] / [\text{Efficiency} + \text{Safety}]$$

The goal is to decrease weight and noise and increase efficiency and safety.

Criteria Problems	Low weight 5	Low noise 4	High safety 4	High efficiency 3	
High installed power	High 3*5	Low 1*4	Low 1*4	Medium 2*3	29
Catastrophic accident	Low 1*5	Low 1*4	High 3*4	Low 1*3	24
Community noise	Low 1*5	High 3*4	Low 1*4	Low 1*3	24
High fuel consumption	Low 1*5	Low 1*4	Low 1*4	High 3*3	22

Weighted Criteria: 1, 2,3,4,5

Rows represent problems while columns represent criteria

Rating Scale: 1= low, 2 = medium, 3 = High

**Figure 17:** Decision Matrix.

The decision matrix shows that the weight is the most important parameter followed by safety, noise, and efficiency. The justification of the rating scale employed was based on Dr. Robert Handschuh's drive system technology objectives, as shown in Figure 20.

Technical Objectives	Project Areas									
	Gears	Bearings	Arrangements	Housings	Rotor Brake	Lubrication	Shafts & Couplings	Clutches	HUMS	Analytical Tools
Power Density	H	H	H	H	H	M	H	H	L	H
Internal Noise	M	L	M	L	L	L	L	L	L	M
Acquisition Cost	M	M	M	M	M	L	H	M	L	L
Operation & Support Cost	L	L	M	M	M	L	M	M	H	L
Reliability & Maintenance Cost	H	H	L	M	M	L	M	M	H	H
Damage Tolerance / Fail Safe	M	M	L	L	L	M	M	L	M	M
Diagnostics / Prognostics	L	L	L	L	L	L	L	L	H	L

H - Extremely Important; M - Somewhat Important; L - Marginally Important

August 10-11, 2005 Propulsion-16

**Figure 20:** Drive System Technology Objectives<sup>29</sup>.

The normalized OEC is expressed mathematically as follows:

$$OEC = 2 \frac{\frac{BASELINEWEIGHT}{OPTIMIZEDWEIGHT} * \frac{BASELINENOISE}{OPTIMIZEDNOISE}}{\frac{OPTIMIZEDEFFICIENCY}{BASELINEEFFICIENCY} + \frac{OPTIMIZEDSAFETY}{BASELINESAFETY}}$$

The normalization procedure takes into account that the OEC is a non dimensional parameter and also the ratios relating baseline values to optimized values must be greater than 1. The factor of 2 is multiplied to ensure that when the baseline values are equal to the optimized values, the OEC will have a value of 1. Therefore, the initial OEC has a value of 1.

## CHAPTER 4

### DRIVETRAIN DESIGN CONSTRAINT

Drive system design determines the drivetrain run, efficiency, and weight based on inputs such as drive rated power and rotational speed, RPM. The main purpose of a drivetrain is to deliver/channel power from the engines to the rotor/tail rotor/ accessories. Transmission design has a “square-cube law” constraint embedded in it. The square cube law states that the power squared is proportional to the weight cubed. Mathematically it can be expressed as follows:

$$\left(\frac{P_2}{P_1}\right)^2 = \left(\frac{W_2}{W_1}\right)^3$$

Since,  $P_2 = \Omega_2 T_2$ ,  $P_1 = \Omega_1 T_1$ , and assuming constant RPM.

$$\left(\frac{W_2}{W_1}\right) = \left(\frac{T_2}{T_1}\right)^{\frac{2}{3}}, \text{ If the RPM is not constant then } \left(\frac{W_2}{W_1}\right) = \left(\frac{T_2 \Omega_2}{T_1 \Omega_1}\right)^{\frac{2}{3}}$$

The AMCP states that the ratio,  $\left(\frac{W_2}{W_1}\right) = \left(\frac{T_2}{T_1}\right)^{0.7}$  for gears. Therefore, the gear weight

obeys the square cube law. The AMCP states that the shaft weight is proportional to the 0.38 power of torque and it can be expressed mathematically as follows:

$$\left(\frac{W_{2s}}{W_{1s}}\right) = \left(\frac{T_{2s}}{T_{1s}}\right)^{0.38}$$

This variation is consistent with current design of shafts in practice today. Shafts rotate at higher RPM, therefore, it has less torque, and thus, less weight.

Therefore, the transmission weight is the sum of the gear and shaft weights and it can be expressed mathematically given the fact that the transmission weight is proportional to the sum of the shaft torque raised to the 0.38 and the gearbox torque raised to the 0.7.

Therefore,  $\frac{WT2}{WT1} = \frac{T2S^{0.38} + T2^{0.7}}{T1S^{0.38} + T1^{0.7}}$ , as predicted by the AMCP for constant RPM. For

variable speed, the transmission weight ratio is mathematically expressed as

$$\frac{WT2}{WT1} = \frac{\Omega2S^{0.38}T2S^{0.38} + \Omega2^{0.7}T2^{0.7}}{\Omega1S^{0.38}T1S^{0.38} + \Omega1^{0.7}T1^{0.7}}$$

According to the equation published by Timothy Krantz, the main rotor gearbox weight is given below<sup>2</sup>.

$$W = K(hp)^{0.76} \frac{(engineRPM)^{0.13}}{(RotorRPM)^{0.89}}, \text{ where K is the technology factor and has the value of}$$

118 based on 1980 technology, 94 based on 2000 technology, and a value of 72 for future technology.

The manipulation of the weight equation above yields an equation that depends on overall reduction ratio and the output torque is given below<sup>2</sup>.

$$W = KQ^{0.76} RR^{0.13}, \text{ where RR is the overall reduction ratio and is given as the ratio of}$$

engine RPM to Rotor RPM. The Research and Technology laboratories (RTL) weight formulae predicts the overall gearbox weight, which is the sum of the main rotor gearbox, tail rotor gearbox, and the intermediate gearbox and is given below<sup>4</sup>.

$$W_{gb} = 172.7 \left( \frac{HP_{MR}}{RPM_{TR}} \right)^{0.7693} \left( \frac{100HP_{TR}}{RPM_{TR} \left( \frac{HP_{MR}}{RPM_{TR}} \right)} \right)^{0.079} n_{gb}^{0.1406}$$

where  $n_{gb}$  is the number of

gearboxes. Based on data from JHL and given that they are three gearboxes, the gearbox weight variation with RPM reduction is illustrated in Figure 3.

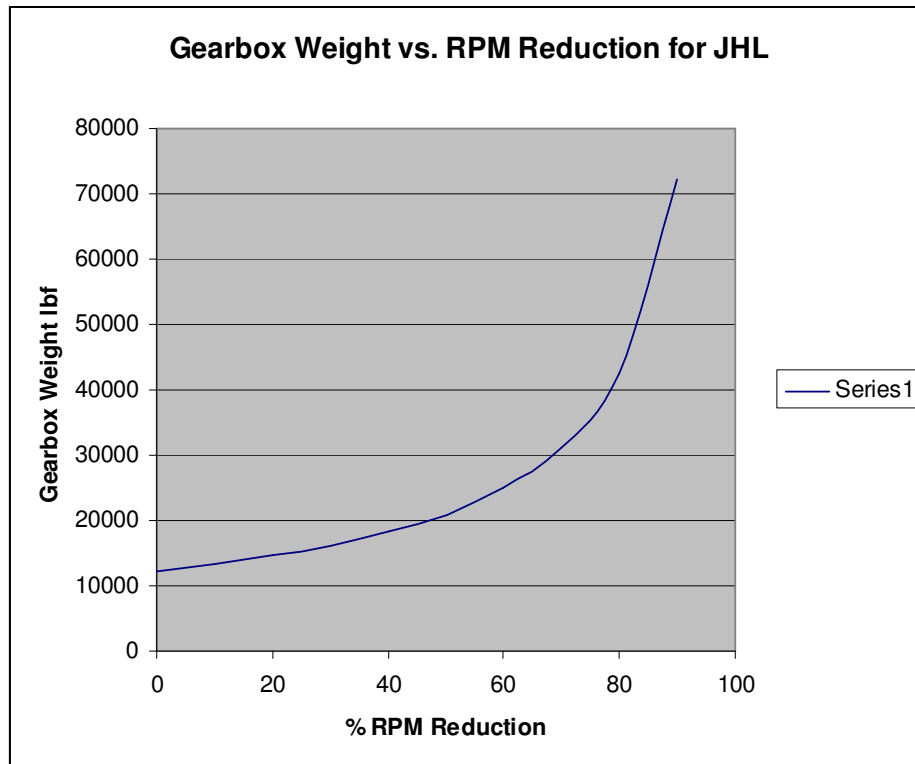


**Figure 3:** Gearbox Weight vs. RPM Reduction for JHL.

The drive system weight is the sum of the gearbox weight and the shaft weight. According to work done by Arling Schmidt<sup>3</sup>, shaft design requires the following steps: determining whether the operation is subcritical or supercritical, knowing the maximum power, RPM, and length of the shaft. The shaft weight is the sum of the tube weight, coupling weight, and bearing weight. According to work done by Arling Schmidt, the shaft weight for subcritical operation is given below<sup>3</sup>.

$$W_s = \frac{(0.7L + 5.9a + 1.5)(P/100)^{0.67}}{(N/1000)^{0.67}}$$

where L is the length of the shaft and a is the

number of segments. Shaft weight variation with RPM reduction is illustrated in Figure 4.

The data was obtained from Andrew Bellocchio's thesis<sup>6</sup> on preliminary design for the Joint Heavy lift Helicopter (JHL). The shaft analysis was performed on the engine shaft, main rotor shaft, tail rotor shaft, intermediate tail shaft, and the tail take-off shaft.

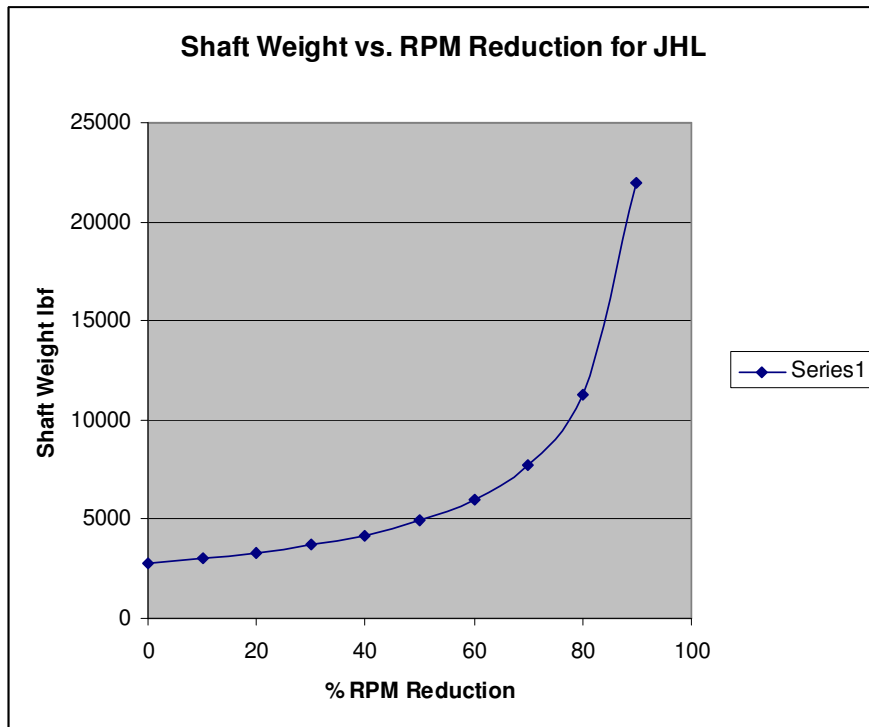


**Figure 4:** Shaft Weight vs. RPM Reduction for JHL.

The shaft weight obeys the square cube law and the gear weight approximately follows the square cube law, which implies that, the transmission weight follows the square cube law as shown in Figure 5.

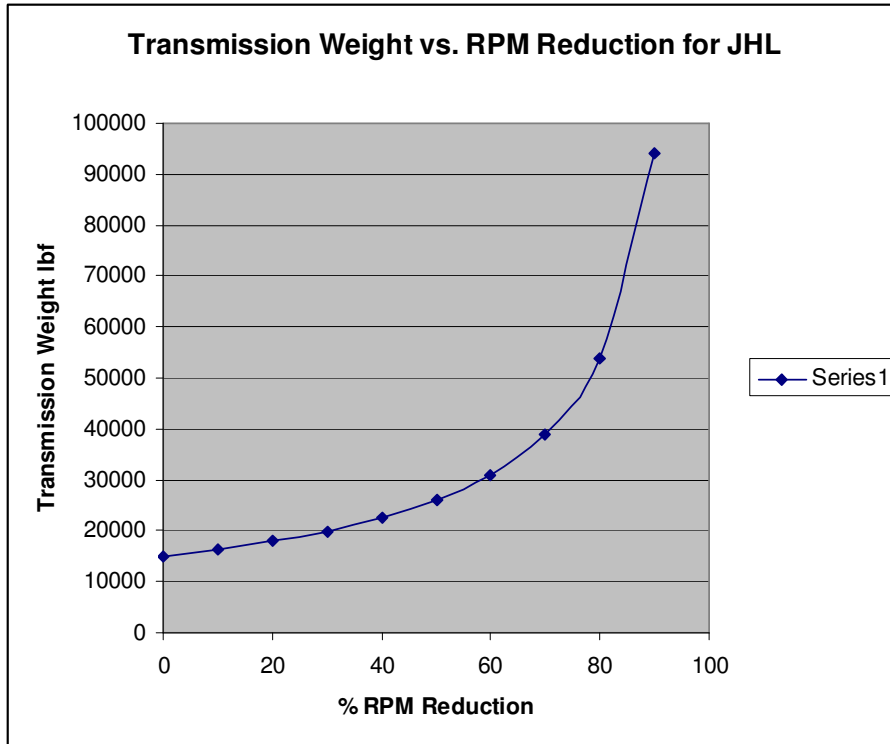


**Figure 5:** Transmission Weight vs. RPM Reduction for JHL.

Therefore, as the vehicle weight increases, the power required increases and, thus, the transmission weight increases. The drivetrain design has a “Square-cube” law constraint which sets the stage for research dedicated to minimizing the drivetrain weight by looking at different types of transmissions and determine which of these has a lower weight. This sets the stage for variable speed transmission also called continuously variable transmission (CVT). Continuously variable transmission implies lack of discontinuities or spikes in the output torque and speed. There are several types of CVT namely belt driven, traction, and variable geometry. Variable speed transmission is a promising prospect because of the ability to vary the rotor RPM, so that each section of the rotor can operate at its best lift to drag ratio. Traditionally, varying the speed is done through the engine; however, the specific fuel consumption deteriorates when the

turboshaft speed is changed as turboshaft engines are optimized for a fixed turboshaft speed. The whole basis of a variable speed transmission is to be able to slow down the rotor in cruise, thus minimizing the profile power and also being able to travel at advance ratios greater than 1, as the maximum speed of a rotorcraft is limited by compressibility effects on the advancing side and blade stall on the retreating side. The CVT is one area of research that has the potential to design a drivetrain/propulsion system that can handle high torque with light weight gears. A study done to compare the weight of a 2-stage planetary gear system of a K-MAX helicopter with a pericyclic CVT revealed the following advantages of using a P-CVT over a traditional planetary gear system<sup>5</sup>. The advantages are: (1) ability to achieve a large gear reduction of  $>50:1$  using a single stage that comprises of four face gear members; (2) A larger contact ratio of  $> 5:1$  resulted in improved power density; (3) reduction in Vibration/Noise; (4) A 17% weight reduction was achieved in comparison to the 2-stage planetary gear system of the K-MAX helicopter. A high fidelity analysis is needed to optimize the weight of the drivetrain by analyzing different speed ranges of the helicopter rotor.

## CHAPTER 5

### CONTINUOUSLY VARIABLE TRANSMISSION CONCEPTS

There are several types of CVT namely belt, traction, variable geometry, and hybrid/electric. Pulley type CVT falls under the category of belt type CVT, toroidal type CVT falls under traction type CVT, and pericyclic continuously variable transmission (P-CVT) falls under hybrid/electric CVT. The types of CVT that will be discussed are pulley, toroidal, and P-CVT. There are several other types of CVT such as hydrostatic and hydrokinetic that use variable displacement pumps to vary the flow and variable blade angles respectively. The pulley type CVT consists of a drive pulley, rubber or metal belt, and a driven pulley. The pulleys are variable diameter pulleys, such that when either pulley reduces its pitch diameter the other pulley increases its pitch diameter to keep the belt taut. The drive pulley is connected to the crankshaft while the driven pulley is connected to the drive shaft. Infinite gear ratios are obtained between a maximum speed and a minimum speed as the pulleys vary the diameters relative to each other. The ratio of the speeds is inversely proportional to the pitch diameters assuming no slipping.

Mathematically it can be expressed as  $\frac{\omega_{driven}}{\omega_{drive}} \equiv \frac{D_{drive}}{D_{driven}}$ . A pulley type CVT is

illustrated in Figure 7.

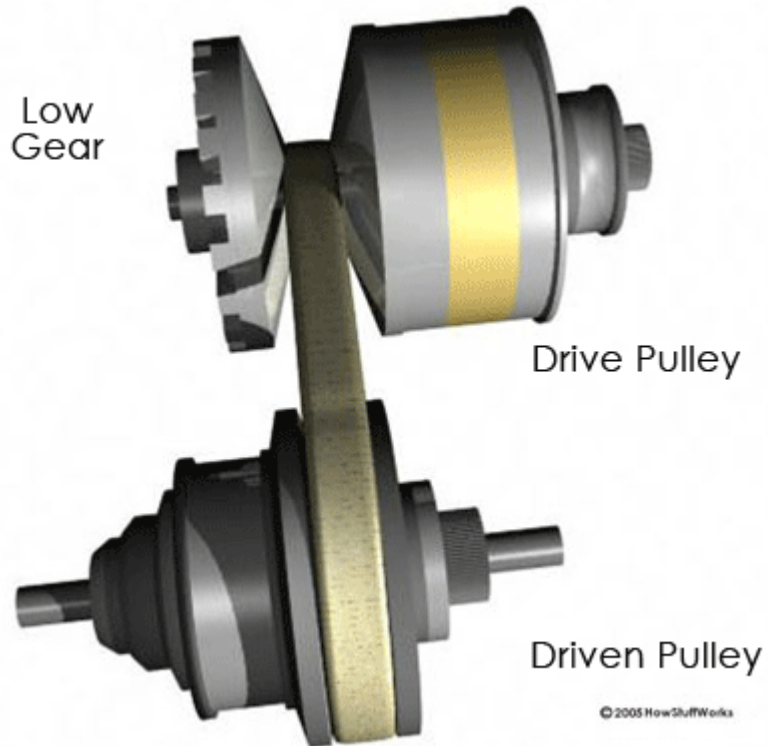


**Figure 7:** Pulley Type CVT.

(<http://www.howstuffworks.com>)

The toroidal CVT has rollers and discs. The input disc is equivalent to the drive pulley, the output disc is equivalent to the driven pulley, and the rollers are equivalent to the belt. The mating of the rollers with the input disc at the center results in the rollers mating with the output disc at the rim which decreases the speed of the output disc and when the mating of the rollers occurs with the output disc at the center results in the rollers mating with the input disc at the rim which increases the speed of the output disc. A toroidal CVT is illustrated in Figure 8.

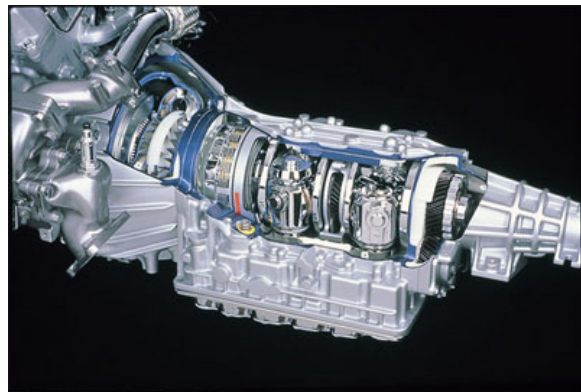
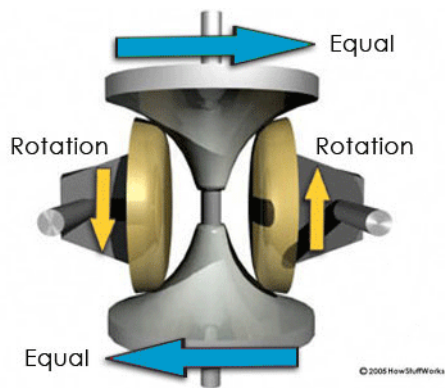


**Figure 8:** Toroidal Type CVT.

(<http://www.howstuffworks.com>)

The P-CVT is an electromechanical CVT consisting of a reaction control rotor, pericyclic motion converter, and an output control rotor. The mating of the reaction control rotor with pericyclic motion converter at the reaction control rotor side results in the mating of the output control rotor with the pericyclic motion converter at the output side<sup>5</sup>. This arrangement varies the speed of the output rotor. An illustration of a P-CVT split torque design is shown in Figure 9.

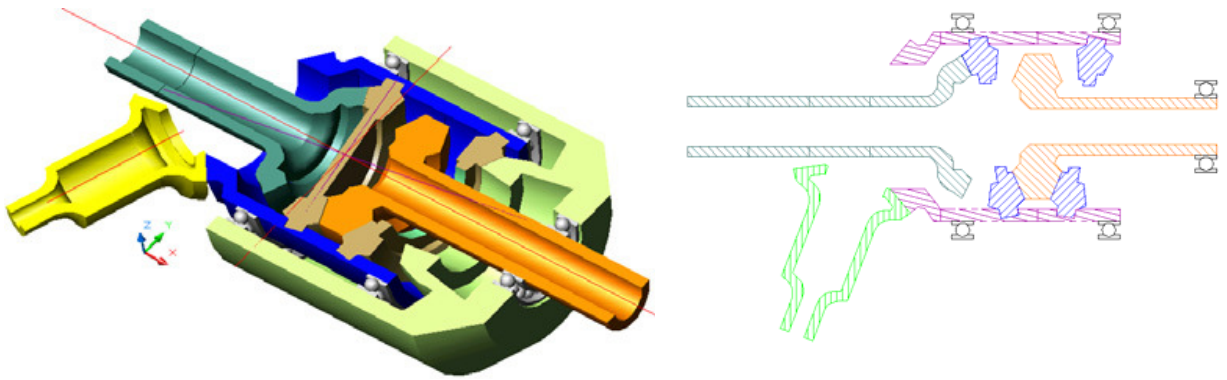


**Figure 9:** Split Torque P-CVT<sup>5</sup>.

The P-CVT falls under the class of a nutating mechanical transmission. The P-CVT undergoes nutation, rotation and precession to achieve variable speed operability at a design coneing angle that is selected based on gear design mating principles and it is typically in the range of 2 to 5 degrees<sup>5</sup>. The P-CVT mechanism is illustrated in Figure 18.

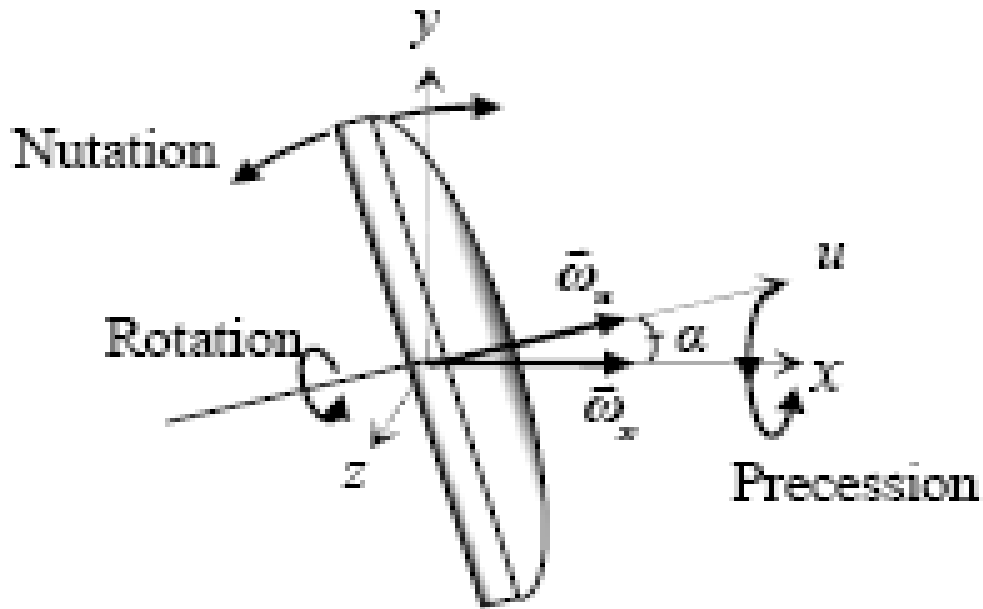


**Figure 18:** P-CVT Electromechanical Transmission<sup>5</sup>.

The advantages of the P-CVT according to Alfonse J. Lemanski<sup>5</sup> are:

- High Contact ratios ( $> 5:1$ ) which results in a quarter of the teeth of the PMC mating with the reaction control rotor and a quarter of the teeth of the PMC mating with the output rotor. This allows for high torque transfer and efficiency resulting in high power density, low gear vibration excitation and noise
- P-CVT analysis done on a K-MAX helicopter has resulted in a 17% weight reduction and a 40% reduction in envelope size
- Large single stage reduction ( $> 50:1$ )
- Static laboratory tests and flight test of the A-160 Hummingbird UAV has proven the “optimal speed rotor” concept

- NASA-Army-Industry-University design study has demonstrated importance of variable speed technology for Heavy lift Missions. Studies looked into Nutating Mechanical Transmissions (NMT)

## CHAPTER 6

### METHODOLOGY AND RESULTS

This section will provide the mathematical framework, methodology and simulation, and optimization flow chart of the weight analysis, acoustic analysis, safety analysis, static finite element analysis, housing, and lubrication analysis.

- **OBJECTIVE : TO REPLACE FIRST AND SECOND STAGE PLANETARY GEAR SYSTEM OF THE JHL (10:1 ratio) WITH A SPLIT TORQUE TYPE P-CVT**
- **The split torque type P-CVT will consist of 50% variable speed P-CVT cascaded in series with a fixed ratio PVT. The variable P-CVT system will have a high speed of 115 RPM and a low speed of 57.5 RPM as shown in Figure 56**

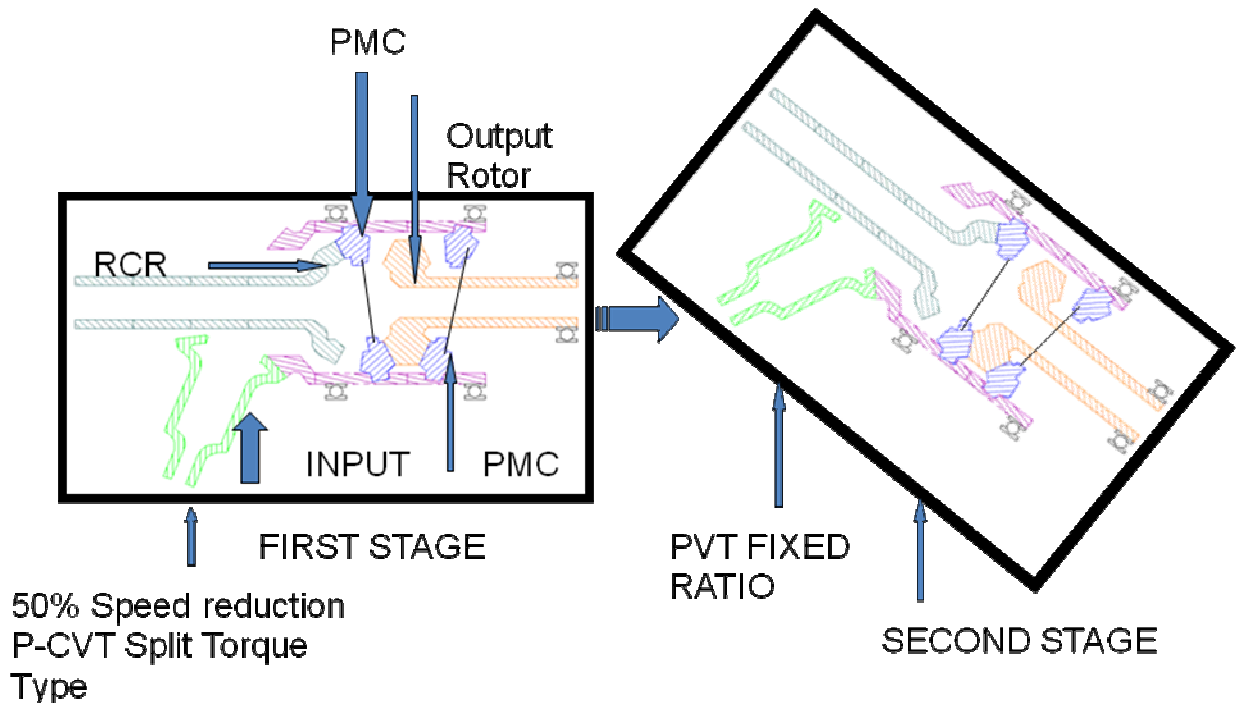


**Figure 56:** Split Torque Type P-CVT Gearbox<sup>5</sup>.

The single main rotor heavy lift helicopter layout is shown in Figure 10.

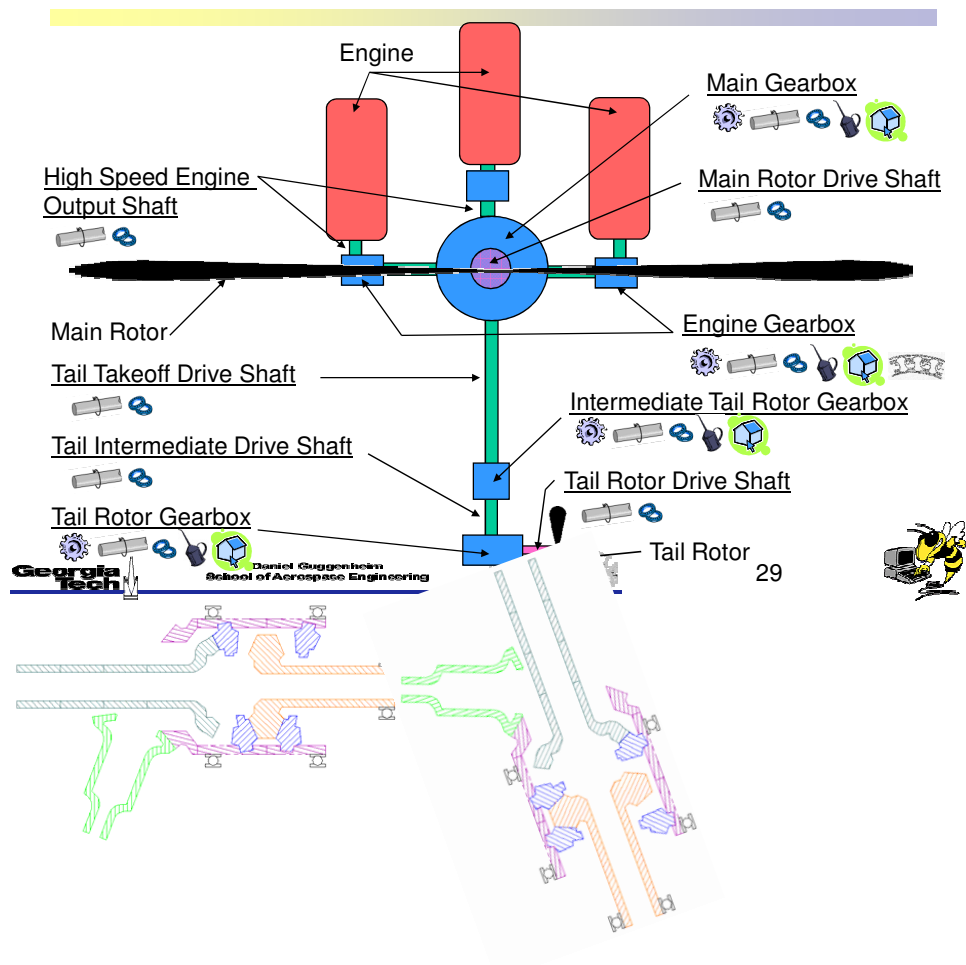


**Figure 10: JHL Diagram and P-CVT Split Torque Connected in Series<sup>6,5</sup>**

The drivetrain schematic is shown in Figure 19.

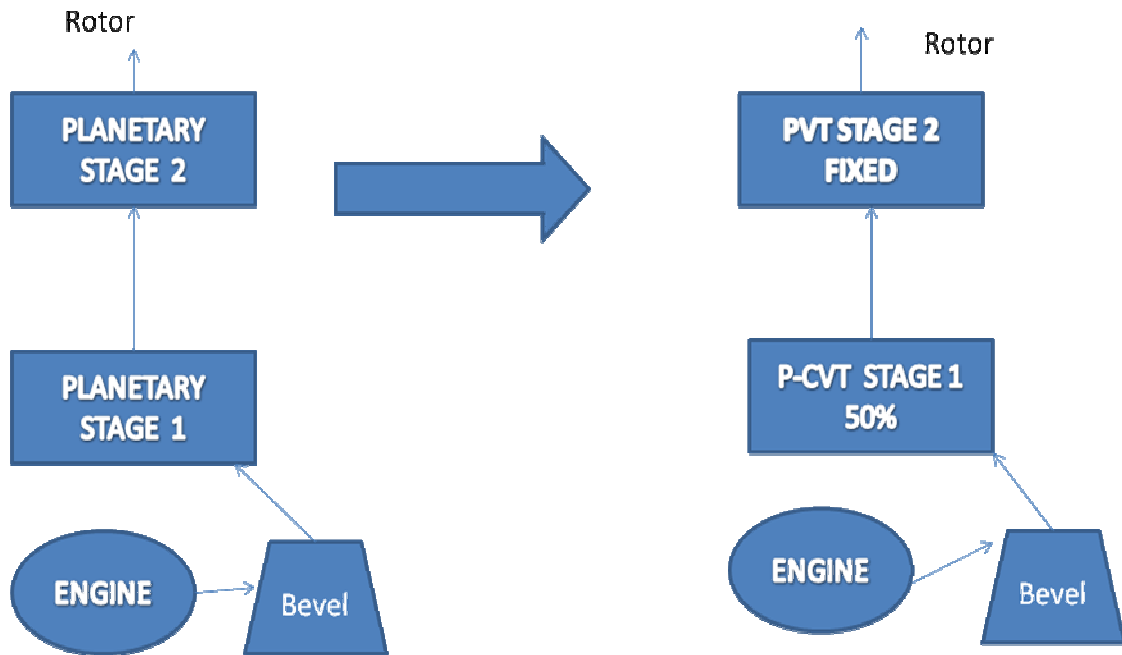


**Figure 19:** Drivetrain Schematic.

### 6.1 Weight Analysis

The P-CVT analysis obtained from references [5] and [20] was done as follows:

The below calculations are for the variable speed PVT system.

Low speed reduction ratio : 20:1

High speed reduction ratio: 10:1

Apply the equation below for number of teeth and RCM speed calculation

$$\frac{\omega_{Arm}}{\omega_4} = \frac{1}{\left(1 - \left(1 - \frac{\omega_1}{\omega_{Arm}}\right) \cdot \frac{N_1 \cdot N_3}{N_2 \cdot N_4}\right)}$$

input speed : 1151.6rpm

low speed : 57.5 rpm

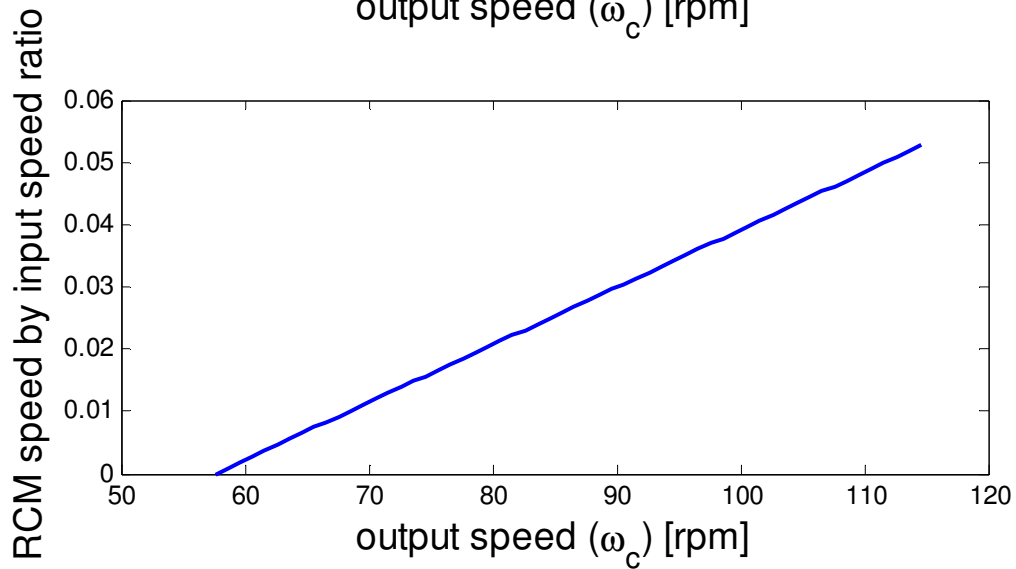
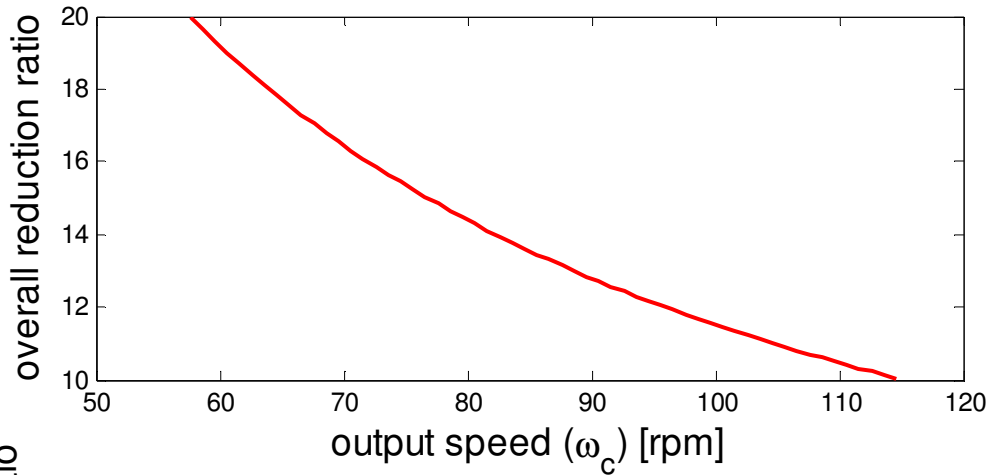
high speed : 115.2 rpm

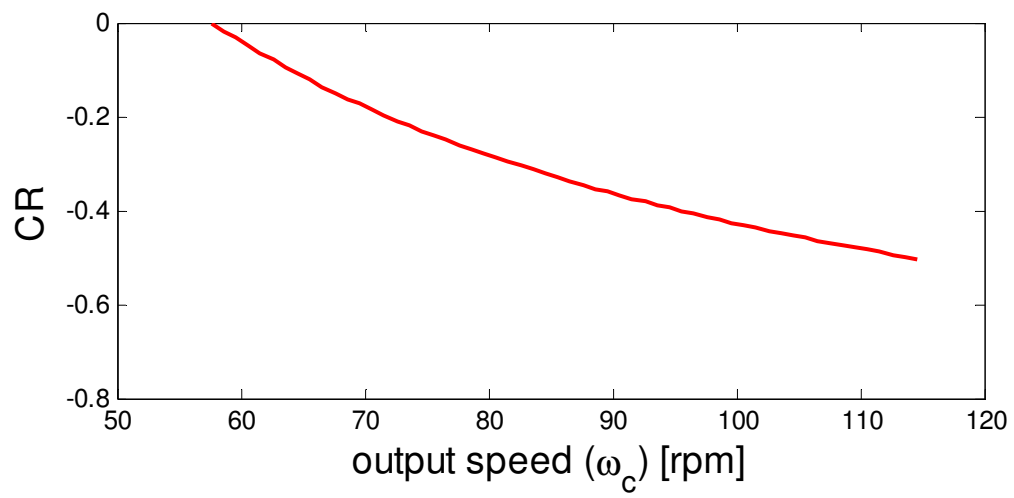
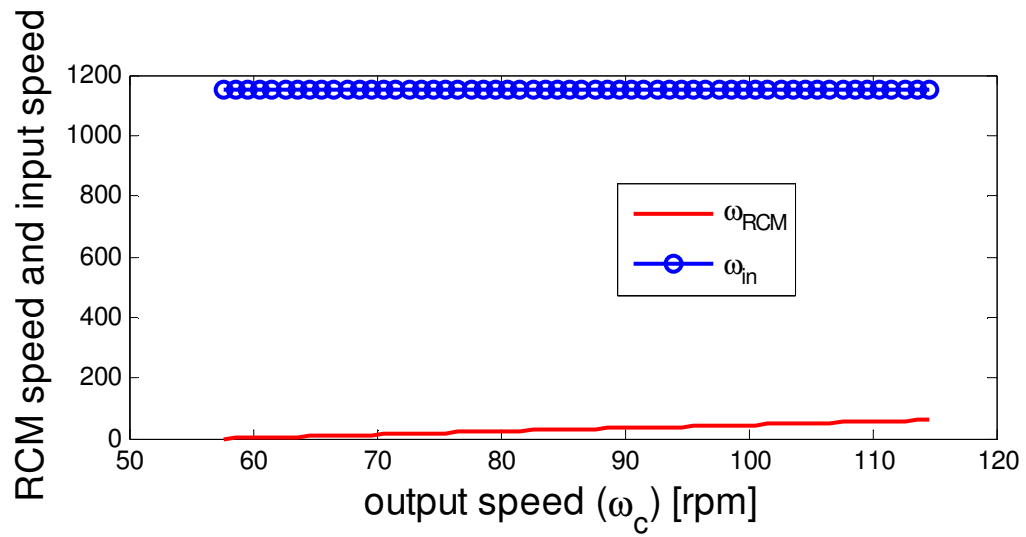
Possible Number of teeth for this design:

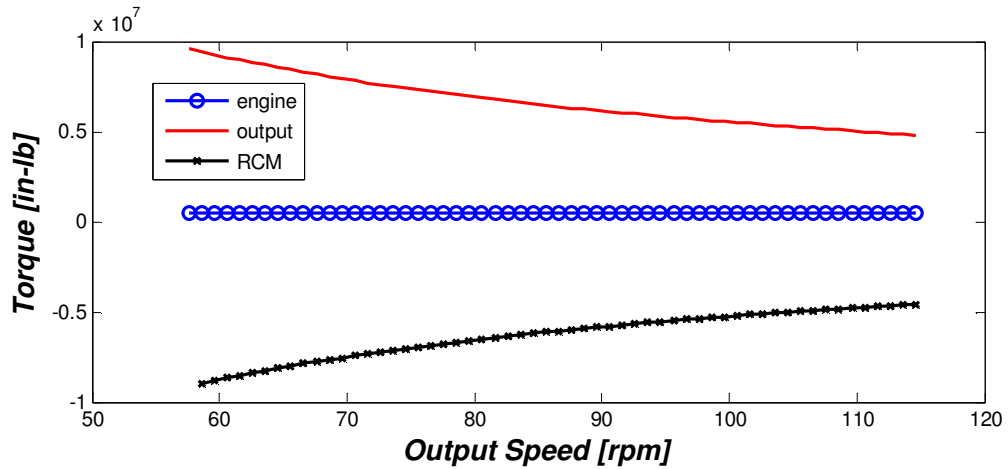
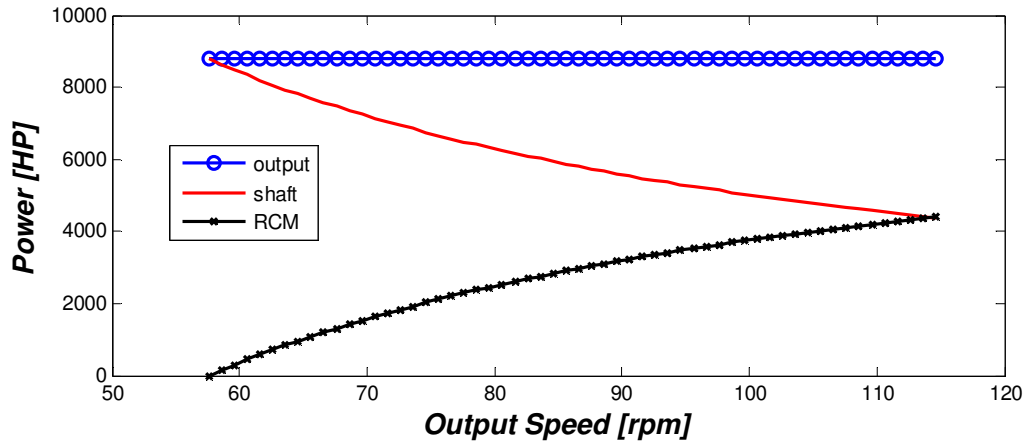
<i>N<sub>r</sub></i>	<i>N<sub>pr</sub></i>	<i>N<sub>po</sub></i>	<i>N<sub>o</sub></i>
14	15	57	56
18	20	19	18
18	20	38	36
19	21	21	20
19	21	42	40
19	20	20	20
28	30	57	56

-> selected for the analysis

Calculated RCM speed and Circulating power ratio, power flow and torques







The P-CVT analysis<sup>5</sup> conducted above can be found in Appendix B and the mathematical derivation of the governing equations of the P-CVT<sup>25</sup> can be found in Appendix D. The objective was to calculate a range of diameters and corresponding facewidths that would give tooth bending stress values below the allowable bending stress of the material. The allowable bending stress of the material intersected the curve that had the highest tooth bending stress based on the stress curves plotted for the output, reaction control and PMC rotors. Based on this analysis, the diameter of the gears is chosen and the weight can be

computed using the face width, diameter, and weight density. The mathematical analysis for the planetary gears can be found in Appendix A. The tensile stress of the gears obtained by varying the pitch diameter is illustrated in Figures 11 and 12 respectively.

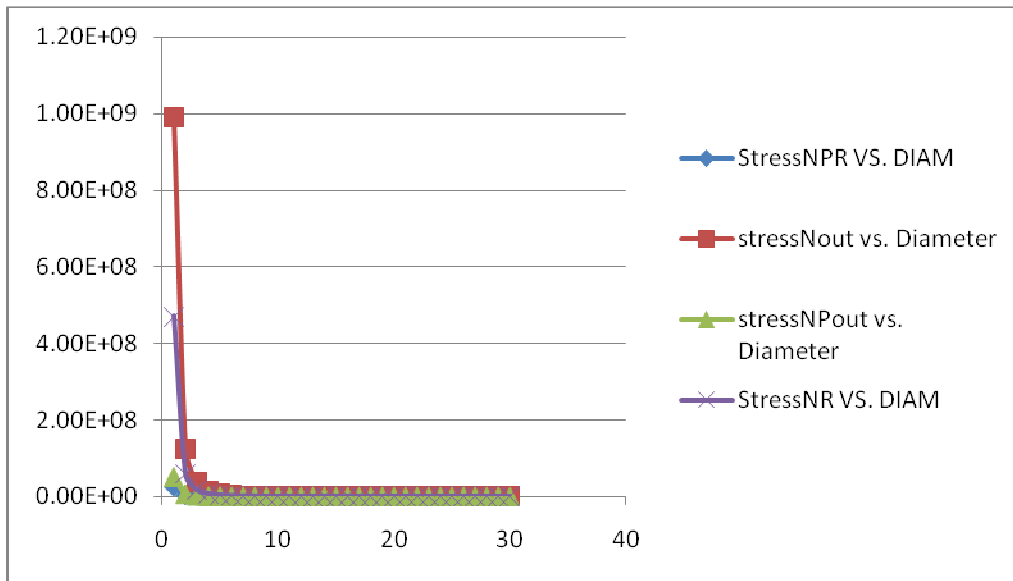


**Figure 11:** Tensile stress for the four facegears of the first stage P-CVT.

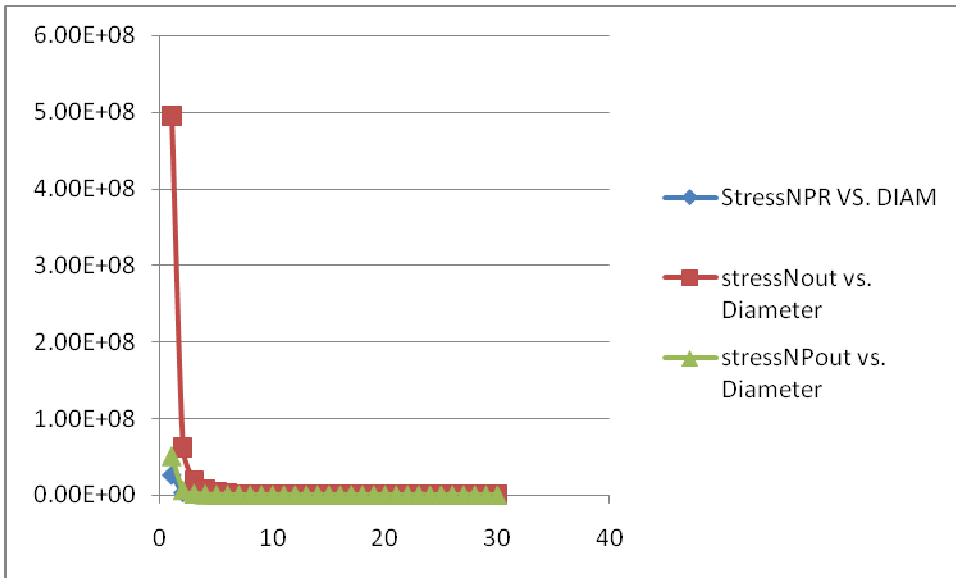


**Figure 12:** Tensile stress for the four face gears of the second stage PVT.

The optimization procedure followed for the P-CVT adhered to the design flow chart<sup>20</sup>, as illustrated in Figure 21.

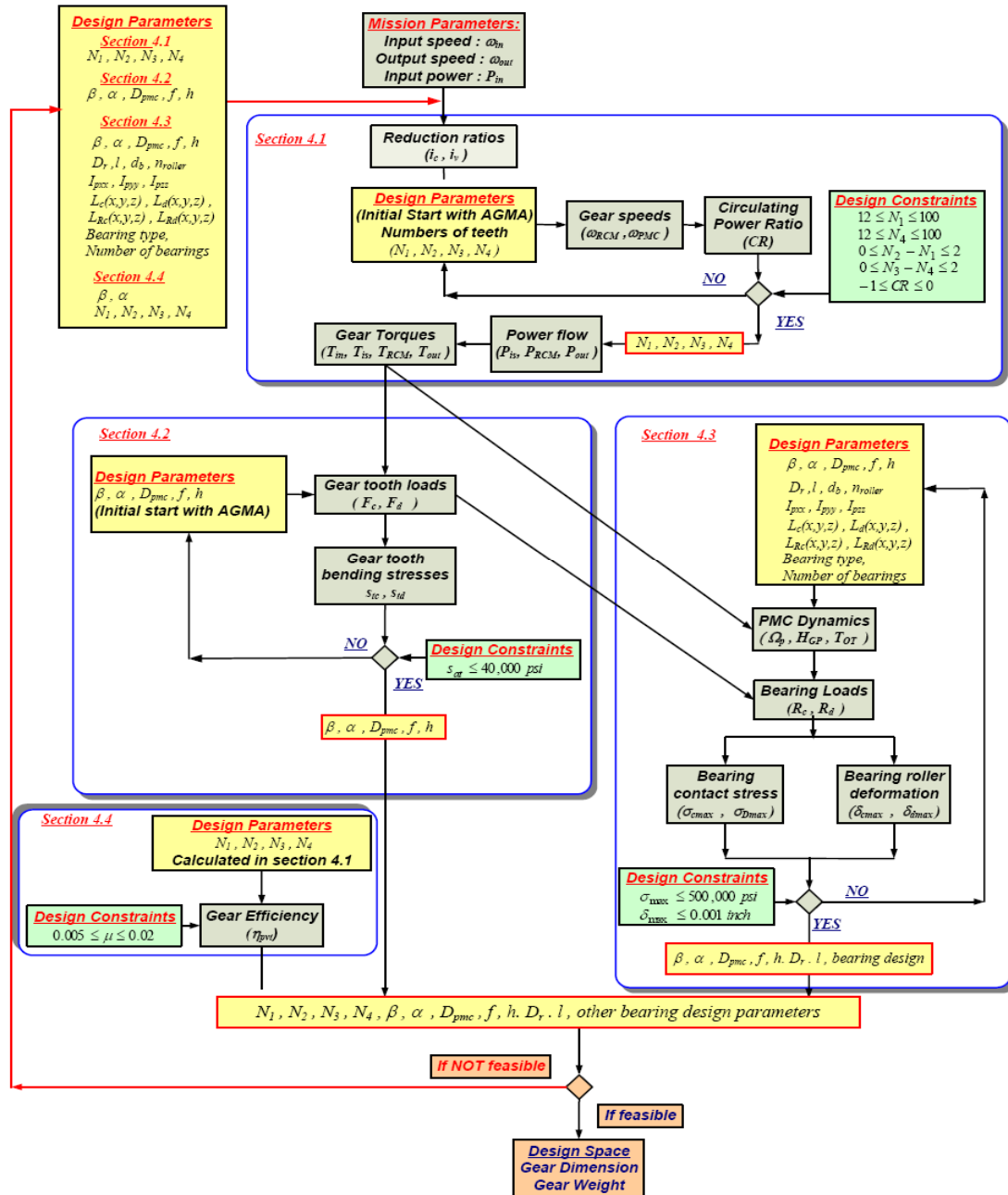


**Figure 21:** Design Flow Chart for Weight Analysis<sup>20</sup>.

The following Tables 1 and 2 lists the design parameters and constraints<sup>20</sup>.

**Table 1:** Design Parameters<sup>20</sup>.

	<u>Symbols</u>	<u>Definition</u>
1.	$N_1, N_2, N_3, N_4$	Numbers of teeth
2.	$\beta$	Nutation angle
3.	$\alpha$	Tooth pressure angle
4.	$D_{pmc}$	Gear diameter
5.	$f$	Tooth face-width
6.	$h$	Gear-cylinder height
7.	$D_r$	Gear bore diameter
8.	$L$	Bearing roller length
9.	$d_b$	Roller diameter
10.	$n_{roller}$	Number of rollers
11.	$I_{pxx}, I_{pyy}, I_{pzz}$	Moment of inertias
12.	$\vec{L}_c, \vec{L}_d$	Tooth contact location
13.	$\vec{L}_{Rc}, \vec{L}_{Rd}$	Bearing center location
14.	<i>Bearing type and amount</i>	

**Table 2:** Design Constraints<sup>20</sup>.

<b>Section</b>	<b>Constraints</b>	<b>Definition</b>
3.1	1) $N_{\min} \leq N_1 \leq N_{\max}$	Limits of RCM teeth
	2) $N_{\min} \leq N_4 \leq N_{\max}$	Limits of output teeth
	3) $0 \leq N_2 - N_1 \leq 2$	(PMC – RCM) tooth
	4) $0 \leq N_3 - N_4 \leq 2$	(PMC – output) tooth
	5) $-1 \leq CR \leq 0$	Split Power branch
3.2	6) $s_t \leq 40,000 \text{ psi}$	Tooth bending stress
3.3	7) $\sigma_{\max} \leq 500,000 \text{ psi}$	Roller contact stress
	8) $\delta_{\max} \leq 0.001 \text{ inch}$	Roller deformation
3.4	9) $0.005 \leq \mu \leq 0.02$	C. of friction

Based on references [5] and [20], we are usually interested in three main issues which are cross-functionally related to each other. These are:

- 1 – Weight of the system
- 2 – Reliability of the system
- 3 – Maintainability or serviceability requirements

From industry experience<sup>5</sup>, these three are related to the torque and the operating speeds. The gearbox weight analysis and shaft analysis procedures are credited to Mr. Zihni Saribay<sup>5</sup>.

### **Gearbox Weight Analysis Procedure**

- Obtain the overall reduction ratio of the planetary gear train 1 and planetary gear train 2
- Find the proper numbers of teeth of the PVT gears to achieve this reduction ratio. Probably you may not be able to get exactly the same reduction ratio but a ball park will be acceptable
- Determine the torques and the tooth loads of the PVT gears
- Obtain the bending stresses of the planetary gear trains (PGT)
- Because you are trying to compare two different gear mechanisms your stress comparisons should be based on the material allowable rather than the comparison to the already designed PGT system
- Calculate the range of diameters that will show a range of stresses below the allowable limit of the material by using the formula in the paper<sup>5</sup> and the related AGMA coefficients
- The objective function will be the minimization of the weight and constraint is the tooth bending stress

## Shaft Analysis procedure

- Identify the tooth loads
- Identify the location of the bearings
- In general transmission practice, we usually treat the shaft as a pinned-pinned constraint beam problem or in some cases clamped-pinned beam problem. In this case to eliminate statically indeterminate situation pin-pin can be sufficient
- Calculate the inertial moment that is produced by the rotating gear
- Calculate the moments and loads on the PMC bearings
- The moments produced are in opposite directions in the torque split design
- There is a schematic below that gives ideas about the simple model
- By using equivalent moments and loads acting at the **red dot** on the figure 22 and the cylindrical hollow beam with pin-pin boundaries you can calculate minimum dimensions and even optimize the entire gear train for minimum weight that has tooth bending and shaft bending stresses

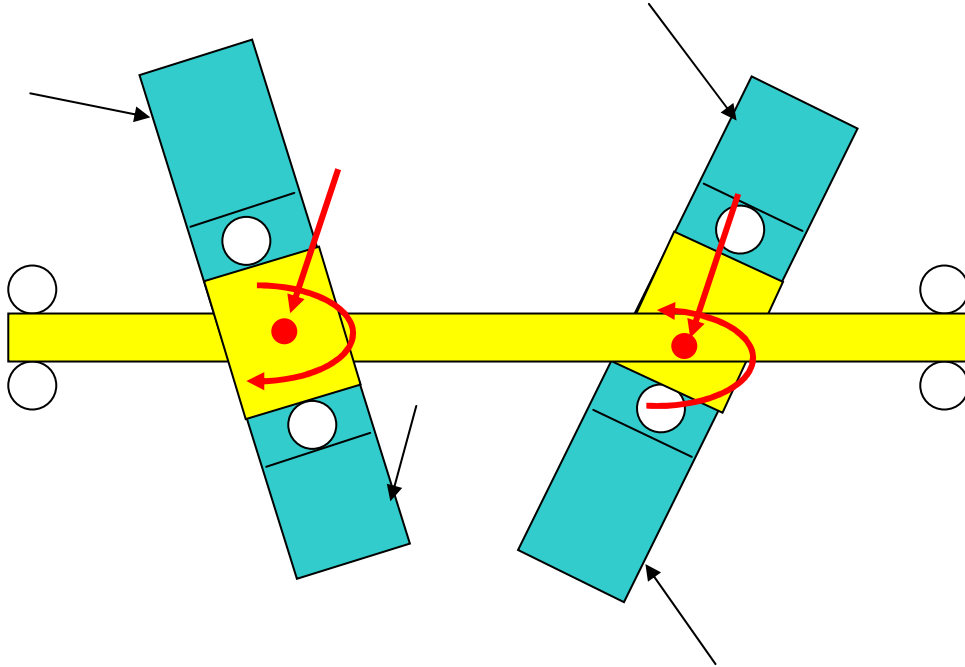


**Figure 22:** Double Nutator mounted on a Shaft pinned at both ends.

The parameters and combination of these parameters are listed below in order to optimize a P-CVT<sup>25</sup>.

- Single or double nutator
- Nutation half angle
- Duration of tooth/roller contact
- Basic spherical radius
- Nutator roller mounting method
- Nutator roller radii/cam teeth thickness
- Number of rollers on nutator/teeth on cams

- Nutator support bearing configuration
- Roller centerline coning angle
- Roller length

The weight Analysis of the JHL yielded the following results, as shown in Table 3 and Table 4. The weight analysis methodology can be found in Appendix B.

**Table 3:** Weight Breakdown of the Split Torque Type P-CVT.

Total Shaft Weight for Split Torque Type P-CVT (lbs)	5,000
Total Gearbox Weight for Split Torque Type P-CVT (lbs)	1,823
Total Bearings Weight (lbs)	1,630
Total Housing Weight (lbs)	289

**Table 4:** Weight Comparison of the Drivetrains.

JHL Planetary		JHL Split		Split Torque Type	
Drivetrain	Weight	Torque	Drivetrain	Weight	P-CVT Weight (lbs)
(lbs)		(lbs)			
15,203		14,750			8,742

The P-CVT split torque type transmission offers a 42.5% weight reduction over a planetary drive system and a 40.7% weight reduction over a split torque drive system.

The major weight savings comes from the gearbox due to the use of face gears.

## 6.2 Acoustic Analysis

The acoustic analysis equations are obtained from reference [7]. The SPL versus time for the planetary stages of the JHL is shown in figures 13 and 14 respectively. The equation used in the analytical study implies that the vibration of the planetary gear system is the sum of the vibration of the pinions<sup>7</sup>. The excitation was assumed to be an impulse function.

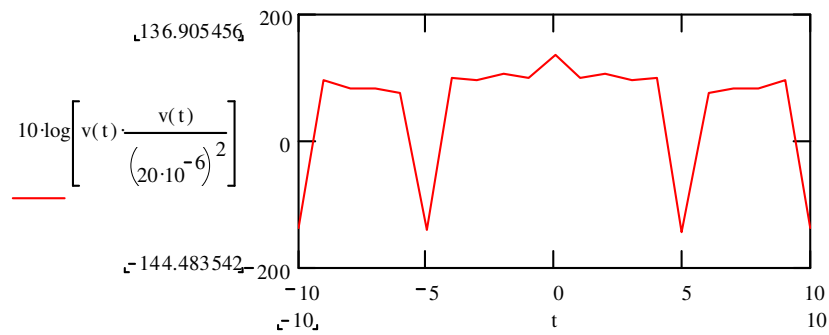


**Figure 13:** SPL vs. Time for 1<sup>st</sup> stage Planetary Gear System.

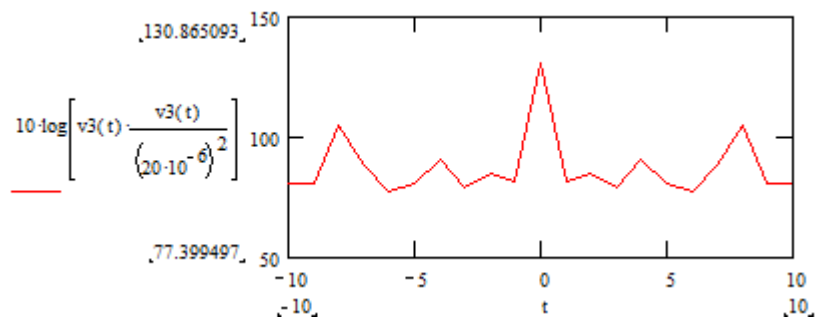
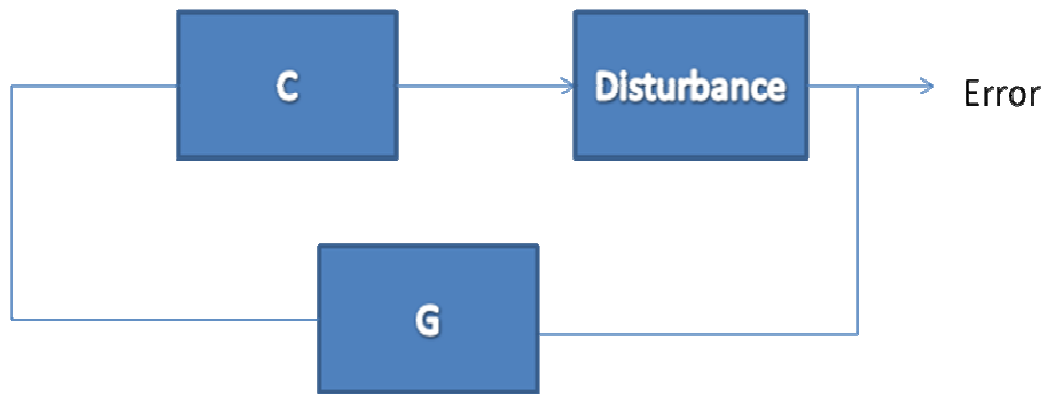


**Figure 14:** SPL vs. Time for 2<sup>nd</sup> Stage Planetary Gear System.

## Active Noise Control

- Free Field Control Scheme : wave interference
- Equally distanced from a field point, the sound source and control source have same power to cause a null at a specified point
- For sound power control ( Global Minimization), the distance between the sound source and the control source must be less than a third of a wavelength



C: is the Plant transfer function includes all path and transducer dynamics

G: Controller Transfer Function : Proportional integral derivative control (PID)

- $See(\omega) = Sdd [ 1/(|1-G(j\omega)C(j\omega)|^2)]$
- See is the Spectral Power Density
- Sdd is the disturbance
- Goal is to minimize the See by maximizing the denominator
- Major noise contributor is the drivetrain

- Use of Active Noise Control and Finite Element Analysis (FEA) to model the CVT elements interaction with the gearbox housing
- Noise generated is due to the resonances in the gearbox housing. Therefore, emphasis must be placed on housing design
- The Active noise control portion using boundary element solvers was not performed for this thesis due to the fact that it is a research topic unto itself, however, the ground work is set for a pursuit in the acoustics regime of CVT's

The major goal is reduce the tonal components of the gear meshing noise which are in the range of 500 Hz TO 4 kHz. Human hearing is most sensitive in the midband frequencies between 1 and 3 khz. The vibration of the gear meshing noise is transmitted via gearbox struts to the helicopter cabin. A new experimental methodology in active vibration control has been proposed by EADS Corporate Research center and Eurocopter Deutschland and the results are published in an AIAA paper<sup>21</sup>. This methodology of employing active gear strut technology has been successful in the BK117 flight test of 2004<sup>21</sup>. The results show a 19.5 dB reduction in Sound Pressure Level ( $L_p$ ) for the first harmonic independent of the flight condition and about 4 to 8 dB reduction in sound pressure levels for other harmonics based on flight conditions<sup>21</sup>. Based on the successful deployment of the active gear strut technology in the BK117, the Split torque type P-CVT for the JHL will incorporate this technology in the gearbox design. The active gear strut deployment in a helicopter is illustrated in Figure 23.

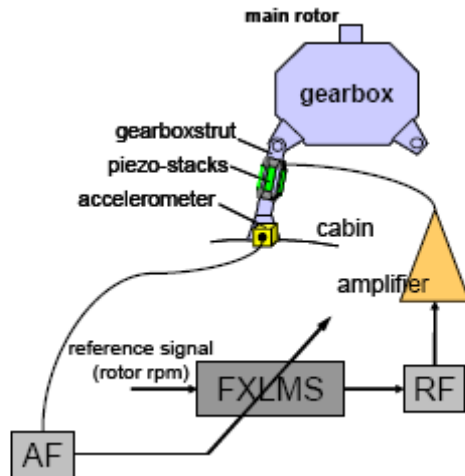


**Figure 23:** Schematic of the Active gear strut technology deployment in a helicopter<sup>22</sup>.

This diagram shows a butterworth low pass filter connected to an accelerometer which is used to block high frequency components and aliasing. A reference signal, which is the RPM of the rotor serves as an input in terms of the frequency to be controlled and is fed to the narrowband multi-channel filtered-x version of the adaptive LMS algorithm that tracks the frequency and amplitude variations of the noise/vibration<sup>21</sup>. The output of the low pass filter is fed into the amplifier and the amplified signal is used to excite the piezo stacks. The need for a reference signal to be the rotor RPM stems from the fact that the gear mesh frequencies vary with rotor RPM.

A control system describing this algorithm's ability to control several tonal components is shown in Figure 24 and the active gear strut is shown in Figure 25.

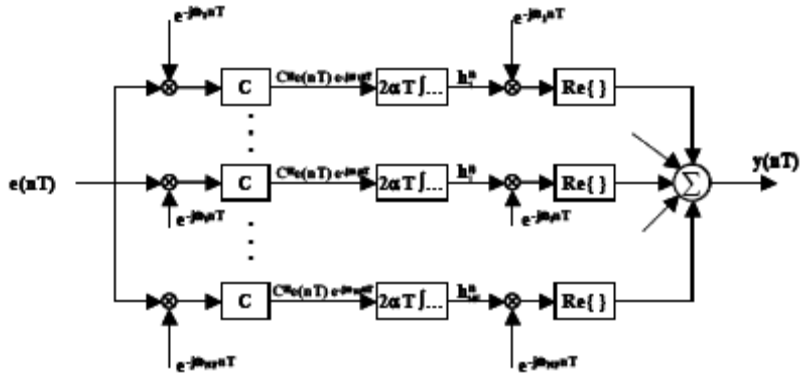


**Figure 24:** FXLMS Algorithm<sup>21</sup>.

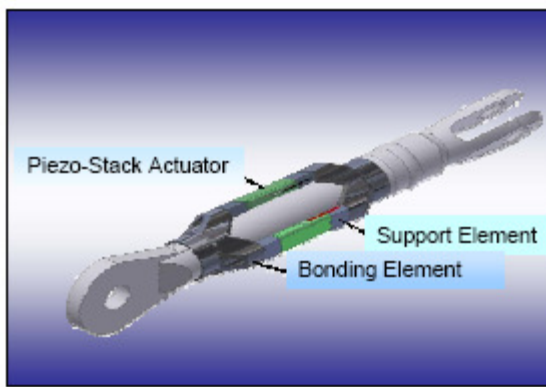


**Figure 25:** Active gear Strut<sup>21</sup>.

It is important to note that active noise control is useful for controlling low frequencies while passive noise control is useful for controlling high frequencies. Also modifications to housing shape can lead to sound pressure level reduction as well.

### 6.3 Safety Analysis

This section describes the safety assessment of the split torque type P-CVT for a single main rotor heavy lift helicopter. The safety assessment of the split torque type P-CVT was selected as a project for the safety by design class taught by Dr. Daniel Schrage at Georgia Institute of Technology. The Safety assessment consisted of:

- Fault tree construction for nontraction based CVT as part of the static analysis
- The FTA for P-CVT is based on reaction control rotor failure, PMC failure, output rotor failure, input shaft failure, control systems failure, regenerative braking system failure, and power system failure. The reliability is the product of these failures
- Monte Carlo Simulation using stochastic petrinets as part of the dynamic analysis, failure hazard analysis, and reliability block diagrams
- Preliminary certification and time line of the certification process
- The safety assessment of the P-CVT for the single main rotor heavy lift helicopter was conducted by Sameer Hameer, Trey Kasling, Baris A. Sen, Santosh Hemchandra, Vagan Babajanyan

The aim of this work is to perform a preliminary safety assessment of the Pericyclic Continuously Variable Transmission (P-CVT) system for deployment in the single main rotor Heavy-Lift Helicopter. When compared to traditional traction based CVT systems, the P-CVT offers the dual advantages of a high-contact ratio and the ability to achieve large speed reductions (50:1 in some cases). A Failure Hazard Analysis followed by an FTA/RBD analysis yielded an overall system failure rate of 140.35 failures per million

hours. A Stochastic-Petri Net analysis was performed to estimate overall system availability and mission success rate. The Stochastic petrinets is dynamic analysis software developed by Dr. Vitali Volovoi at the Georgia Institute of Technology. Based on the analysis recommendations for a certification basis as well as a time-line for certification are also provided.

This goal of this project was to do a reliability analysis on a pericyclic continuously variable transmission (P-CVT) for a single main rotor Heavy-Lift Helicopter. At the time of starting, there were only conceptual designs for a Heavy-Lift Helicopter. So we chose to use the University of Alabama single main rotor Team's joint heavy lift proposal for the American Helicopter Society Competition sponsored by Boeing in 2005 as our baseline single main rotor helicopter.

The next step was to look at a typical mission for the single main rotor heavy lift helicopter to find the operational stages. Once this was defined, a function hazard assessment (FHA) was done to determine the risk of failure of any component for every mission stage. The FHA combines the consequence of a failed component with the likelihood of that failure to give a risk assessment.

Failure rates were also determined for the mechanical and electrical components of the P-CVT. These were input into the ITEM software to formulate a fault tree analysis of the P-CVT to find the overall failure rate of the transmission. A reliability block diagram was also drawn to find the mission success rate.

Petri Nets were used to look at the overall mission success rate of the transmission over a large number of operational hours. The failure rates were input into the software

with repair times and put through a monte-carlo simulation. This simulation gave us the probability of how long the transmission would be available for operational use.

The certification requirements for a single main rotor heavy lift helicopter were looked at along with the specific standards that apply to the P-CVT.

### **Mission Description**

The mission requirements for a single main rotor heavy lift helicopter were realized from NPS Helicopter Design Team<sup>22</sup>. A 300nm radius of action must be achieved with the ability to carry a 37,500lb payload. The helicopter should be able to transport a light armored vehicle, medium tactical vehicle replacement, or a heavy expanded mobility tactical truck at cruise speeds from 200 to 250kt<sup>22</sup>.

### **Functional Description**

A typical mission profile would include preflight, takeoff, cruise, objective, return and land. Each one of these is broken up into more detailed components. During preflight, the pilot would run through the checklist for the helicopter. The payloads would be exchanged and weapons loaded. The pilots would also establish and maintain communications with the tower and other aircraft. The next stage is the take-off where the pilot starts the engine and engages the rotor. The pilot gets the proper clearances from tower, sets the blade pitch and begins to leave the ground. Cruise includes the climb out stage, and achieving a desired airspeed and altitude.

Once the objective is in site, the helicopter will descend and come into a hover to land. By either ground commands or the pilot's discretion, the pilot lands the helicopter and the payloads get exchanged. When the exchange is complete, the helicopter returns to hover and climbs out to the desired altitude and airspeed to return to base. During the

final landing stage, the helicopter descends, maintains a hover, and slowly touches down and the mission is complete.

### Preliminary System Safety Assessment

One of the main aims of the PSSA is to determine overall system reliability. The first step in this process is to perform a component-wise breakdown of the P-CVT system based on the description provided in the previous sections. This is presented in Figure 26.

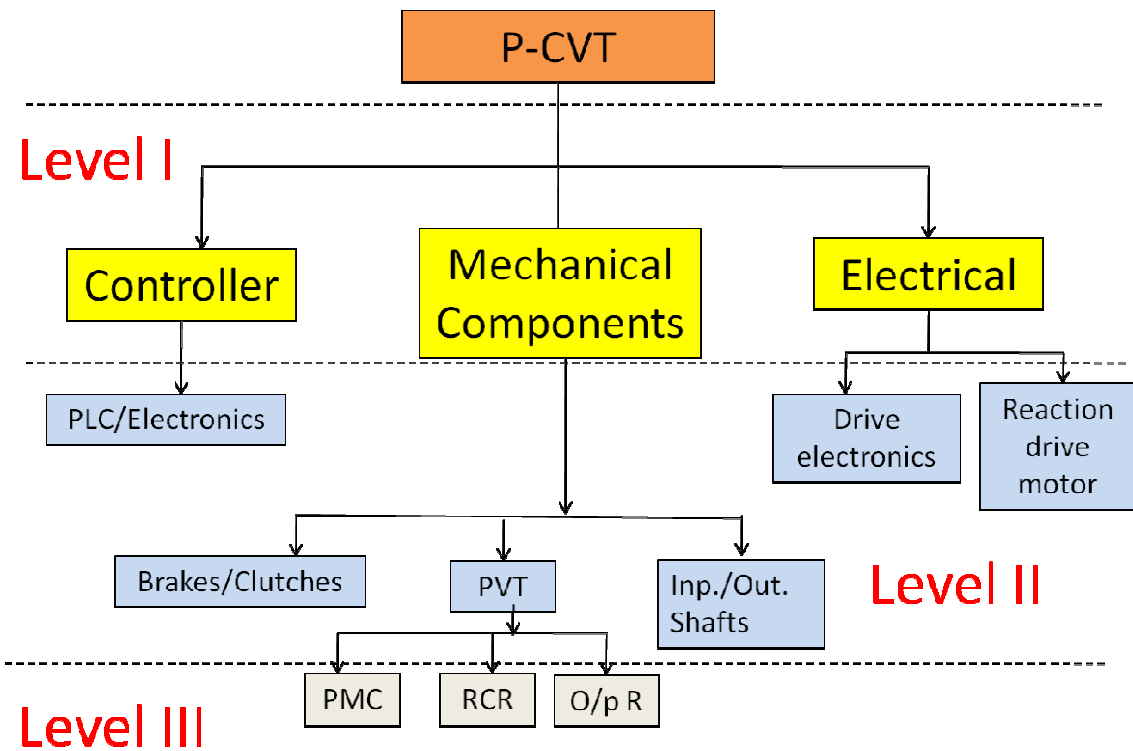


**Figure 26:** Component-wise breakdown of the P-CVT.

## Functional Hazard Assessment

In order to analyze the risk associated with the P-CVT, a functional hazard assessment was performed over the operational range of the aircraft system. The P-CVT was broken down into the following main subcomponents:

### Failure Modes & Rates

Three categories of failure types were formulated to group the potential failure modes for each of these P-CVT components. A summary of these categories is given in Table 5, along with a description of example modes for each.

**Table 5:** Failure types.

Failure Type	Description of Example Modes
Fatigue	Crack initiation due to static, dynamic, Foreign Object Damage (FOD), and corrosion related stress increases
Fracture	Elimination of component load path(s) due to crack propagation
Mechanical	Cessation or inhibition of functional operation due to friction (e.g. lubrication leak), gear slip, component warp, and FOD

These three failure types were chosen to be consistent with traditional fatigue & fracture analytical methods, which seek to quantify a failure rate, damage fraction, retirement life, and inspection interval for components. First, all cracks are fatigue cracks in origin, unless they are caused by Foreign Object Damage (FOD), like a loose nut or bolt impacting a part and forming a high stress crack initiation point. But, FOD is not usually considered when establishing a fatigue life, because it is a random event and a designer assumes that the manufacturer is taking appropriate inspection steps to eliminate FOD. Second, all fractures begin as cracks that then propagate through the part under loading. In practice, we analyze the fatigue and fracture of parts based on the dynamic loads – low

cycle Ground-Air-Ground (GAG) and high cycle rotor induced loads – measured in flight test; the material S-N curve – which is a Weibull function fit to test data of oscillatory load vs. cycles-to-failure – established from coupon testing; and, the endurance limit for the part based on the material and lab fatigue tests. A flight spectrum is established which indicates a percent flight time that the aircraft will execute particular maneuvers. If the flight loads encountered exceed the endurance limit for the part then it will damage. The extent of the damage is determined by using the Weibull function to approximate the cycles-to-failure for that flight load and the number of rotor cycles at that condition, given the RPM and allocated flight time in the spectrum. The damage is added up over the entire spectrum and a life in terms of flight hours is determined, which establishes the retirement life for the part. We also conduct a crack growth analysis to determine the threshold crack initiation size necessary for a crack to grow. Most programs, like the V-22, use an initial crack size equivalent to the effective shot-peen depth of 0.010". If the propagation threshold size is less than that value, then we apply the flight loads to determine the exponential rate at which the crack will grow and the number of flight hours until it reaches the critical crack length. This establishes the inspection interval for the part. In the case of the P-CVT, we do not have test data available to establish lives to this level of detail. Instead, we based failure rates on those of similar components in other transmission systems prevalent in the automobile industry, which serve as a rough starting point for the safety analysis presented in this report. The P-CVT component failure rates are given in Table 9.

## Risk Analysis

The risk associated with each failure is a function of its likelihood of occurrence (failure rate) and the consequence to the system should that failure occur. Different systems will have different definitions for the consequence associated with each hazard level. The scope of the safety analysis will also determine the aircraft system level to which the consequences are applied. For this analysis, the consequences for each hazard level are defined with respect to the impact of the failure on the overall aircraft. Table 6 presents a summary of the hazard levels.

**Table 6: Hazard Levels.**

Hazard Level	Consequence
Minor	Does not prevent system function but requires timely service, resulting in self-contained component damage and repair/replacement
Medium	Does not prevent short-term function but requires immediate service, resulting in damage to other aircraft components and several repairs/replacements
Major	Critical loss of function that does not prevent autorotation, resulting in moderate-to-severe damage to entire aircraft and probable injury or fatality
Catastrophic	Ceases system function preventing autorotation, resulting in probable loss of aircraft and fatality

The fifth hazard level used in the risk analysis, which is not defined in Table 6, is "No Effect". This level is self-explanatory, meaning that the failure has no effect on the system. Table 7 summarizes the level of risk as a function of the hazard consequence due to a failure and the rate at which that failure occurs.

**Table 7: Risk Matrix.**

		Likelihood				
		$< 10^{-9}$	$< 10^{-7}$	$< 10^{-5}$	$< 10^{-2}$	$> 10^{-2}$
Hazard Consequence	Catastrophic					
	Major					<b>HIGH</b>
	Medium			<b>MED</b>		
	Minor		<b>LOW</b>			
	No Effect					

The next step in this FHA was to set the hazard level for each failure type across the operational spectrum of the aircraft. Operating conditions have an important impact on

the level of risk, particularly between flight and ground operations. Once the hazard levels were set, they were combined with the component failure rates to determine the operational risk to the system (see Table 8).

**Table 8:** System Operational Functional Hazard Assessment.

P-CVT FHA		Operational Stages							
		Pre-Flight	Take-Off		Cruise	Objective	Return	Land	
Component	Failure Type	1	2a	2b	3	4	5	6a	6b
Input Shaft	Fatigue	Minor	Minor	Medium	Medium	Medium	Medium	Medium	Minor
	Fracture	Medium	Medium	Catastrophic	Catastrophic	Catastrophic	Catastrophic	Catastrophic	Medium
Output Shaft	Fatigue	Minor	Minor	Medium	Medium	Medium	Medium	Medium	Minor
	Fracture	Medium	Medium	Catastrophic	Catastrophic	Catastrophic	Catastrophic	Catastrophic	Medium
Reaction Control Rotor	Fatigue	Minor	Minor	Medium	Medium	Medium	Medium	Medium	Minor
	Fracture	Medium	Medium	Catastrophic	Catastrophic	Catastrophic	Catastrophic	Catastrophic	Medium
	Mechanical	Medium	Medium	Major	Major	Major	Major	Major	Medium
PMC	Fatigue	Minor	Minor	Medium	Medium	Medium	Medium	Medium	Minor
	Fracture	Medium	Medium	Catastrophic	Catastrophic	Catastrophic	Catastrophic	Catastrophic	Medium
	Mechanical	Medium	Medium	Major	Major	Major	Major	Major	Medium
Output Rotor	Fatigue	Minor	Minor	Medium	Medium	Medium	Medium	Medium	Minor
	Fracture	Medium	Medium	Catastrophic	Catastrophic	Catastrophic	Catastrophic	Catastrophic	Medium
	Mechanical	Medium	Medium	Major	Major	Major	Major	Major	Medium
Bearings	Fracture	Medium	Medium	Catastrophic	Catastrophic	Catastrophic	Catastrophic	Catastrophic	Medium
	Mechanical	Medium	Medium	Catastrophic	Catastrophic	Catastrophic	Catastrophic	Catastrophic	Medium
Housing	Fatigue	Minor	Minor	Minor	Minor	Minor	Minor	Minor	Minor
	Fracture	Medium	Medium	Medium	Medium	Medium	Medium	Medium	Medium

### Fault Tree Analysis

The next step in the FTA is to build the fault tree for the system from the above. The various failure modes of each of the level II and level III components from the FHA form the lower most level of the fault-tree. Thus from this setup the probability of failure of each of the sub-systems in Level I can be determined. The resulting fault-tree for the P-CVT is presented below,



These failure rates were using in the FTA that was performed using ITEM. The net overall system failure rate for the P-CVT as well as the failure rate of each sub-system was determined. These results are summarized in Table 10.

**Table 10:** FTA/RBD analysis summary of results.

Subsystem	Critical Component	Failure Rate (per million hrs)
PVT	PMC/RCR/OR	1.506
Mechanical	Brakes	20.30
Controller	Component Failure	60.0
Electrical	Reaction Control Motor	59.96
Overall	Reaction Control Motor	140.35

From the above table it is clear that the controller and electrical systems are the most susceptible to failure. Hence the overall reliability of the P-CVT may be improved by adding redundancy in these sub-systems. This completes the FTA.

### **Reliability Block Diagrams**

Reliability block diagrams (RBDs) are similar to fault trees but differ in that the RBDs are used to calculate the probability of success where as fault trees are used to calculate the probability of failure of the system. For the P-CVT, the fault trees that are described this document were converted to reliability block diagrams using ITEM software. OR gates are represented by reliability blocks in series whereas AND gates are represented as reliability blocks in parallel. Typical arrangements derived from the fault-tree in the previous section are presented below.

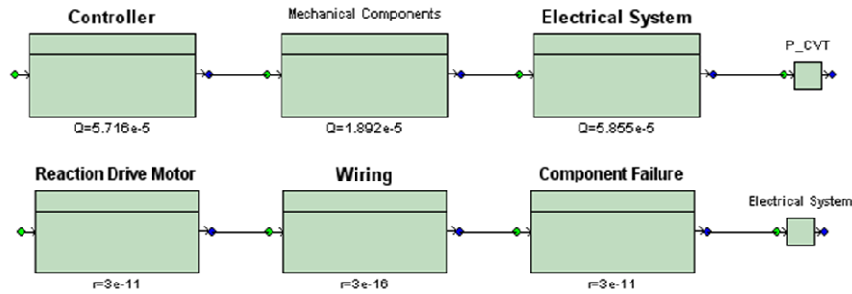


**Figure 28:** Typical RBDs derived from the Fault-tree, level I (above) Electrical system (below).

Using these two arrangements the fault trees at each sub-system level were converted into reliability diagrams and ITEM software was used to link the failure rate values of the components in the FTA to the RBD so the reliability of the P-CVT can be calculated. It was found that the probability of success or that the reliability in the RBD and FTA analysis summaries of the P-CVT is given as .99986.

### Stochastic Petri Net analysis

For the Stochastic Petri Net (SPN) analysis, the aircraft system component failures were grouped into the following three categories based on their level of risk:

- Minor
- Major
- Hazardous

The levels of risk used for this categorization were from the worst-case operational stage, given in Table 8. For system level components called out in the FTA, but not subcomponents of the P-CVT, the failure rates were obtained from the FTA. The failure rates for the components in each group were then summed to arrive at a total failure rate for the group. Table 11 summarizes the components in each group, as well as the total failure rate calculation. With these group failure rates defined, two separate analyses were

done to establish the probability of system availability and the probability of mission success via a Monte Carlo simulation.

**Table 11:** SPN Component Groups & Failure Rates.

<b>Minor</b>		<b>Major</b>		<b>Hazardous</b>	
<b>Component</b>	<b>Rate</b>	<b>Component</b>	<b>Rate</b>	<b>Component</b>	<b>Rate</b>
Loss of Power (Controller)	3.00 E -5	Housing	3.00 E -6	Bearings	3.00 E -7
Wiring Fault (Controller)	7.00 E -8	Brake	1.50 E -5	Output Rotor	5.00 E -8
Electronic Component (Controller)	3.00 E -5	Clutch	5.00 E -7	PCM	5.00 E -7
Electrical Component (Electrical System)	3.00 E -5			Reaction Control Rotor	5.00 E -7
Wiring (Electrical System)	3.00 E -10			Output Shaft	3.00 E -9
Reaction Drive Motor (Electrical System)	3.00 E -5			Input Shaft	3.00 E -9
<b>TOTAL</b>	<b>1.20 E -4</b>		<b>1.85 E -5</b>		<b>1.36 E -6</b>

### Availability

The analysis of system availability was constructed on the basic premise of failure and repair cycles. Each of the three component groupings comprises a state in the model,

along with an operational state. The failure gates were given exponential distributions with parameter  $\lambda$  given by their respective failure rates. The repair gates were given a fixed-time distribution. Table 12 summarizes the distributions used in the availability analysis.

**Table 12:** Availability SPN Distributions.

Description	Distribution
Operational to Minor	$\sim\text{Exp}(1.20\text{E-}4)$
Operational to Major	$\sim\text{Exp}(1.85\text{E-}5)$
Operational to Hazardous	$\sim\text{Exp}(1.36\text{E-}6)$
Minor to Operational	Fixed(40)
Major to Operational	Fixed(40)
Hazardous to Operational	Fixed(40)

A Monte Carlo simulation was run on the availability model, and the results are presented in Figure 29. This analysis shows that the projected aircraft system incorporating a P-CVT will have approximately a 98% probability of being available at any given time.

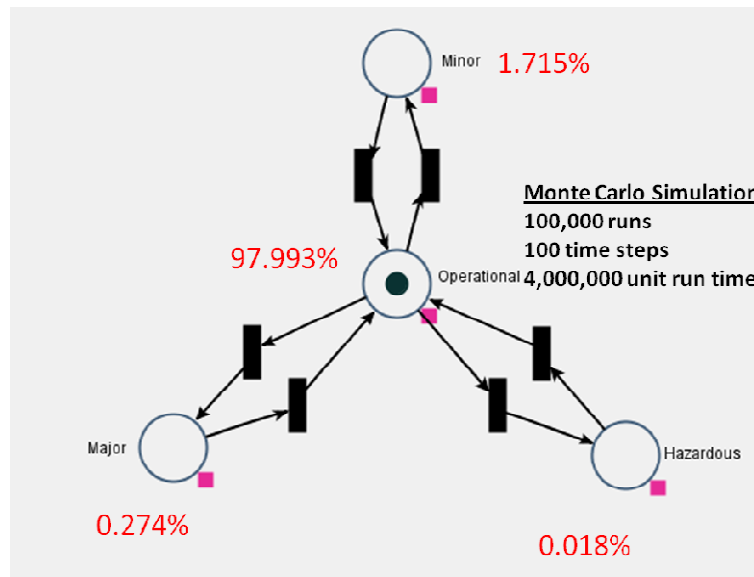


**Figure 29:** Availability SPN.

## Mission Success

The analysis of mission success was constructed on the basic premise of failure types and their effect on system functionality (i.e. mission success). Each of the three component groupings comprises a transition gate in the model, along with a no failure gate. The three states in this model are defined as follows:

- Mission Success (No Failure or Minor Failure)
- Mission Success with Delays (Major Failure)
- Mission Failure (Hazardous Failure)

The failure gates were given exponential distributions with parameter  $\lambda$  given by their respective failure rates. The no failure gate was given a fixed-time distribution. 13 summarizes the distributions used in the mission success analysis.

**Table 13:** Mission Success SPN distributions.

Description	Distribution
Mission Failure	~Exp(1.36E-6)
Success w/ Delays	~Exp(1.85E-5)
Success (minor failure)	~Exp(1.20E-4)
Success (no failure)	Fixed(20)

A Monte Carlo simulation was run on the mission success model, and the results are presented in Figure 30. This analysis shows that the projected aircraft system incorporating a P-CVT will have approximately a 99% probability of mission success.

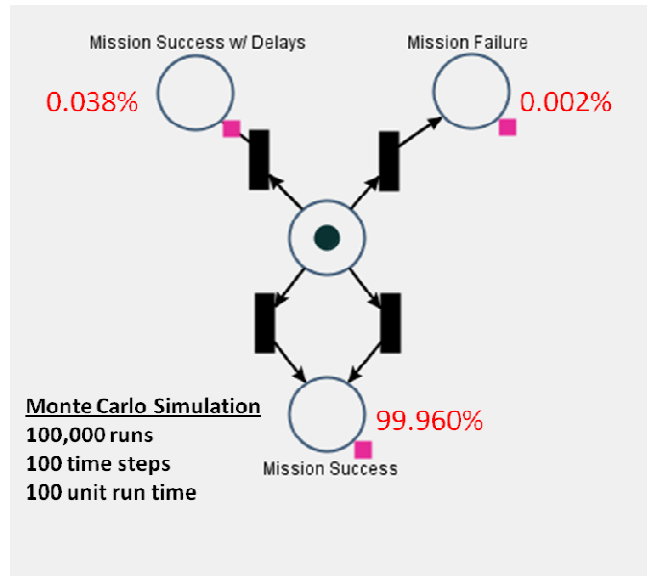


**Figure 30:** Mission Success SPN.

### **Certification Basis and Schedule**

Certification is a process that is used to qualify aircraft and rotorcraft for airworthiness. Airworthiness is achieved when the vehicle has been verified to meet safety criteria prescribed in the Federal Aviation Regulations (FARs) by the Federal Aviation Administration (FAA). If the air vehicle is being designed for military applications, then the Military Handbooks (MILs) published by the Department of Defense (DoD) are to be used in the qualification process. In all cases, the Federal or the Military Authority typically oversees the design, production, and qualification tests as well as computer tools to make sure that the means used to meet their criteria is valid.

Currently, next generation air vehicles will have multiple roles and functions in the civil, commercial and military sector. As a result, an aircraft or a rotorcraft might have to obtain certification as a safe vehicle by meeting the criteria in the MIL and FAR documents. It is therefore important to look at what is outlined in these regulations in order to meet safe flight criteria for the pericyclic continuously variable transmission (P-CVT) for a single main rotor heavy lift helicopter.

The P-CVT in its most basic form has been discussed in previous the sections of this report. It is necessary in terms of airworthiness that the P-CVT and its complimentary components meet safety standards set for the system as whole.

In order to address the certification basis of the P-CVT, two documents were reviewed by the team; FAR – Part 29 [24] and MIL – 516B [22]. Most importantly, parts of these documents that are of value to the P-CVT as a system are as follows:

**Table 14:** Parts of FAR 29 that are applicable to the P-CVT.

FAR Part	Description
29.63	Takeoff: Category B
29.64	Climb
29.75	Landing
29.141	Rotorcraft Flight Characteristics
29.395	Control Systems
29.571	Fatgue Evaluation of Structure
29.671	Control Systems: General
29.1027	Transmission and Gearboxes
29.1343	Electrical equipment and Installations
29.1351	Electrical Systems
29.1355	Distribution Systems

**Table 15:** Parts of MIL-516B that are applicable to the P-CVT.

MIL-516 Part	Description
7.3.2.5	Transmission/Gearbox Lubrication Systems
7.3.2.6	Dynamic Coupling of Aircraft Components
9.7	Crash Survivability
12	Electrical Systems
12.2	Electrical Wiring System
15.3.1	Electronics

To summarize these parts the following statements are true about the certification basis of the JHL. The rotorcraft must be crashworthy and in the event of a crash, the disintegration of the transmission will not harm the occupants as well as severely limit the space that the crew occupies. In the event of power loss due to engine malfunction or other environmental factors such as static electricity build up or lightening, the power generator and the battery must be able to sufficiently supply power to the P-CVT in order to avoid a catastrophic loss of vehicle (LOV). The integration of electrical components with the P-CVT and the resulting system must safely operate for all flight conditions and avoid failure modes that will result in LOV. In the event of a failure, the integrated electrical system and the P-CVT must revert to a fail-safe state in order to enable the pilot and the crew to safely recover the vehicle in autorotation.

The wiring for the electrical system that is integrated into the P-CVT must be appropriate for the environment that it will be operating in all flight conditions and once again must meet fail-safe criteria. Redundancy of the electrical system must also be designed into the transmission in order to compensate for the loss of one or more of the electrical components so that the P-CVT can function in its nominal state.

In the above discussion, the flight conditions that are covered by both documents include Take-Off, Climb, Cruise, Hover, Landing and Descent. In addition, maintainability and safe-life criteria must be met by the P-CVT system in order for the rotorcraft to be reliable and available due to decreased inspection and repair intervals. It is also very important to closely work with the certification authority so that any other system, the integration of that system with the P-CVT, and the interface between the two systems meets fail-safe, safe-life and additional safety criteria that is realized in the

airworthiness qualification process that is not described in any of the FAR and MIL documents. With this prologue, the certification plan is presented next.

### **Certification plan**

Certification plan in general tells FAA how an applicant intends to demonstrate the compliance of the design to the Federal Aviation Regulations (FAR's). The plan should assist the applicant in substantiating the design and assist FAA in expediting its approval. Preparation of the certification plan should begin as soon as the basic design has been determined in order to realize benefits from up-front consideration of the FAR's. The certification plan should be submitted to the FAA as soon as possible after the design concept is firm. Certification plan should consist of the following items:

1. Description: Brief description. Should be submitted separately if detailed.
2. FAR's: The applicable regulations need to be listed, by sections and sub-sections
3. Compliance: Show how the compliance will be proved by indicating laboratory testing, flight testing, analysis, similarity, etc
4. Conformity: Indicate what parts and installation conformity will be required.
5. Data: List the data to be submitted to show compliance.
6. Proposed DER's: The project ACO must determine the appropriateness of each DER for each project
7. System Criticality: The results of the preliminary function hazard analysis need to be made known.

8. Schedule            Provide a schedule which shows the following significant milestones:
- i. Identify when a preliminary hazard analysis will be submitted and when all detailed data submittals will be made
  - ii. When (and where) the tests requiring an FAA will be run
  - iii. When conformity inspection (parts, systems and installations) requests will be submitted
  - iv. When final certification is required

### **Compliance**

Keeping these regulations in mind, in order to certify a helicopter, one should look for the FAR 25 and 29. In general 27 is given for the normal category rotorcraft. The primary intention of single main rotor heavy lift helicopters with P-CVT type transmission is to use them for transportation. In this sense, particularly for this project the focus has been spent for the FAR Part 29 (FAA Airworthiness Standards: Transport Category Rotorcraft) and MIL-516B (DoD Airworthiness Certification Criteria). The compliance can be achieved by performing the standard tests given in the FAR's, These tests can be listed as

FAR 29.681    Limit load static test

FAR 29.683    Operation tests

FAR 29.723    Shock Absorption tests

FAR 29.725    Limit Drop Test

FAR 29.727 Reserve Energy Absorption Drop Test

FAR 29.727A Reserve Energy Absorption Drop Test

FAR 29.923 Rotor Drive System and Control Mechanism Tests

FAR 29.965 Fuel Tank Tests

FAR 29.1015 Oil Tank Tests

FAR 29.1043 Cooling Tests

FAR 29.1363 Electrical Systems Tests

### **Compliance specific to a single main rotor heavy helicopter with P-CVT**

However, it should be noted that in addition to the standard parts in a helicopter, now there are additional parts due to the P-CVT. These components can be summarized as:

#### Mechanical Components

- Input/Output/Rotor Shafts, Pericyclic Motion Converter (PMC), Reaction Control Rotor (RCR), Bearings, Housing , Lubrication Systems.
- Need to check for fatigue, fracture, crash survivability.

#### Electrical Components:

- Wires, Circuitry, Power Supply.
- Need to check for temperature, electric loading, electromagnetic fields.

Control Components:

- Software, CPU
- Similar to the electrical components, they need to be checked for temperature, electric loading, electromagnetic fields.

Given the fact that a helicopter is already certified, one should still check for special items on the FAR's related with the lubrication, transmission etc. These tests and standards can be summarized as follows:

Regulation	Description
FAR Part 21	Certification procedures for products and parts
FAR Part 29	Airworthiness Standards: Transport Category Rotorcraft  Subpart E - Powerplant  29.923 – Rotor drive system and control mechanism test  29.1027 – Transmission and gearboxes: general  Subpart F – Equipment  29.1337 – Power plant Instruments  29.1351 – General  29.1353 – Electrical equipment and installations  29.1363 – Electrical System tests  29.1435 – Hydraulic Systems

The Powerplant, subpart-E on the FAR Part 29 has to be handled very carefully for the certification of a helicopter with P-CVT . The standard tests for the Powerplant listed on the FAR Part 29 are given below:

*(a) Endurance tests, general*

*(b) Endurance tests; takeoff run.*

- (c) *Endurance tests; maximum continuous run*
- (d) *Endurance tests; 90 percent of maximum continuous run.*
- (e) *Endurance tests; 80 percent of maximum continuous run.*
- (f) *Endurance tests; 60 percent of maximum continuous run.*
- (g) *Endurance tests; engine malfunctioning run.*
- (h) *Endurance tests; overspeed run.*
- (i) *Endurance tests; rotor control positions.*
- (j) Endurance tests, clutch and brake engagements
- (k) *Endurance tests; OEI power run*
- (l) Special tests.
- (m) Endurance tests; operating lubricants

Here on this list, specifically (j) *Endurance tests, clutch and brake engagements*, (l) *Special tests* and (m) *Endurance tests; operating lubricants* are of relevance for the P-CVT. Since the new transmission system has additional number of clutches and brakes, the tests related with their endurance should be applied to them as well. Proper lubrication of the new parts are also important, and they should meet the criterion as given in the FAR's. The lubrication standards are given in 29.923– Rotor drive system and control mechanism test in a better way. The 29.923 from the FAR 29 reads:

- (a) The oil system for components of the rotor drive system that require continuous lubrication must be sufficiently independent of the lubrication systems of the engine(s)

(b) Pressure lubrication systems for transmissions and gearboxes must comply with the requirements of 29.1013, paragraphs (c), (d), and (f) only, 29.1015, 29.1017, 29.1021, 29.1023, and 29.1337

(c) Splash type lubrication systems for rotor drive system gearboxes must comply with 29.1021 and 29.1337(d).

Similarly, 29.1337 Power plant Instruments is also relevant to the P-CVT. The important sub-sections of the FAR 29.1337 are:

(a) *Instruments and instrument lines*

(b) *Fuel quantity indicator*

(c) *Fuel flowmeter system*

(d) *Oil quantity indicator*

(e) Rotor drive system transmissions and gearboxes utilizing ferromagnetic materials must be equipped with chip detectors designed to indicate the presence of ferromagnetic particles resulting from damage or excessive wear within the transmission or gearbox

Here, item (e) is relevant for the P-CVT certification. Finally for 29.1351:

29.1351– General

(a) *Electrical system capacity*

(b) *Generating system*

(c) *External power*

Apart from the FAR 29, the MIL-516 should also be checked for the certification and compliance purposes:

<b>MIL-516 Part</b>	<b>Description</b>
7.3.2.5	Transmission/Gearbox Lubrication Systems
7.3.2.6	Dynamic Coupling of Aircraft Components
9.7	Crash Survivability
12	Electrical Systems
12.2	Electrical Wiring System
15.3.1	Electronics

The tests and standards used for certification of transport type rotorcraft were outlined on the previous sections.

### **Recommendations**

It should be noted that the use of P-CVT for a helicopter is not a standard issue, and in addition to the aforementioned tests, some additional tests should also be made. This report does not aim to establish a complete certification procedure for the helicopters using a P-CVT, but it rather tends to give the big picture to show what is important. In this sense, there are a couple of suggestions which may be used for certification process.

The first suggestion is related with the transmission control section. The Control unit's sub-section of the FAR 29 lists the following items:

29.1141 Powerplant control

29.1142 Auxiliary power unit controls

29.1143 Engine controls

It is our understanding that an additional item should be added to this list, which is related with the Transmission control (29.XXX Transmission control). Also, 29.923 (a) reads:

*Any additional dynamic, endurance, and operational tests, and vibratory investigations necessary to determine that the rotor drive mechanism is safe, must be performed.*

For a P-CVT based JHL helicopter this definition needs to be strengthened. The dynamic, endurance and operational tests should be clearly identified relevant to the P-CVT certification, maybe as a new sub-section.

### **Certification Schedule**

The FAA type certification process needs to cover the following items:

1. Familiarization
2. Formal Application
3. Preliminary certification board
4. Certification program plan
5. Technical meetings

6. Pre-flight type certification
7. Type inspection authorization
8. Conformity inspections and certification flight tests
9. Aircraft evaluation group determinations
10. Final type certification board
11. Type certificate
12. Post certification activities

The schedule for this process is given as the following:

Year	1				2				3			
Month	1	2	3	4	1	2	3	4	1	2	3	4
Familiarization	█											
Formal Application	█	█										
Preliminary type certification Board	█											
Certification Program Plan	█											
Technical meetings	█	█	█	█	█	█	█	█	█	█	█	█
Pre-flight type certification board		█	█	█	█	█	█					
Type inspection authorization				█								
Conformity inspections and certification flight tests					█	█	█	█	█	█	█	
Aircraft evaluation group determinations				█								
Final type certification board									█	█	█	█
Type certificate											█	
Post certification activities												█

## 6.4 Static Finite Element Analysis

The goal of this project is to develop a static finite element model for a nontraction pericyclic continuously variable transmission (P-CVT) that has an application in rotorcraft drivetrain design. The finite element model will be created using ANSYS. The drivetrain is composed of shafts, gears, and tapered roller bearings. The model creation will involve the use of 3-D finite elements such as solid cylinders and contact elements to model the gears. The development of the finite element model will predict the stress and displacement distribution of the drivetrain under study. The finite element analysis helps in determining if the designed product meets its functional requirements. Displacement boundary conditions will be applied. The tapered roller bearing resists radial loading, axial loading, and resists moment in the radial direction. The finite element procedure will involve defining the elements, defining the material properties, creating the geometry, mesh the elements, and then apply the boundary conditions.

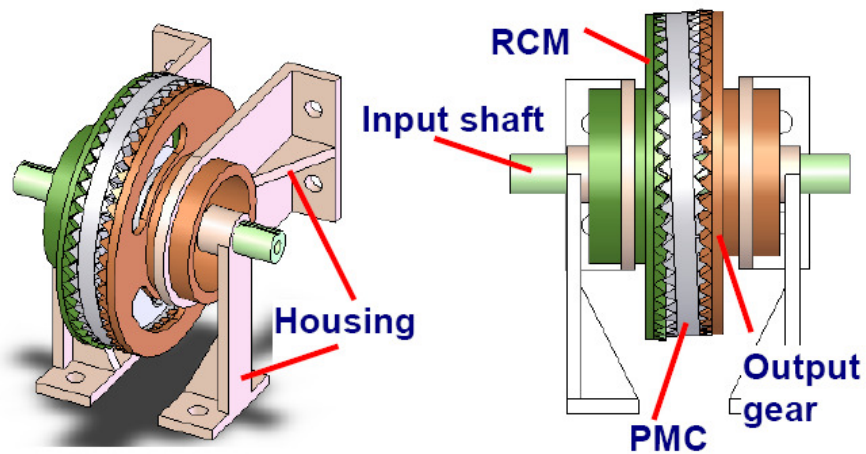
The Finite element process arises from complexity in geometry, loading and material properties. It requires a complicated domain and a mesh. The steps involved in the finite element process are obtaining a weak form of the governing differential equation which is a mathematical model of a physical process such as a solid mechanics, or heat conduction problem. The next step is to integrate by parts, and then impose boundary conditions. Next a solution of the form  $U$  equals a sum of the products of the nodal values of  $U$  and the interpolation functions is chosen. The weight function is arbitrary and is assumed to be equal to the interpolation function.  $U$  and  $W$  are substituted back into the differential equation to form algebraic expressions of the form,  $\underline{F}=\underline{K}\underline{X}$ . Next the

techniques of linear algebra such as Gaussian elimination can be used to determine the displacements.

## Model

### The Original Model

- The roller cam model (RCM)
- The roller is considered the PMC
- Figure 31 shows the PCVT assembly and the location of the bearings. The input shaft is mounted to the housing by cylindrical roller bearings. The PMC is mounted on the input shaft by cylindrical roller bearings and it's mounted to the housing by tapered roller bearings. The output rotor is mounted to the housing by cylindrical bearings.



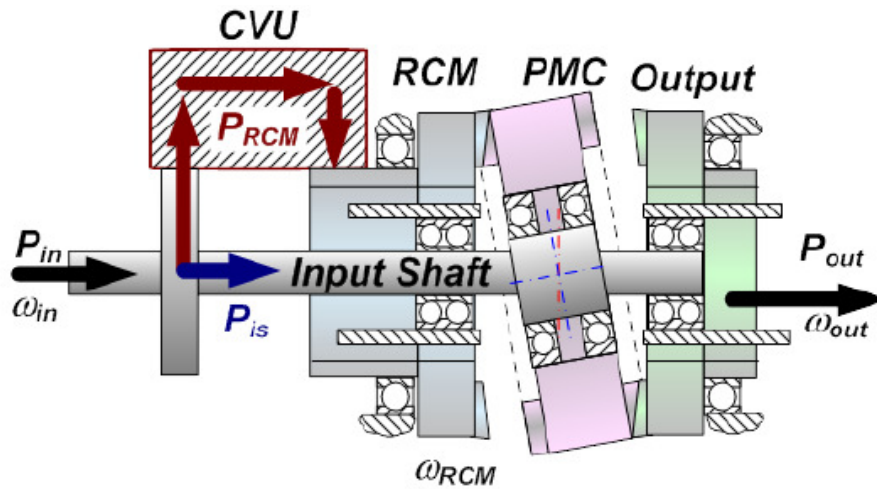


Figure 31: Cross Section View of the PCVT<sup>[20]</sup>.

## The Ansys Geometry Model

### 3D Geometry Model

The 3D geometry model was created by hollow cylinders for the shafts and gears. The shaft diameter is 11” and 36” length. The gear sizings are detailed in “material properties & physical dimensions” section.(Figure 32)

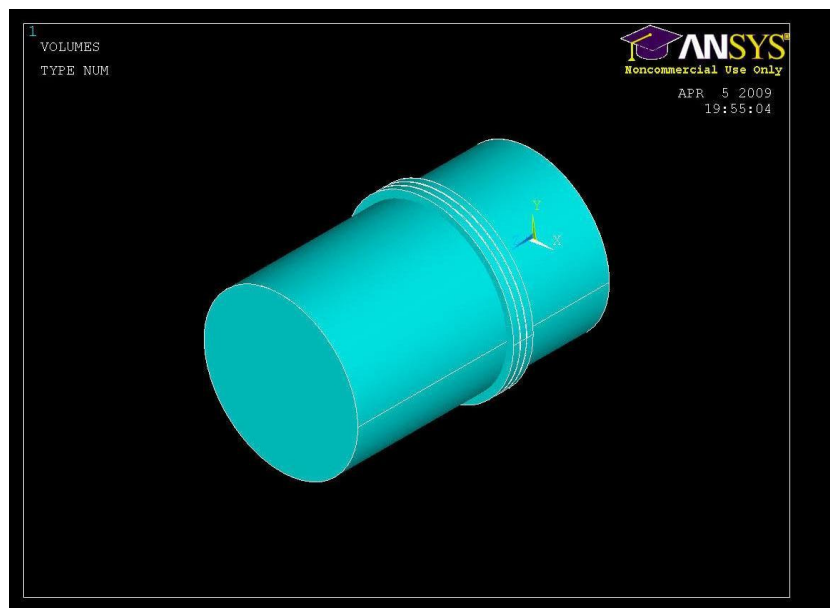
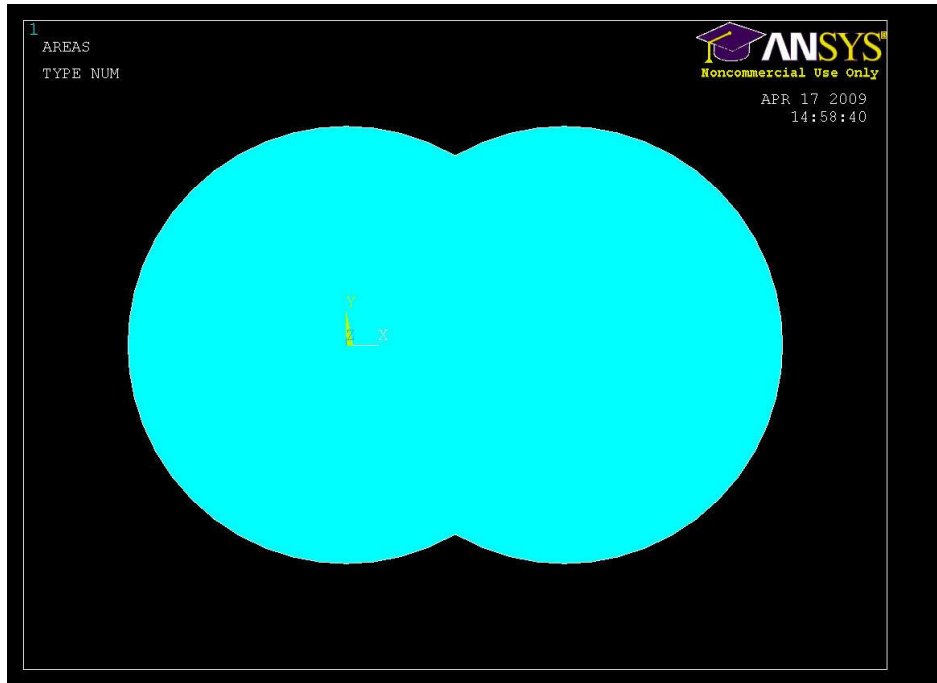


Figure 32: The 3D Geometry Model.

## The 2D Geometry Model

Two gears are modeled in 2 dimensions showing the meshing of the gears that are hinged at their center.(Figure 33)



**Figure 33:** The 2D Geometry Model.

# Material Properties & Physical Dimensions

## Material Properties

Material used is AISI 9310 Steel with modulus of elasticity of 27.6 Msi and Density of 0.273 lbs/in<sup>3</sup> and poisson's ratio of 0.27. (All dimensions are in engineering units)

## Reaction Control Rotor

N= Number of Teeth = 28

$D_{Inner} = 24$  in

$D_{Outer} = D_{Inner} + 2 / p$

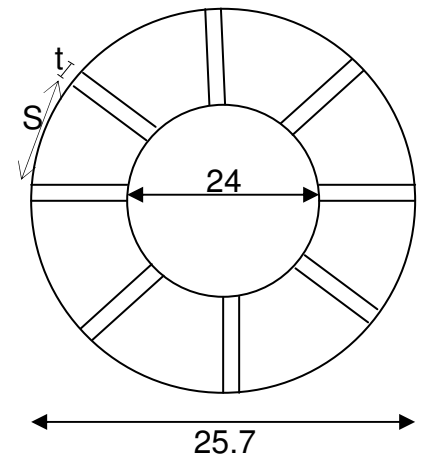
Where p is diameter pitch & is equal to:

$p = \text{Number of Teeth} / D_{Inner} = 28 / 24 = 1.1667$

So D outer will be:

$D_{Outer} = 24 + 2 / 1.1667 = 25.71$  in

H = Cylinder Height = 1 in



## Section View of Teeth:

F = Face Width

$H_t$  = Height of Teeth

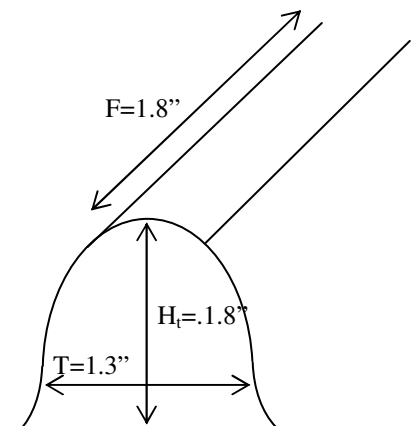
t = Thickness of teeth

$t = 1.5708 / 1.1667 = 1.346$  in

$H_t = 2.157 / 1.1667 = 1.849$  in

F = 1.8 in

Spacing between teeth: S = 1.345 inches



**PMC Reaction Control Side**

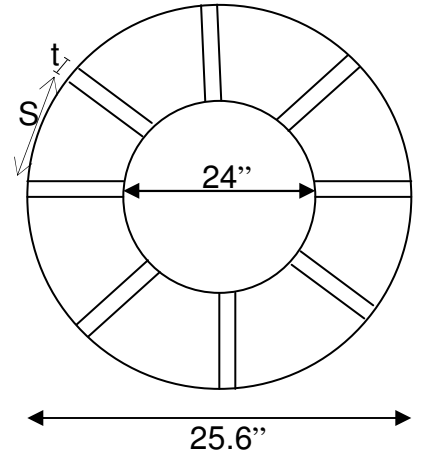
$$N_{PR} = 30$$

$$P = N/D = 30/24 = 1.125$$

$$H = 1 \text{ in}$$

$$D_{inner} = 24 \text{ in}$$

$$D_{outer} = 24 + 2/1.25 = 25.6 \text{ in}$$



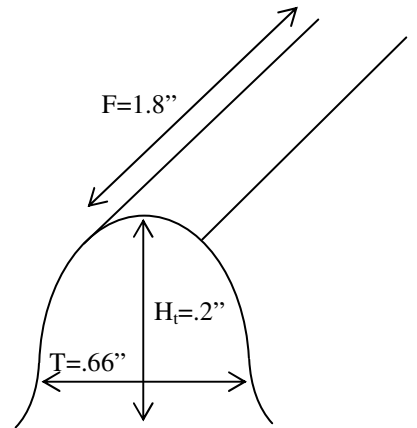
**Section View of Teeth:**

$$F = 1.8 \text{ in}$$

$$H_t = 0.208 \text{ in}$$

$$T = 0.6614 \text{ in}$$

$$S = \text{Spacing between teeth} = 0.6607 \text{ in}$$





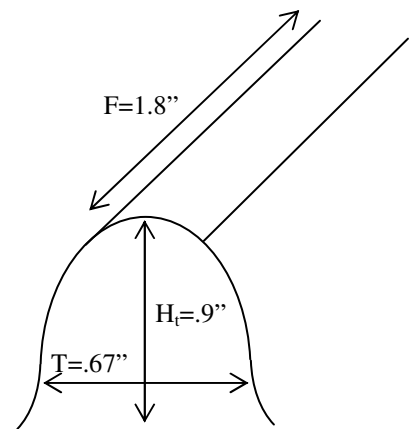
**Section View of Teeth**

T=.6733in

H=.9246in

F=1.8in

S=.6726in



# Boundary Conditions

## 3D

The boundary conditions are next applied to the model .There are two bearings at the two ends of the shaft which are simplified as two hinges at the end having zero displacements (figure 34)

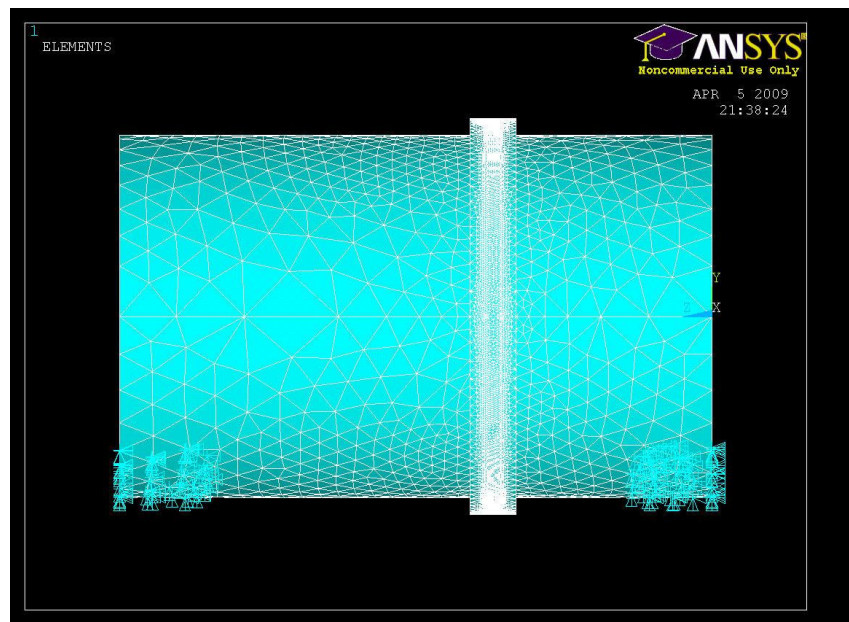


**Figure 34:** Zero Displacements are applied to the corners of the shaft.

Since the gears are rotating, torques need to be applied to the gears. Since ANSYS cannot model moments for boundary conditions, the torques are modeled as two couple forces of 10,000 lbs & -10,000 lbs acting on the top & bottom of each gear. (Figure 35)

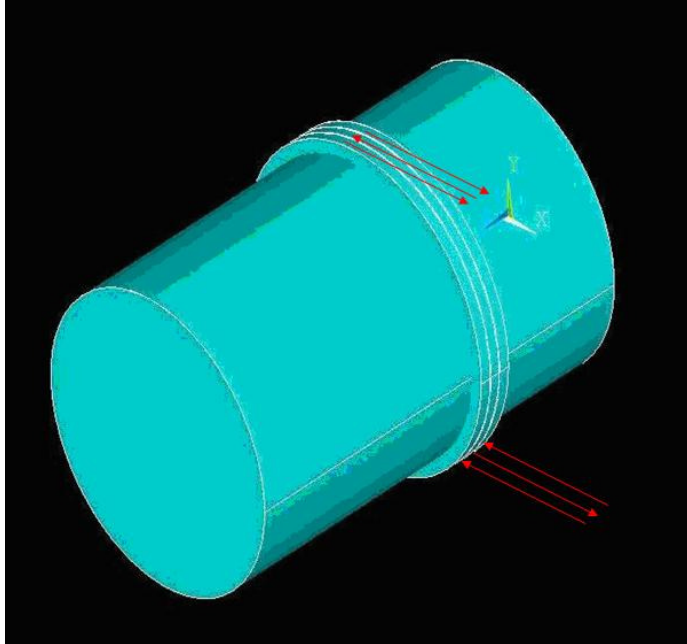


**Figure 35:** Couple forces are applied to each gear to act as torque.

## 2D

Since the gears are mounted to the shaft, zero displacements are applied on the center of the gears; also the coupled forces are applied to the top & bottom of the gears as they were in the 3D model. (Figure 36)

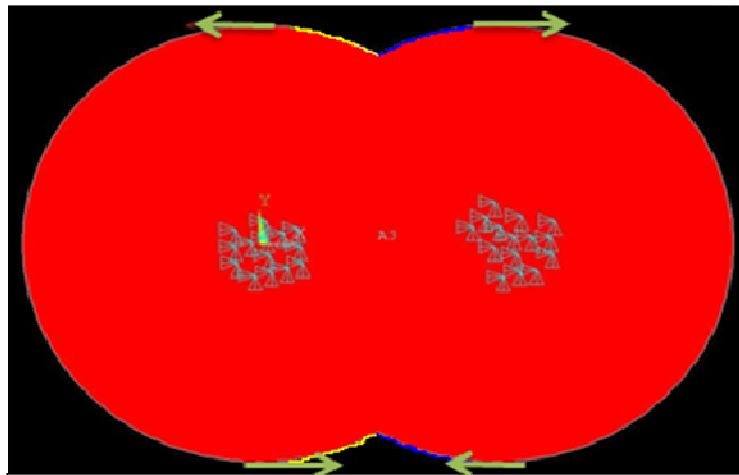


**Figure 36:** Applying force & displacement boundary conditions to the 2D model.

# Analysis & Model Convergence

## 3D

The type of model Convergence was h-convergence where we kept the order constant and increased the mesh density until there was a tolerance value of about 5% between the current and previous value of the stress. The 3-D model element type used was solid element 185. From ANSYS 11 SOLID 185 is described below. SOLID185 is used for 3-D modeling of solid structures. It is defined by eight nodes having three degrees of freedom at each node: translations in the nodal x, y, and z directions. The element has plasticity, hyperelasticity, stress stiffening, creep, large deflection, and large strain capabilities. It also has mixed formulation capability for simulating deformations of nearly incompressible elastoplastic materials, and fully incompressible hyperelastic materials.

SOLID185 is available in two forms:

- Structural Solid (KEYOPT(3) = 0, the default)
- Layered Solid (KEYOPT(3) = 1)

The assumptions are listed as follows:

- Assumed Static Analysis: Modeled in a static (steady state ) FE analysis
- Bearings [instead of using bearing supports we used simply supported joints
- Shaft was simply supported at both ends
- modeling teeth as surface contact elements
- chose zero alignment from the vertical: The real angle was 2.5 deg

- model face spur gears as solid cylinders
- The contact elements were created using GUI in ANSYS

The mesh was varied from a coarser mesh to a finer mesh until a 5% tolerance value was achieved between the previous and current stresses. (Figures 37 to 42)

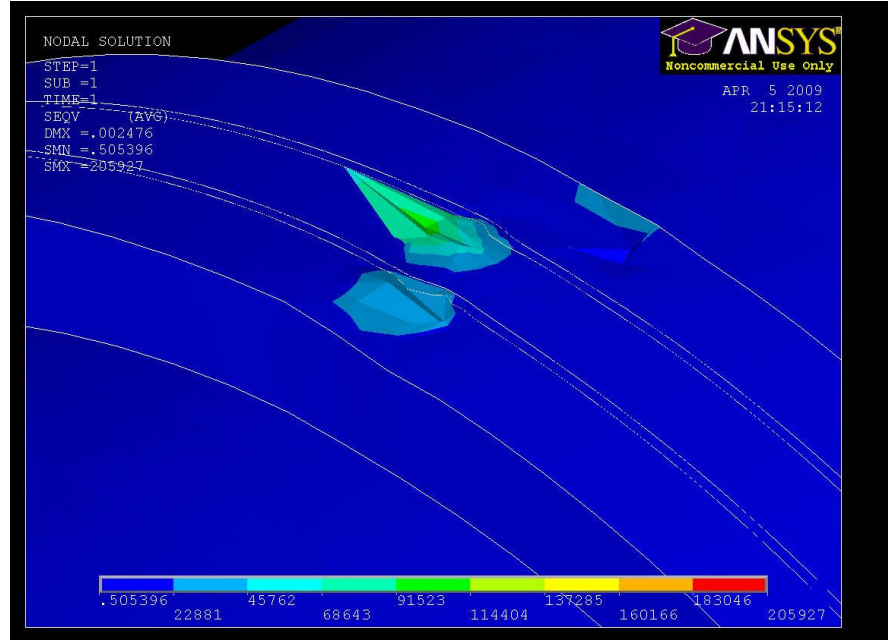


**Figure 37:** Mesh Density=6.

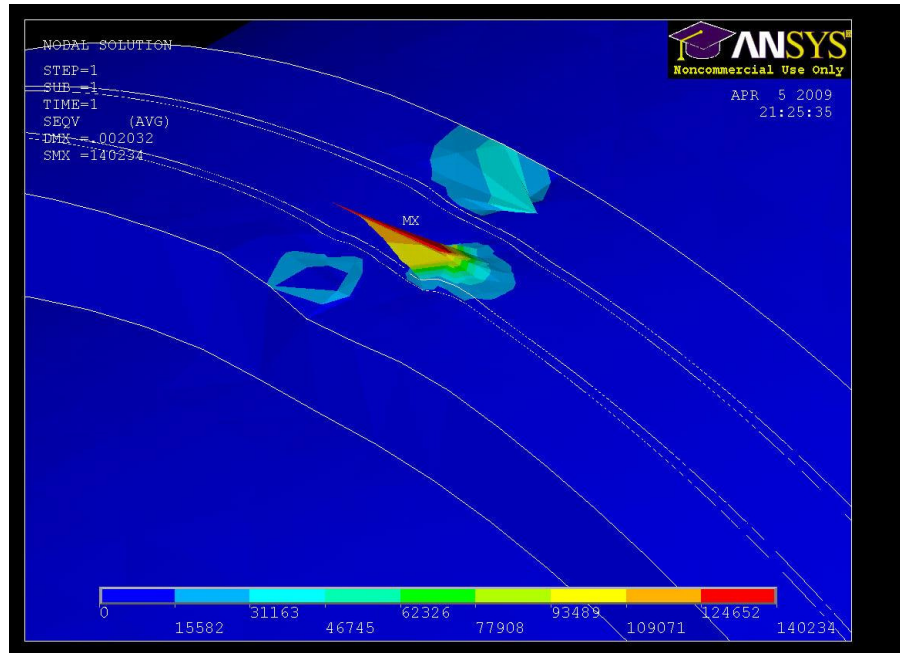


**Figure 38: Mesh Density=5.**

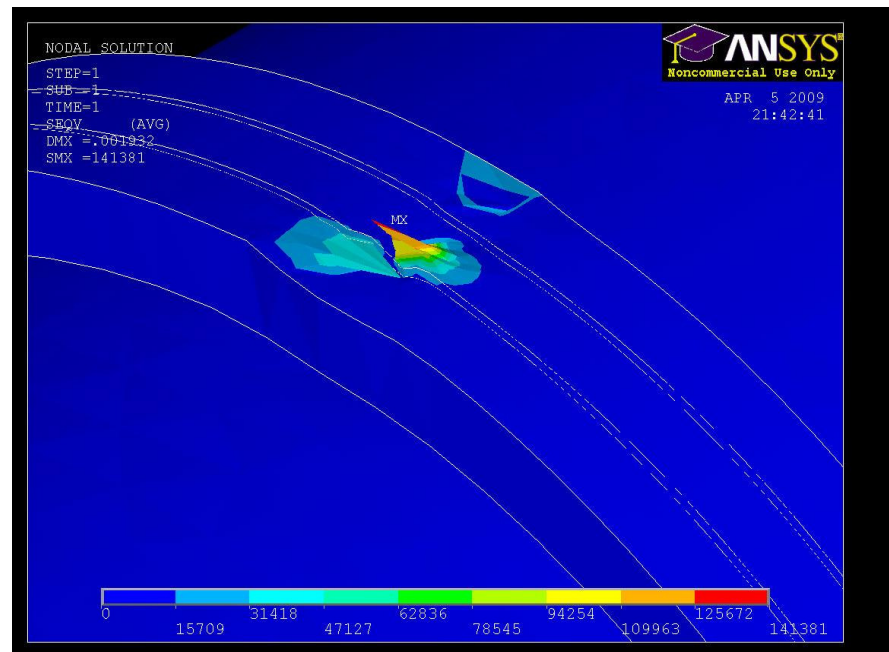


**Figure 39: Mesh Density=4.**

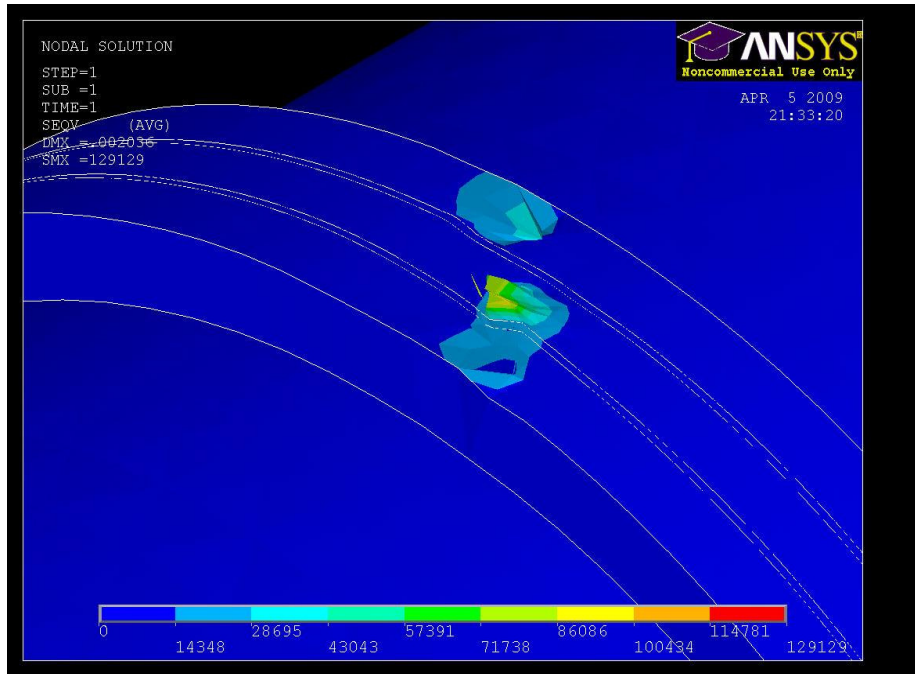


**Figure 40:** Mesh Density= 3.

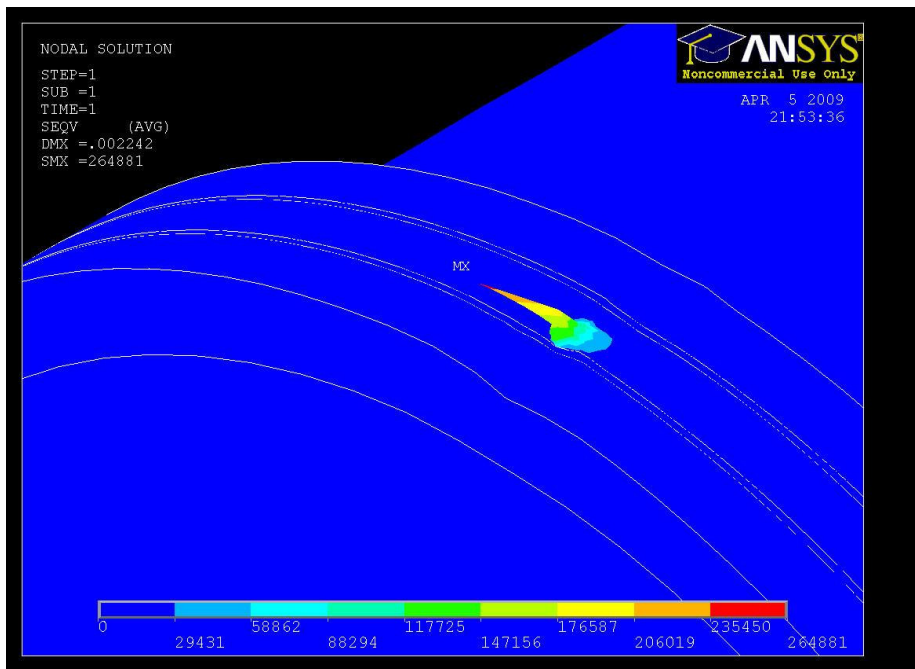


**Figure 41:** Mesh Density=2.

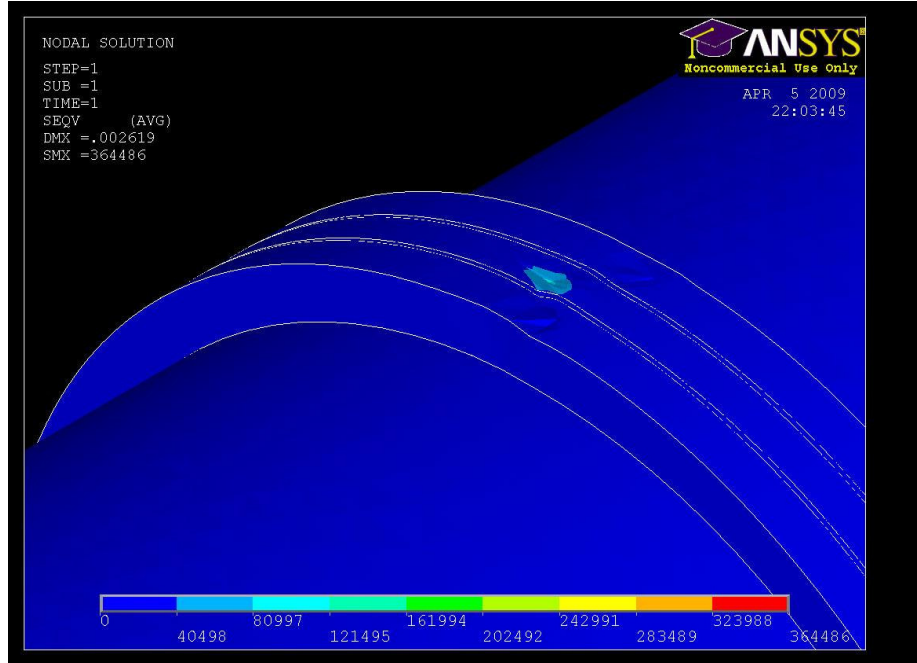


**Figure 42:** Mesh Density= 1 & .3.

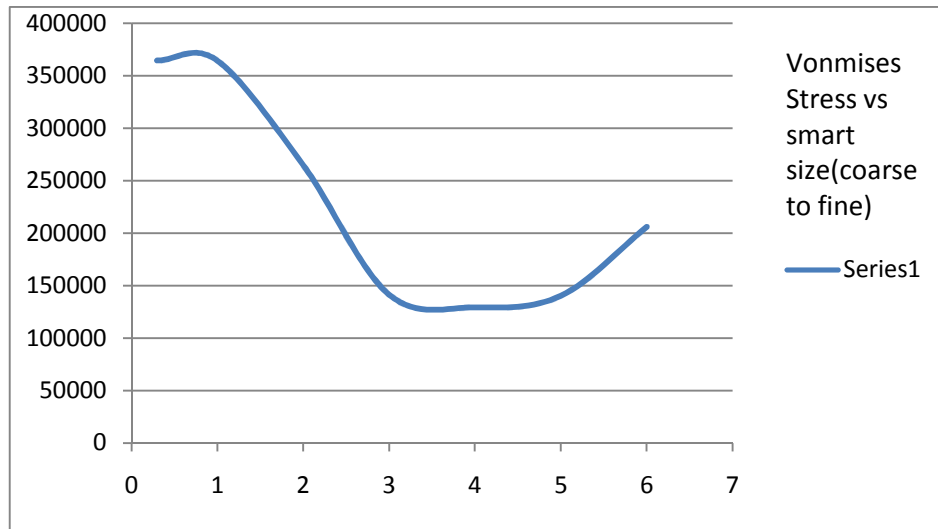


**Figure 43:** 3D Model Convergence.

**Table 16:** 3D Convergence Stress Values.

Smart size from ANSYS (Mesh Density)	Stress (psi)
0.3	364486
1	364486
2	264881
3	141381
4	129129
5	140234
6	205927

As it can be seen from the plot in Figure 44 the convergence stress value is 364486 psi

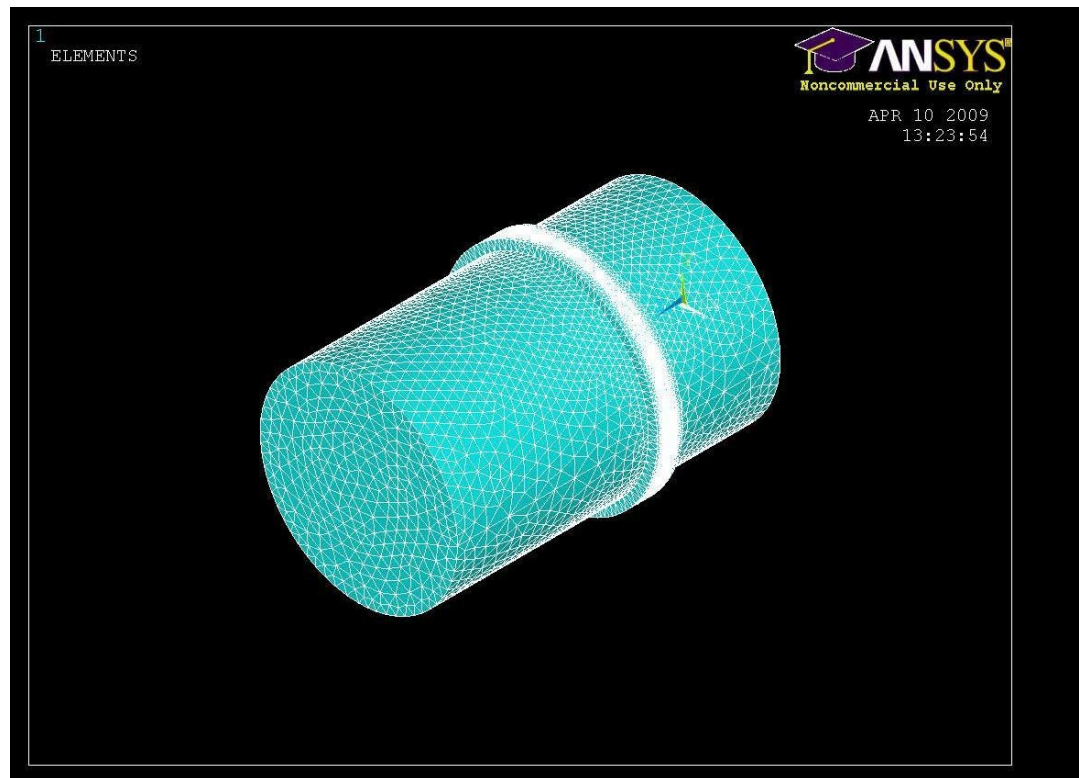


**Figure 44:** Mesh Model for the selected converged stress value.

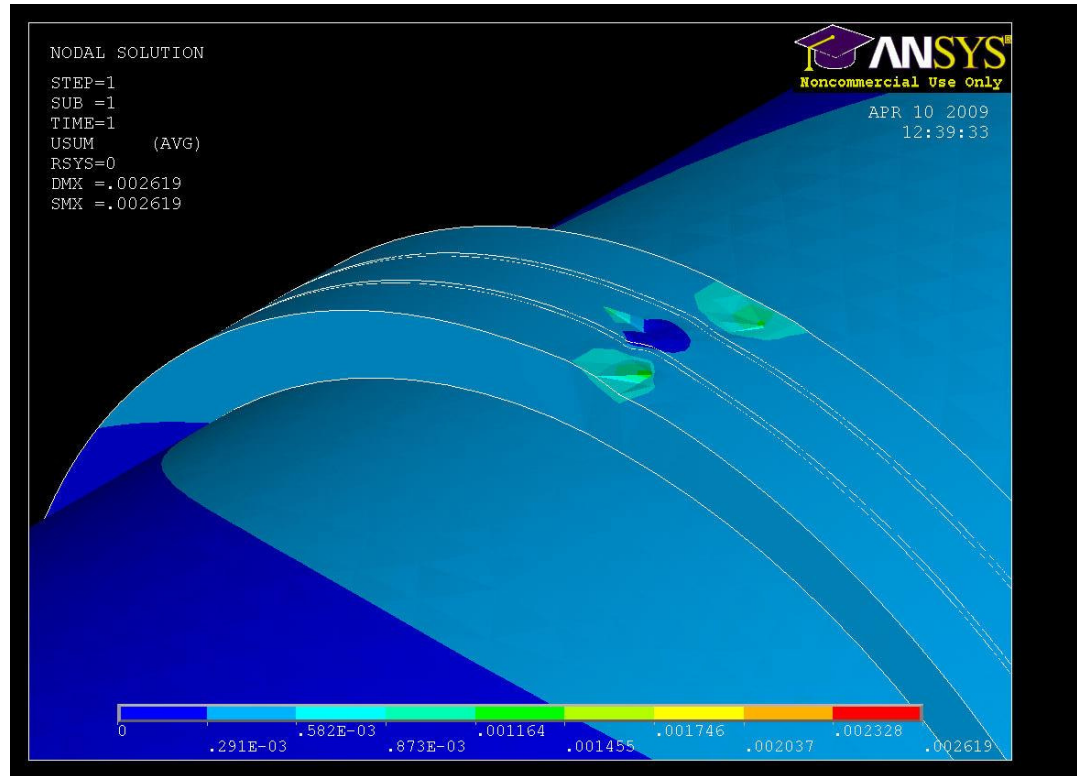


**Figure 45:** Displacement Plot.

## 2D

For the 2-D analysis, 8 node PLANE 183 element type was used and it's described below from ANSYS 11.0. PLANE183 Element Description

PLANE183 is a higher order 2-D, 8-node or 6-node element. PLANE183 has quadratic displacement behavior and is well suited to modeling irregular meshes (such as those produced by various CAD/CAM systems).

This element is defined by 8 nodes or 6-nodes having two degrees of freedom at each node: translations in the nodal x and y directions. The element may be used as a plane element (plane stress, plane strain and generalized plane strain) or as an axisymmetric

element. This element has plasticity, hyperelasticity, creep, stress stiffening, large deflection, and large strain capabilities. It also has mixed formulation capability for simulating deformations of nearly incompressible elastoplastic materials, and fully incompressible hyperelastic materials. Initial stress import is supported. Various printout options are also available.

The model convergence was started with a coarse mesh of smart size 6 and was later converged to a smart size of 1. (Figures 46 to 49)

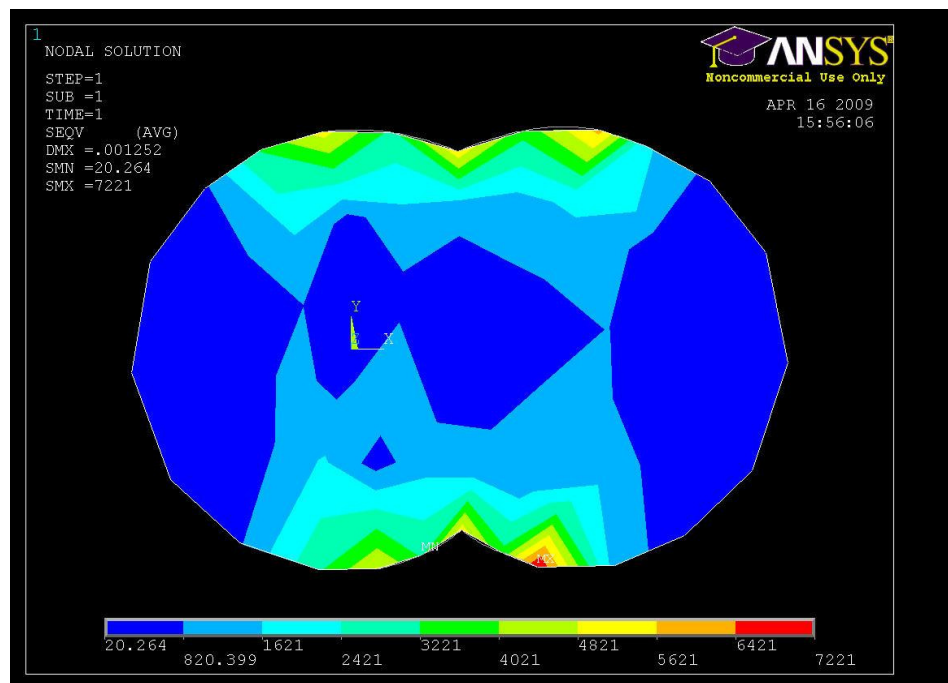


**Figure 46:** 2D Mesh density = 6.

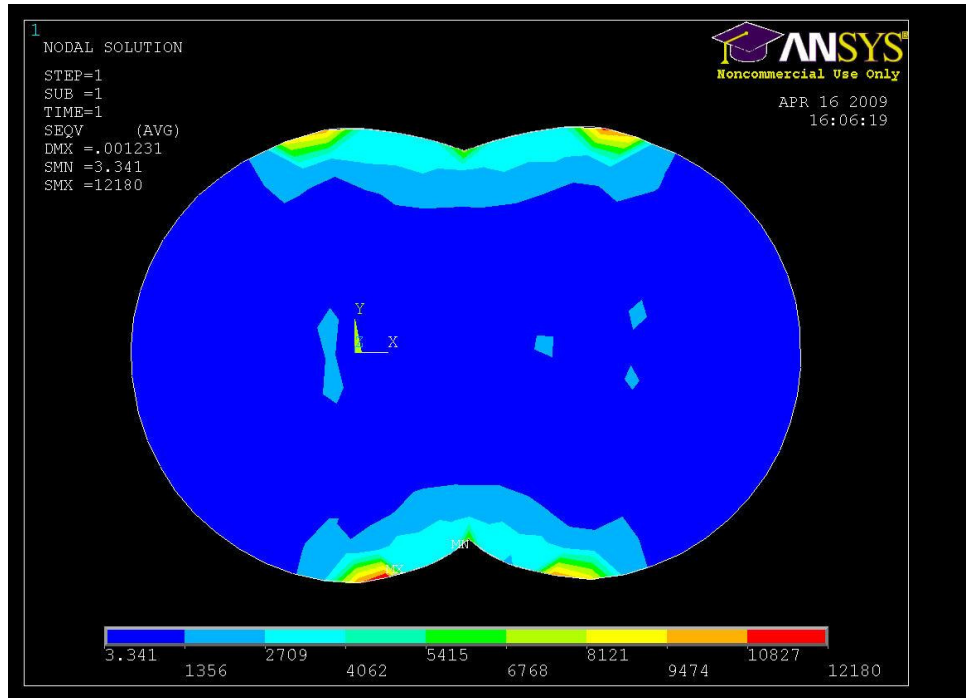


**Figure 47:** 2D Mesh density = 4.

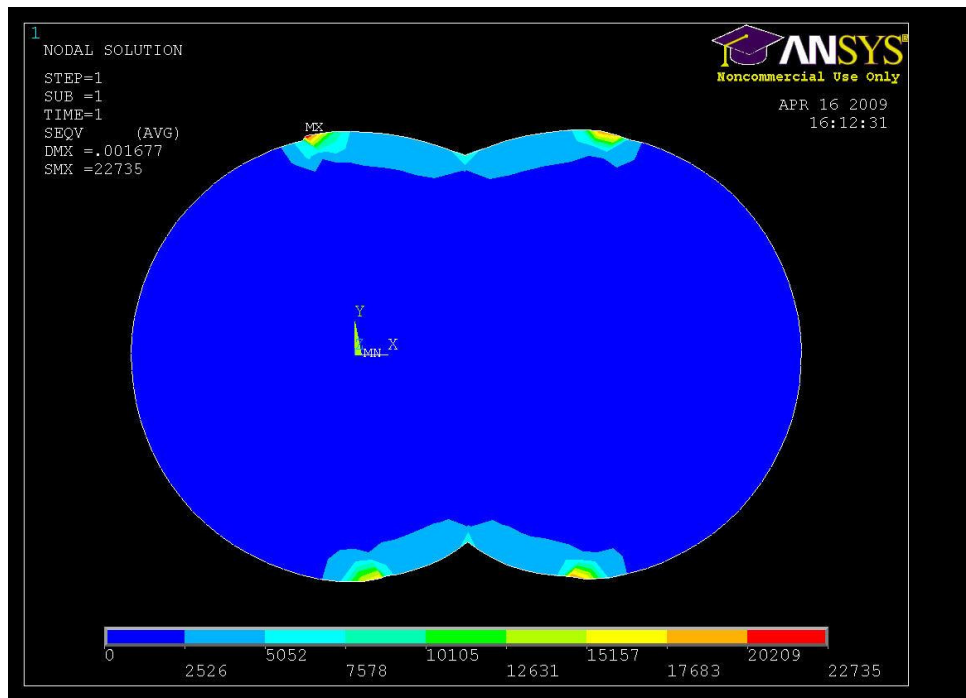


**Figure 48:** 2D Mesh density=2.

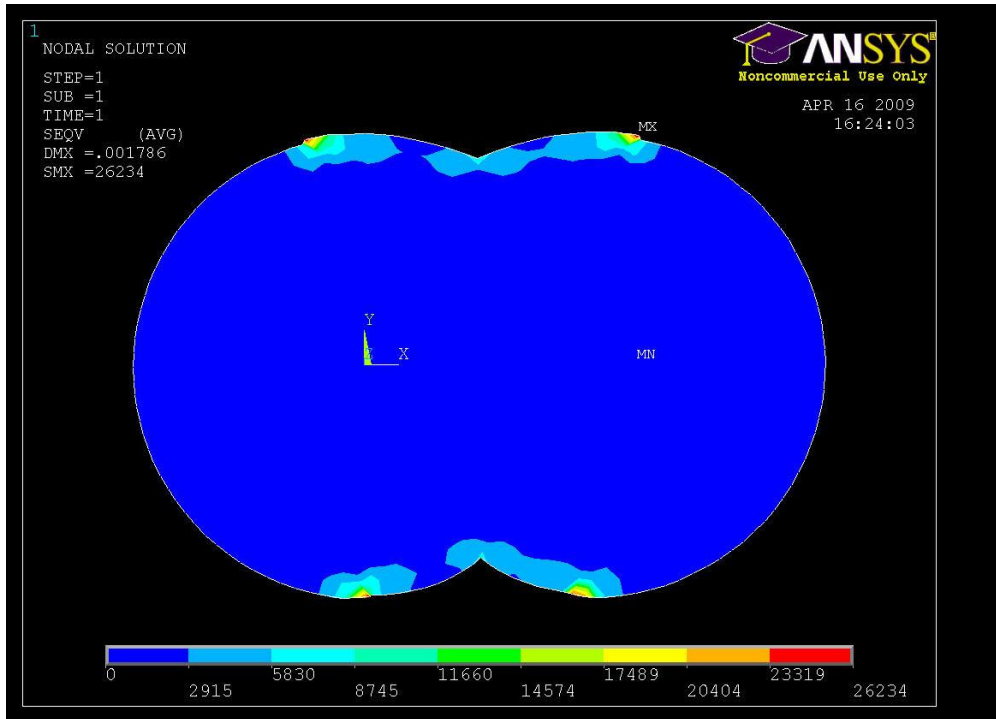


**Figure 49:** 2D Mesh density=1 & 0.3.

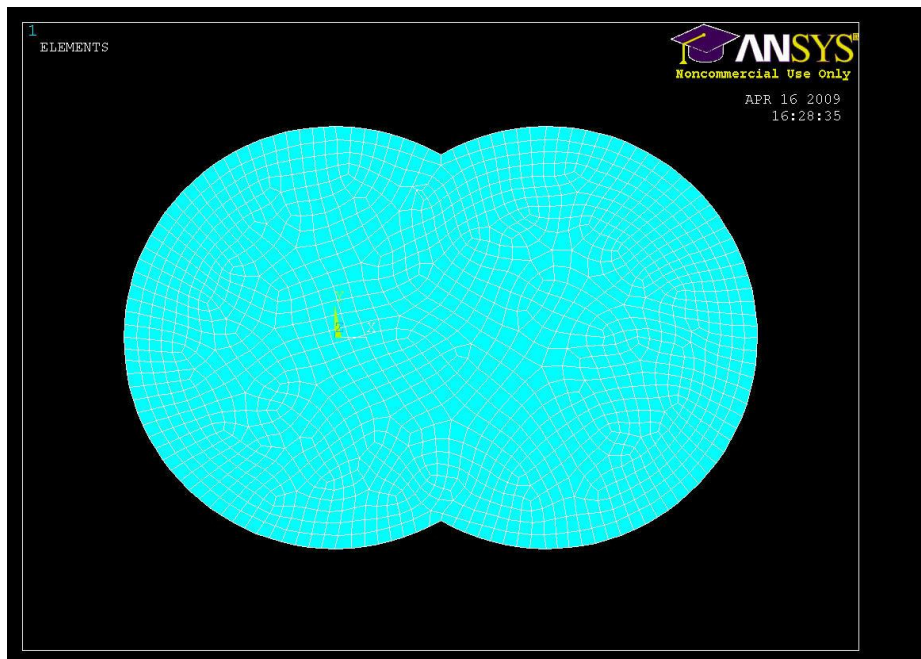


**Figure 50:** Mesh Model for the selected converged stress value.

The total displacement is shown in Figure 51. In the 2D model the total displacement is the vector summation of u & v displacement in x & y directions.

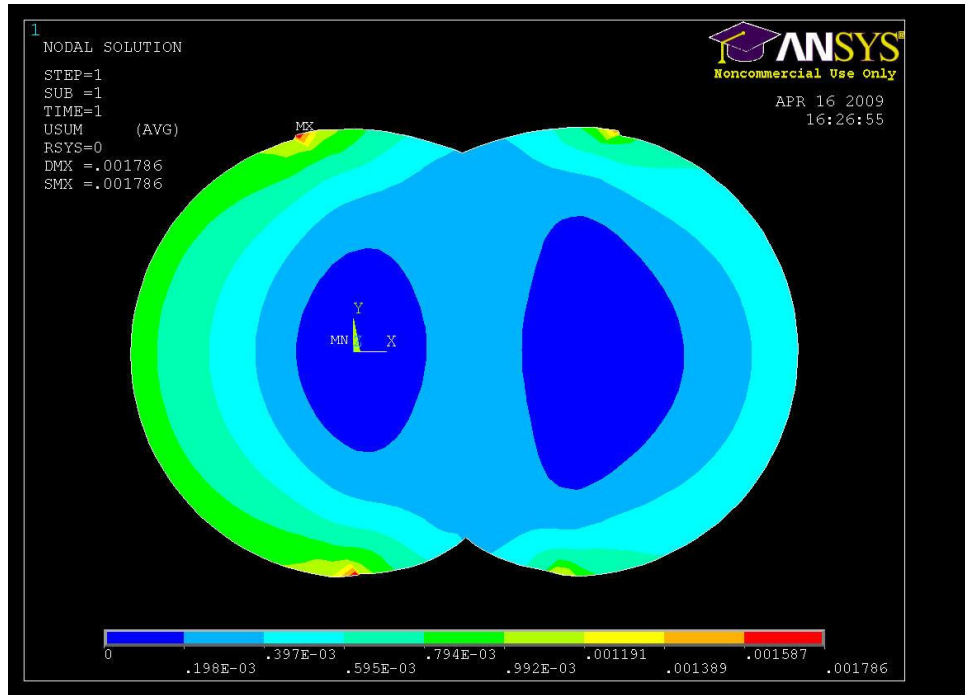


**Figure 51:** Displacement Plot.

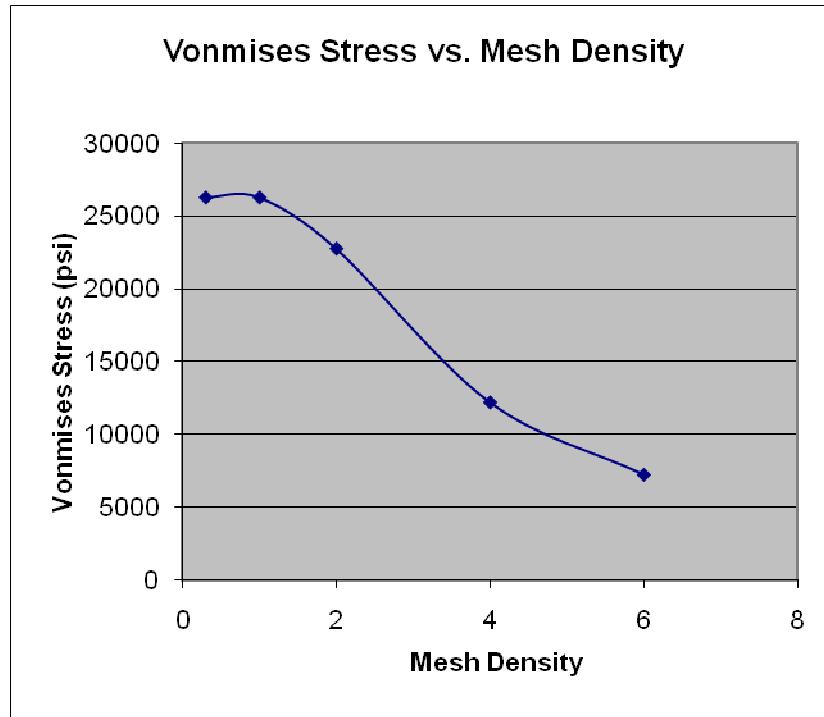


**Figure 52:** 2D Convergence plot.

**Table 17:** 2D Convergence Stress Values.

Smart Size	Vonmises Stress
6	7221
4	12180
2	22735
1	26234
0.3	26234

The validation and verification aspect of the static finite element analysis was performed.

The theoretical equation for the vonmises stress is given below.

**Tensile Stress**

**Face Gears**

$$\sigma_t = [63000 * P * K_o * N_{gear} * K_s * K_m * K_T * K_R * c/k] / [2 * w * R_{gear}^2 * K_v * F * J * K_L]$$

- P= power transmitted
- Ko = application factor
- Ngear = Number of teeth in gear
- ks = size factor
- km = load distribution factor
- KR= Reliability factor
- k = loadshare
- c = ratio of the tooth meshing
- w = RPM of gear
- Kv = Dynamic factor
- Rgear = pitch radius of gear
- F = Facewidth
- J= Geometry Factor
- KT = Temperature Factor
- KL= Life factor

The equation given above<sup>[5]</sup> calculates the tooth bending stress and it's given in Von Mises results. Von Mises stress can be thought of as an equivalent stress resulting from the combination of the principal stresses in x, y and z direction. This value can be compared to the yield stress of the material. The von Mises stress is given by the relation

$$S_{eq}^2 = S_{xx}^2 + S_{yy}^2 + S_{zz}^2 - S_{xx} S_{yy} - S_{yy} S_{zz} - S_{zz} S_{xx} + 3 S_{xy}^2 + 3 S_{yz}^2 + 3 S_{xz}^2$$

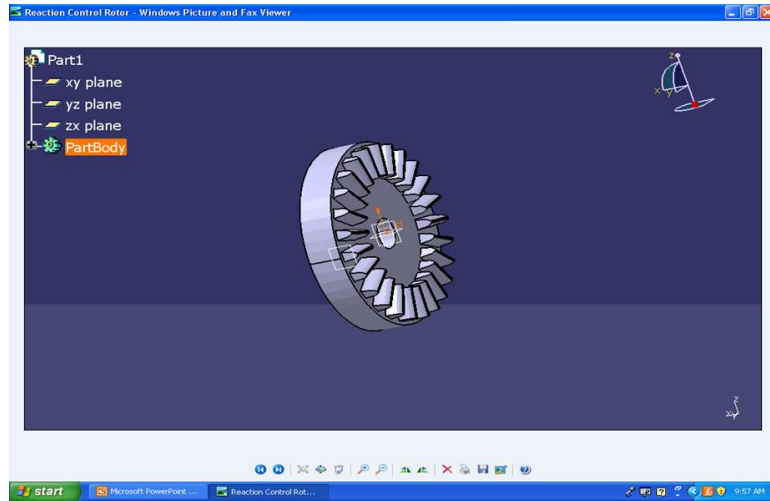
The objective of the stress analysis is to calculate a range of diameters and their corresponding facewidths that would give stress values below the allowable bending stress of the material. The stresses are plotted for all the four face gears namely the stress of the reaction control rotor, stress at the pericylcer unit at the reaction side, stress at the

pericyler unit at the output side, and stress of the output rotor. The allowable bending stress of the material intersects the highest stress curve which happened to be the output rotor in this study. The objective was to get the vonmises stresses from the finite element analysis and compare it with the theoretical tooth bending stress equation. The dimensions of the gears were the same, so the stresses on the gears were almost identical. The gears were assumed as face spur gears, so that they could be modeled as solid cylinders for simplicity. In actuality one would use face bevel gears and they would be modeled as cones. The 3-D model that we used was a shaft that was pinned at both ends and the three gears were mounted on the shaft as shown in the geometry section of our report. The teeth were not modeled due to complexity and inexperience with ANSYS. However, the teeth contact was modeled as gear surface contact. The stress value obtained with the 3-D analysis was an order of magnitude larger than the theoretical result. The reason for this high valued can be justified with the fact that analysis was nonlinear and due to the lack of teeth on the gear which would have resulted in a lower stress value, as depicted in the theoretical equation. The 2-D analysis was simplified to two gears meshing with each other and pinned at their respective centers. The stress value obtained with the 2-D analysis was in relatively good agreement with the theoretical result. The % error was about 27%. The main reason for the difference between the finite element results and the theoretical results lie in the realm of the geometry modeling. The input shaft is journaled to the housing via bearings, the reaction control rotor is connected to the housing by its own bearings, and the PMC is mounted on the input shaft with its own set of bearings. The bearings needed in this design were tapered roller bearings that resist motion in the axial, radial direction, and resists moment in the radial direction. The

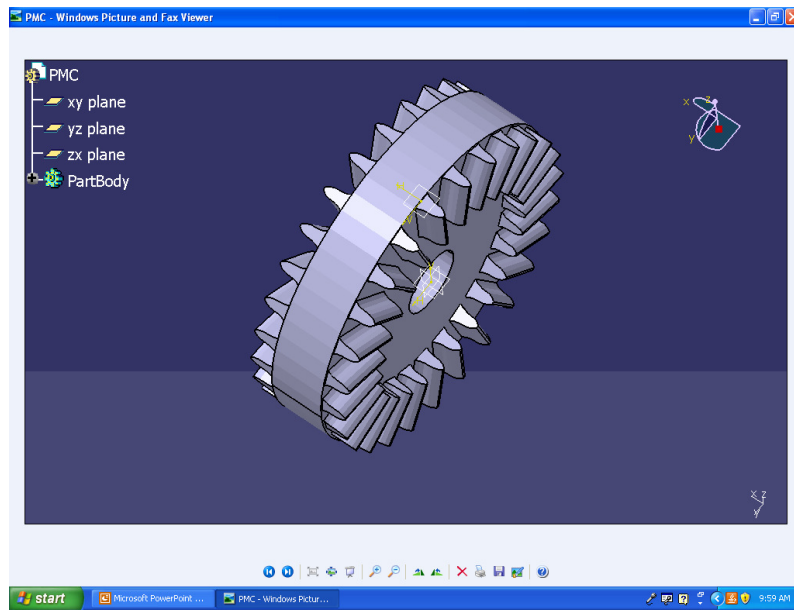
tapered roller bearing could have been modeled as cones sliding past each at a given point. The complete modeling of the P-CVT as described above would have resulted in an physically sound and accurate finite element model that would have yielded results in excellent agreement with theoretical results. This analysis was assumed to be a steady state finite element analysis. However, a dynamic FEA would have been more appropriate since it would take into account the rotations and natural frequencies of the gears and would be an accurate representation of gears meshing in real time on a helicopter.

### **Recommended Future Work**

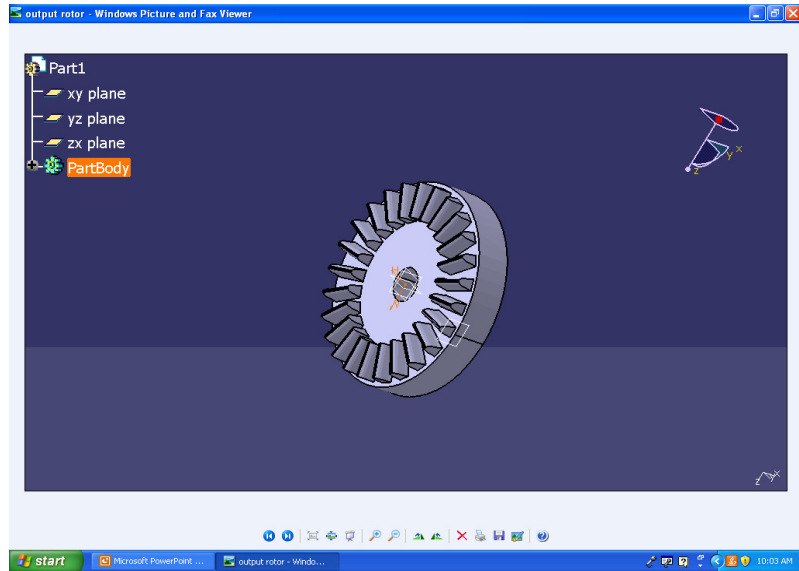
- Modeling the gear with the teeth using the CATIAV5 models as shown in the pictures below
- We intended to use SIMULIA (Abaqus for CATIA) to do the finite element modeling
  - That would include a detailed design of the bearings, shaft Analysis, housing
- Dynamic FEA: Taking into account gear RPM, Shaft RPM, and natural frequencies
- The figures below depict the parts and final assembly modeling in CATIA. The next phase would involve the design and insertion of the bearings in the model, so as to facilitate the finite element analysis using Simulia.



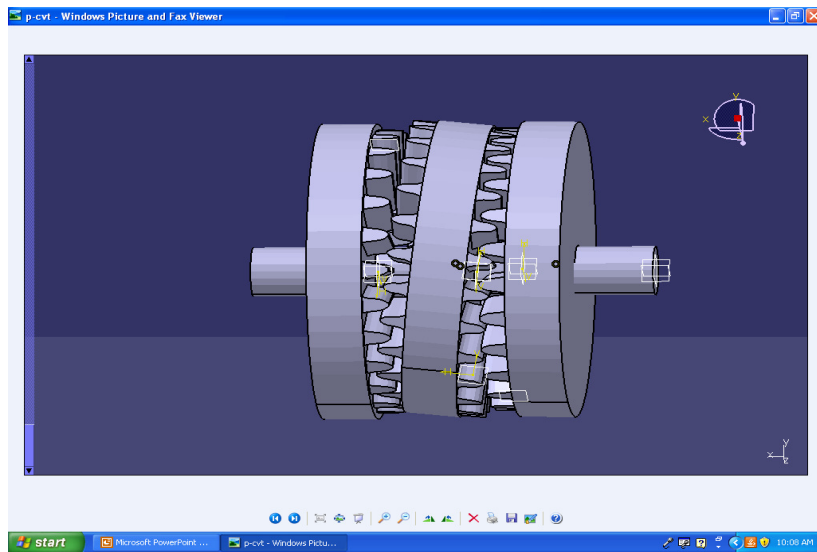
Reaction Control Rotor



PMC



Output Rotor



The final Assembly (PCVT)

## 6.5 Housing and Lubrication Analysis

Helicopter transmission housing design involves the selection, shape, and material of the housing in order to achieve low weight, low noise, high reliability, high maintainability, and low cost transmission housing. There is a trade-off that needs to be considered between light weight housing and noise, as light weight housing is flexible and more noise prone. Therefore, an optimization procedure is required to determine an optimum housing design. The housing that was selected for the optimum split torque type P-CVT was based on Alexander Korzun's paper that described the steel fabricated truss like housing design and its advantages over a magnesium cast housing<sup>26</sup>. The advantages of using the fabricated steel truss like structure over magnesium cast housing are a 15% weight reduction, higher maintainability and reliability, and 30% reduction in cost<sup>26</sup>. The disadvantages of magnesium cast housing are low strength, fatigue, and creep properties<sup>26</sup>. The goal of the optimization process for housing design is to achieve weight reduction and high stiffness. The flow chart of fabricated transmission housing analysis<sup>26</sup> is shown in Figure 53.

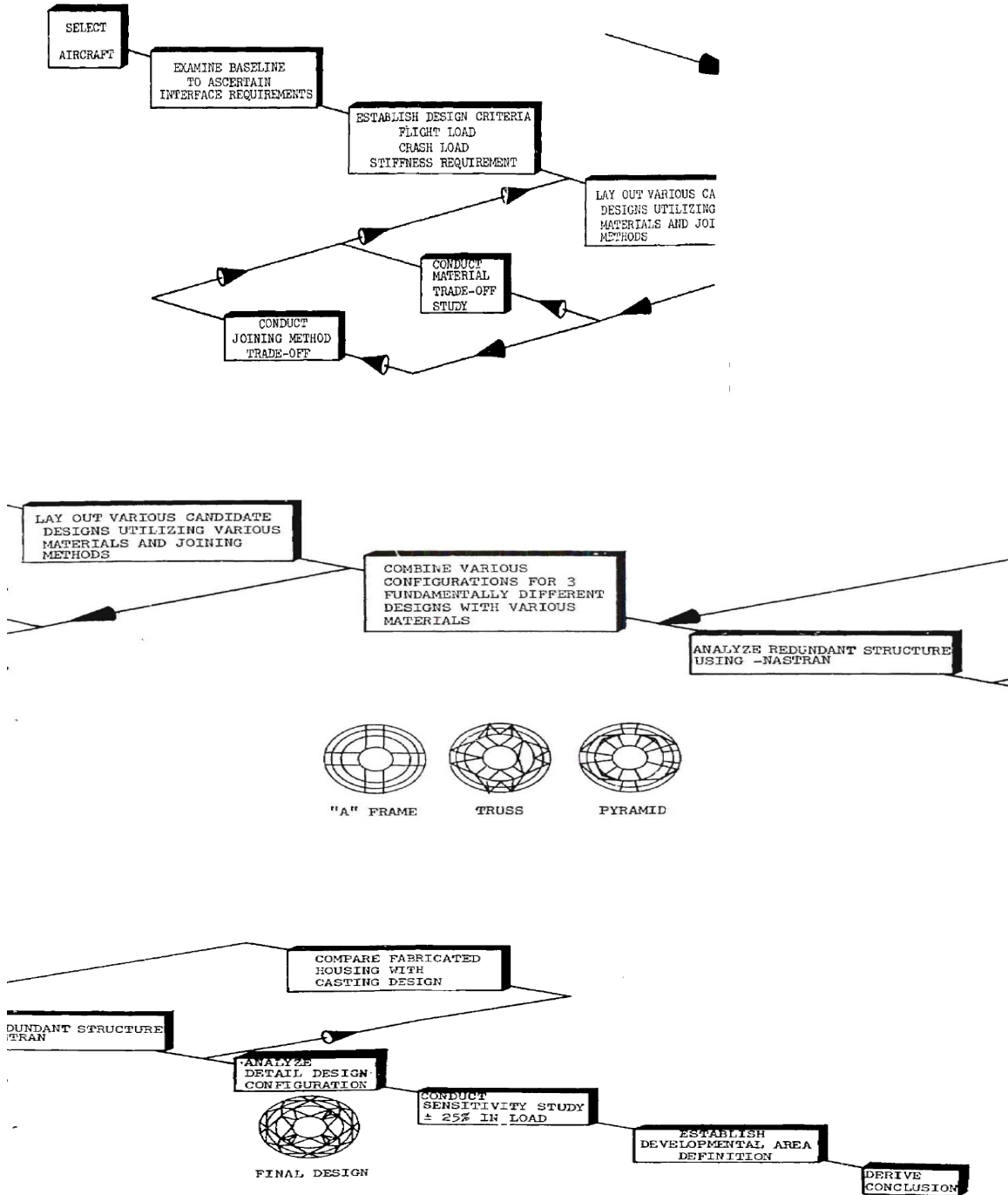
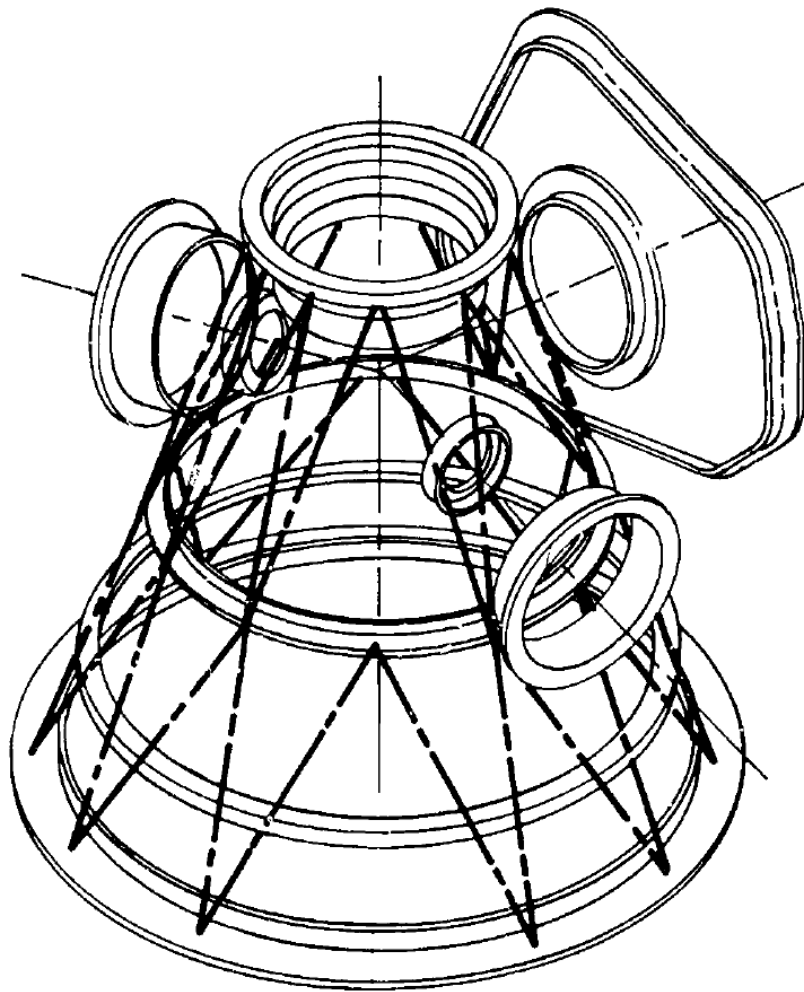
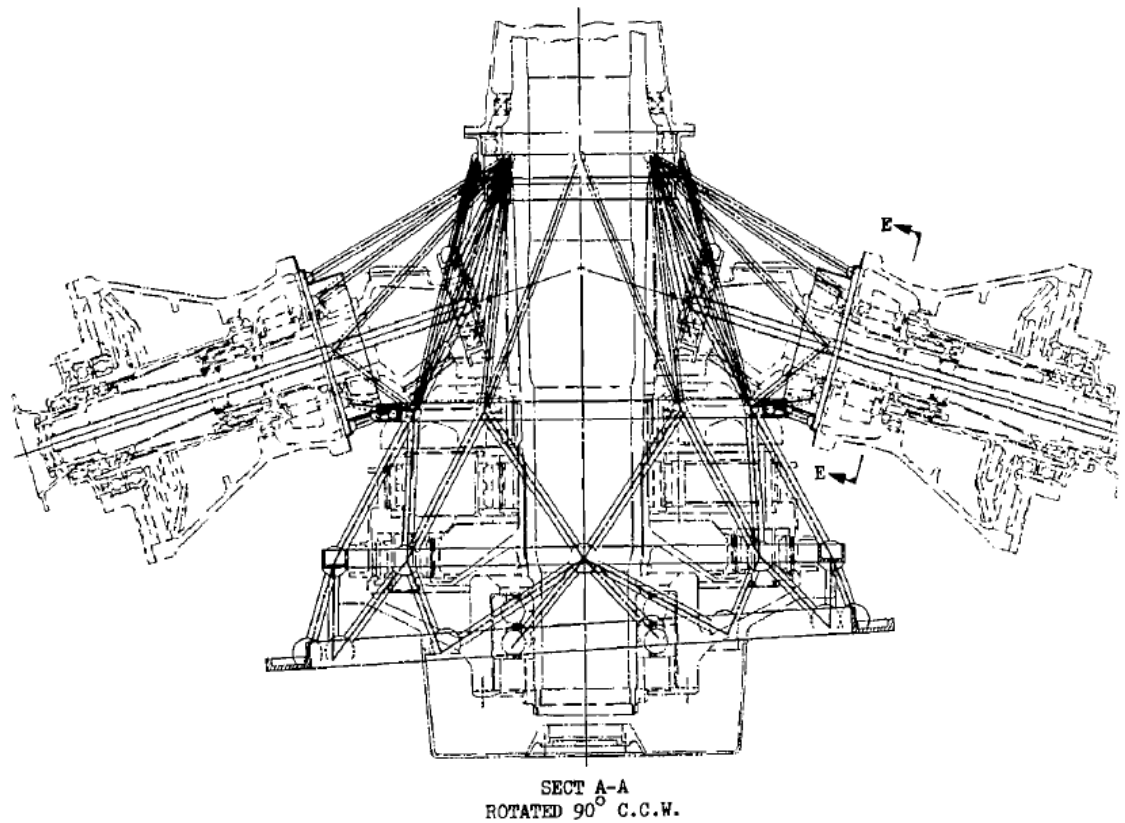


Figure 53: Housing Design Flow Chart<sup>26</sup>.

Based on the study conducted for the CH-54B helicopter, the pure truss structure was selected over the other two candidate designs listed in the flow chart above because it had higher stiffness<sup>26</sup>. The material selected was Custom 455 stainless steel because it has the highest allowable critical buckling strength, highest fracture toughness, and best combination of specific ultimate shear strength, specific ultimate tensile strength, and specific fatigue strength with temperature<sup>26</sup>. Based on the advantages of the steel fabricated truss like housing<sup>26</sup>, the split torque type P-CVT for the JHL will use the pure truss structure made of custom 455 steel for its housing design. The pure truss structure<sup>26</sup> is shown in Figure 54 and its final layout<sup>26</sup> is shown in Figure 55.



**Figure 54:** Pure Truss Design<sup>26</sup>.



**Figure 55:** Detailed Layout of the Fabricated Housing looking Aft<sup>26</sup>.

### **Lubrication system for the split torque type P-CVT**

The FAA requirement requires oil free running for 30 minutes, however, it can run on residual oil. The P-CVT lubrication system described by Lemanski<sup>5</sup> provides oil free running for several hours due to the incorporation of an oil mist system which reduces oil churning and coupled with the use of tribological coatings on the load bearing surfaces which can sustain full torque transfer for several hours, thus, providing oil-off hours for the P-CVT.

## CHAPTER 7

### CONCLUDING REMARKS

The advanced rotorcraft transmission program objectives are to reduce transmission weight by at least 25% , reduce sound pressure levels by at least 10 dB, have a 5000 hr mean time between removal, and also incorporate the use of split torque technology in rotorcraft drivetrains of the future<sup>28</sup>. The analysis of the split torque type P-CVT achieved a weight reduction of 42.5% and 40.7% over planetary and split torque transmissions respectively. In addition, a 19.5 dB sound pressure level reduction was achieved using active gear struts, and also the use of fabricated steel truss like housing provided a higher maintainability and reliability, low cost, and low weight over cast magnesium housing currently employed in helicopters. The static finite element analysis of the split torque type P-CVT, both 2-D and 3-D, yielded stresses below the allowable bending stress of the material, and the goal of the finite element analysis is to see if the designed product has met its functional requirements. The safety assessment of the split torque type P-CVT yielded a 99% probability of mission success based on a Monte Carlo simulation using stochastic- petri net analysis and a failure hazard analysis. This was followed by an FTA/RBD analysis yielded an overall system failure rate of 140.35 failures per million hours, and a preliminary certification and time line of certification was performed. Based on the analysis of the split-torque type P-CVT, the split torque type P-CVT conforms to the hypothesis of the research which states that:

- Is it feasible to design and optimize a split torque pericyclic continuously variable transmission for a single main rotor heavy lift helicopter with the goal of achieving a 50% rotor speed reduction by designing a variator that varies the

speed continuously from zero to 50%. This is opposed to using a two speed transmission which has structural problems and is highly unreliable due to the embodiment of the traction type transmission, complex clutch and brake system

Based on the analysis conducted, it is feasible to design and optimize a split torque pericyclic continuously variable transmission for a single main rotor heavy lift helicopter. It can meet the goal of achieving a 50% rotor speed reduction by designing a variator that varies the speed continuously from zero to 50% as opposed to using a two speed transmission. The two speed transmission has structural problems and is highly unreliable due to the embodiment of the traction type transmission, complex clutch and brake system. The use of spherical facegears and pericyclic kinematics has advanced the state of the art in drivetrain design primarily in the reduction of weight and noise coupled with high safety, reliability, and efficiency.

Revisiting the research questions and the proposed solutions to the questions:

- Two speed transmission versus variable speed transmission?
- Traction versus nontraction CVT?
- Power handling capabilities of CVT?
- Optimization of Variator at fixed ratios versus infinite ratios?
- Safety, Reliability, and efficiency of CVT?

- Two speed transmission has a disadvantage during upshifting (i.e. cruise to hover). The process of going from a low power setting to a high power setting results in drivetrain shock induced loads. A variator concept is needed and has been conceptually designed in Chapter 6
- Traction based CVTs, including pulley based, that rely on friction to transfer torque are discarded based on low reliability, poor bearing life, high rotating inertias, low power capacity, low power density, high parts count, large weight, high vibration, and most importantly low efficiency. Therefore, non-traction based split torque type P-CVT has been selected as the best approach for a single main rotor heavy lift helicopter. The description, mechanism, and advantages of the split torque type P-CVT can be found in Chapters 5, 6.1, 6.2, 6.4, and 6.5
- The power handling capabilities of the P-CVT are much higher than traction based CVTs due to high power density and high contact ratios, as described in Chapter 5
- The variator needs to be optimized for fixed ratios and then a variator selected that has minimum weight for a fixed ratio. Suppose a 50% speed reduction is desired then a variator would vary the speed from zero to 50% continuously as opposed to using a two speed transmission. The Optimization is in Chapter 6
- The safety assessment of CVTs lean towards the P-CVT as it has a higher reliability of over 98% since it uses positive engagement (gearing) to transfer the torque as opposed to traction based which are highly unreliable, as described in Chapter 6.3

- The efficiency of the P-CVT is about 98% and due to a high power density ( small size and weight) and the regenerative braking system employed leads to a lower weight heat exchanger which is usually about 10% of the weight of the drivetrain, as described in Chapter 5

My contributions to the solution to research questions are:

- Provided mathematical and physical derivation of the “square-cube law effect” in drivetrain design
- Assessed gearbox, shafting, and transmission weight variation with RPM for a single main rotor heavy lift helicopter
- Conducted extensive research work on traction based versus non-traction based CVT
- Conducted extensive research work on two-speed versus variable speed transmission
- Conducted a trade-off study on the selection of rotor RPM reduction
- Developed a decision matrix and overall evaluation criteria
- Performed P-CVT optimization and sizing for a single main rotor heavy lift helicopter
- Performed gearbox, shafting, bearings, couplings, and housing weight estimation for the optimum P-CVT for a single main rotor heavy lift helicopter
- Provided transmission and gearbox layout of the optimum P-CVT for a single main rotor heavy lift helicopter
- Performed acoustic analysis of the planetary gear system for a single main rotor heavy lift helicopter

- Conducted extensive research work on the selection of housing, lubrication, and application of active noise control to the optimum P-CVT for a single main rotor heavy lift helicopter
- Performed safety assessment and preliminary certification of the optimum P-CVT for a single main rotor heavy lift helicopter
- Performed static finite element analysis of the optimum P-CVT for a single main rotor heavy lift helicopter

The split torque type P-CVT offers the advantages of a split torque transmission coupled with a nutating mechanical transmission. In addition it also suppresses the “square cube law” effect in drivetrains by providing transmissions that handle high power/torque with light weight gears. The OEC had an initial value of 1 and was expressed mathematically as follows:

$$OEC = 2 \frac{\frac{BASELINEWEIGHT}{OPTIMIZEDWEIGHT} * \frac{BASELINENOISE}{OPTIMIZEDNOISE}}{\frac{OPTIMIZEDEFFICIENCY}{BASELINEEFFICIENCY} + \frac{OPTIMIZEDSAFETY}{BASELINESAFETY}}$$

After plugging in the optimized and baseline values in the expression above results in a final OEC of 1.48 as shown below.

$$OEC = 2 \frac{\frac{15203}{8742} * \frac{25}{19.5}}{\frac{0.98}{0.97} + \frac{140.35}{70.175}} = 1.48$$

The baseline values were obtained from reference [6]. The optimized values were obtained from the analysis conducted in chapters 5, 6, 6.1, 6.2, 6.3, 6.4, 6.5. Based on the

overall evaluation criteria, the split torque type P-CVT offers reduction in weight, noise, and increases efficiency and safety with respect to the baseline drivetrain.

The summary of results is presented below.

- The analysis of the split torque type P-CVT achieved a weight reduction of 42.5% and 40.7% over planetary and split torque transmissions
- The use of active gear struts resulted in a 19.5 dB sound pressure level reduction achieved for the first harmonic and 4-8 dB sound pressure level reduction achieved for the other harmonics
- The use of fabricated steel pure truss housing design resulted in higher maintainability and reliability due to lower parts count, low weight, and low cost over magnesium cast housing currently employed in helicopters
- The static finite element analysis of the split torque type P-CVT, both 2-D and 3-D, yielded stresses below the allowable bending stress of the material
- The safety assessment of the split torque type P-CVT yielded a 99% probability of mission success based on a Monte-Carlo simulation using stochastic- petri net analysis and a failure hazard analysis
- Fault tree analysis and reliability block diagrams analysis yielded an overall failure rate of 140.35 failures per million hours
- Preliminary certification and time line of certification was performed
- The use of spherical facegears and pericyclic kinematics has advanced the state of the art in drivetrain design by incorporating novel mathematical techniques such as differential manifolds to analyze pericyclic kinematics

- The split torque type P-CVT is a split torque nutating mechanical transmission which incorporates the advantages of split torque transmission coupled with a nutating mechanical transmission to form a drivetrain that offers superior qualities than existing planetary and split torque drivetrains

## **CHAPTER 8**

### **RECOMMENDATIONS**

- Perform a dynamic finite element analysis for the split torque type P-CVT
- Conduct an experimental active noise control setup in a laboratory environment
- Detailed analysis of the lubrication system and the control system for the split torque type P-CVT
- Incorporate the Roller/Cam model developed by PSU onto an unmanned aerial vehicle (UAV) in a laboratory environment
- Perform a finite element analysis for the housing of the split torque type P-CVT

## APPENDIX A

### PLANETARY GEAR ANALYSIS

#### MANUAL FOR TRANSMISSION PROGRAMS (PLANETARY GEAR SIZING)

PROGRAM 1: Calculates diameters, speeds, and teeth's of the gears for a 2 stage planetary gear system. The program iterates on the first stage sun teeth, second stage sun teeth, and ratio of 1<sup>st</sup> stage planetary gear. In this code the total planetary stage ratio was 13.629 based on a specific design and the second stage planetary gear ratio is obtained by dividing the overall ratio by the iterated 1<sup>st</sup> stage ratio and the dimensions are calculated and are stored in a matrix form so the designer can pick dimensions that are practical for engineering purposes. The numbers can be chosen based on the design, so wherever you see a number in the code- this means that you can change it based on your design.

#### Variables

Ns1 - 1<sup>st</sup> stage sun teeth  
Ns2 - 2<sup>nd</sup> stage sun teeth  
rt1 - 1<sup>st</sup> stage planetary ratio  
rt2 - 2<sup>nd</sup> stage planetary ratio  
Nr1- 1<sup>st</sup> stage ring teeth  
Nr2- 2<sup>nd</sup> stage ring teeth  
Np1- 1<sup>st</sup> stage pinion teeth  
Np2- 2<sup>nd</sup> stage pinion teeth  
ns1- 1<sup>st</sup> stage sun speed  
ns2- 2<sup>nd</sup> stage sun speed  
na1- 1<sup>st</sup> stage arm speed  
na2- 2<sup>nd</sup> stage arm speed  
np1- 1<sup>st</sup> stage pinion speed  
np2- 2<sup>nd</sup> stage pinion speed  
Diam\_sun1 - 1<sup>st</sup> stage sun diameter  
Diam\_sun2- 2<sup>nd</sup> stage sun diameter  
Diam\_ring1-1<sup>st</sup> stage ring diameter  
Diam\_ring2- 2<sup>nd</sup> stage ring diameter  
Diam\_pinion1- 1<sup>st</sup> stage pinion diameter  
Diam\_pinion2- 2<sup>nd</sup> stage pinion diameter

USAGE: RUN IT IN MATLAB

#### THE CODE:

```
% Transmission5.m a program for calculating diameter,speeds and teeths for  
% a two-stage planetary gear system by Sameer Hameer  
% iterated on the No. of sun teeth and the Ratio of the first stage  
% planetary gear system
```

```

% k is first stage sun teeth
% l is second stage sun teeth
% m is first stage planetary ratio

i=0;
for k=25:1:30
    for l=25:1:30
        for m=2:0.4:5

            i=i+1;
            Ns1(i)=k;
            Ns2(i)=l;
            rt1(i)=m;
            rt2(i)=13.629/rt1(i);% the value "13.629" is obtained : sun gear RPM / Rotor
RPM from design and its the total planetary stage ratio
            Nr1(i)= floor(Ns1(i)*rt1(i)-1);
            Nr2(i)= floor(Ns2(i)*rt2(i)-1);
            if(rem((Nr1(i)-Ns1(i)),2)==0)
                Np1(i)= (Nr1(i)-Ns1(i))/2;
            else
                Nr1(i)=Nr1(i)+1;
                Np1(i)= (Nr1(i)-Ns1(i))/2;
            end

            if(rem((Nr2(i)-Ns2(i)),2)==0)
                Np2(i)= (Nr2(i)-Ns2(i))/2;
            else
                Nr2(i)=Nr2(i)+1;
                Np2(i)= (Nr2(i)-Ns2(i))/2;
            end
            ns1(i)=2000;% sun gear rpm - based on the design
            na1(i)=ns1(i)/rt1(i)
            na2(i)=146.746 %rotor rpm based on the design
            ns2(i)=na1(i)
            Diam_sun1(i)=Ns1(i)/2.7 % p1 = 2.7 diametrical pitch of first stage p2=5.1 diam
pitch of 2nd stage
            Diam_sun2(i)=Ns2(i)/5.1
            Diam_ring1(i)=(Nr1(i)/Ns1(i))*Diam_sun1(i)
            Diam_ring2(i)=(Nr2(i)/Ns2(i))*Diam_sun2(i)
            Diam_pinion1(i)=(1/2)*(Diam_ring1(i)-Diam_sun1(i))
            Diam_pinion2(i)=(1/2)*(Diam_ring2(i)-Diam_sun2(i))
            np1(i)=(Ns1(i)/Np1(i))*(na1(i)-ns1(i))+na1(i)
            np2(i)=(Ns2(i)/Np2(i))*(na2(i)-ns2(i))+na2(i)
        end
    end
end

```

## THEORY:

- The main purpose of a transmission is to deliver power from the engine to the rotors or channeling power to the tail rotor or other accessories like driving pumps
- Transmission design requires minimum losses from the gears, minimum weight which translates into less installed horsepower. The target is to minimize gearbox weight and shaft weight.
- This is a direct result of the “square-cube law”. Power and transmission weight are related as  $P^2 = \text{constant } W^3$
- As you double the power, the weight will be 1.58 times its original weight. As you triple the power, the weight will be 2.08 times its original weight and if you quadruple the power, the weight will be 2.52 times its original weight
- The transmission is sized based on the maximum power required by the rotors for a given flight condition ( hover, cruise, OEI) and not the installed power, as installed power takes into account pressure altitude corrections, XMSN losses etc.

$$HP = QN/63000 \quad Q\text{-ftIb}_f \quad N\text{-RPM}$$

$$\text{POWER} = \text{TORQUE} * \text{ANGULAR SPEED}$$

$$Q_1 N_1 = Q_2 N_2 \quad \text{Assuming no losses}$$

$$\text{Efficiency} = 1 - P_{\text{Loss}}/P_{\text{In}}$$

## GEAR TERMINOLOGIES

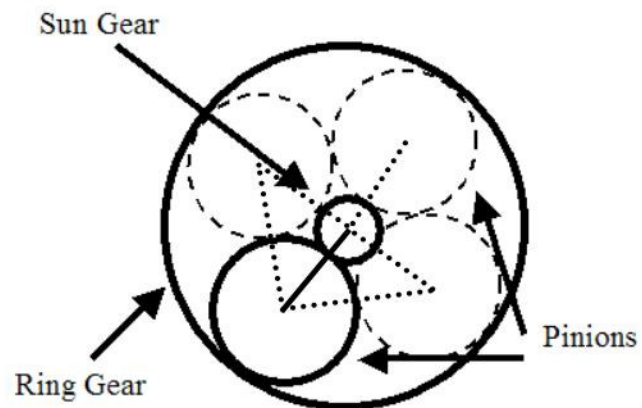
- Diametrical Pitch, P - # of teeth / diameter
- Circular pitch p- distance from one edge of the tooth to another corresponding edge on another tooth

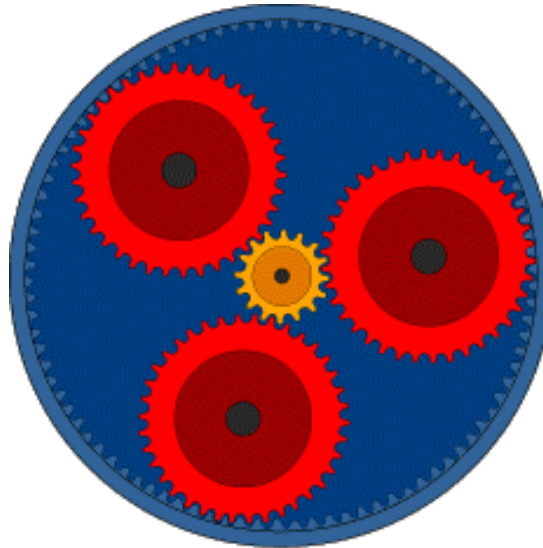
$$P_p = p_i$$

- Face width, F – length of the tooth
- $a = 1/P$ ,  $b = 1.25/P$  for pressure angle = 25 degrees
- Addendum –a
- Dedendum –b
- Weight of gear = F\*Area\*weight density

- The ratio of the speeds is inversely proportional to the ratio of the diameters
- $W1/W2=D2/D1=N2/N1=1/e$  ( assuming no slip between gears – tangential speed = constant), where e is the planetary train factor
- This procedure was employed to calculate the teeth, diameters, speeds, and face width of the gears(from stress analysis)

#### PLANETARY GEAR





©2000 How Stuff Works

### PLANETARY GEAR ANALYSIS

- Assume the Sun gear is rotating counterclockwise
  - Counterclockwise rotation is +ve
  - Clockwise rotation is -ve
  - The ring speed is zero
- The diametral pitch, P, is the same for a given planetary stage
- There are several constraints that need to be taken into account for proper meshing of the teeth

$i$  denotes stage and subscript a, r, s, and p denote arm, ring, sun, and pinion respectively

$N_{ri} = N_{si} + 2N_{pi}$ ,  $N_{si} + N_{ri} / (\text{no. of pinions})$  must equal an integer

### SINGLE STAGE ANALYSIS

Relative to the arm---→

$$e_{\text{sun-ring}} = \frac{n_{ri} - n_{ai}}{n_{si} - n_{ai}}$$

$$e_{\text{sun-ring}} = \frac{-N_{si}}{N_{ri}}$$

$$\frac{n_{ai}}{n_{si}} = \frac{N_{si}}{N_{ri} + 1}$$

$$e_{sun - pinion} = \frac{n_{pi} - n_{ai}}{n_{si} - n_{ai}}$$

$$e_{sun-pinion} = \frac{-N_{si}}{N_{pi}}$$

$$n_{pi} = \frac{N_{si}}{N_{pi}} (n_{ai} - n_{si}) + n_{ai}$$

- arm carrier speed of 1<sup>st</sup> stage = sun gear speed of 2<sup>nd</sup> stage
- Knowing this you can use the equations in the previous slide to express  $n_{a2}/n_{s1}$ , where  $n_{a2}$  is the rotor RPM.
- Radius of the ring gear = Radius of sun + diameter of the pinion
- $D_{ring} = D_{sun} + 2D_{pinion}$
- Divide by the diameter of the sun throughout
- Using the expressions in the previous page
- you get  $N_{ring}/N_{sun} = 1 + 2N_p/N_{sun}$  which is the constraint listed earlier
- Always make your largest reductions at the last stage to save weight (comes from the square-cube law)

## PROGRAM 2: CALCULATES FACEWIDTH

For a given stage assume the facewidth is the same for the sun, pinion and ring gear

Calculation of facewidth involves stress analysis – bending and contact stress

Refer to literature by Shigley in the references section

USAGE: transmission3(arg1,arg2,arg3,arg4,arg5)

Code:

```
% Program to Calculate Facewidth (Spur Gears)
% Name:- Sameer Hameer
% Area:- Transmission (GT-KKU COLLABORATIVE EFFORT)
% Inputs of the function are No. of teeth(N), Rotor Horse Power per Rotor(Hp),RPM(n),
Lewis Form Factor(Y)
% and maximum permissible bending stress(sig_p)
function trans2= transmission3(N,Hp,n,Y,sig_p)

for i=1:0.1:15,
    P(i)=i;
    % circular pitch p
    p(i)=pi/P(i);
    % d is the diameter in inches
    d(i)=N/P(i);
    % V is the pitch line velocity in ft/min
    V(i)= (pi*d(i)*n)/12;
    % The transmitted load W_t in pounds
    W_t(i)= (33000*Hp)/V(i);
    % The Velocity factor K_v
    K_v(i)= 1200/(1200+V(i));
    % The face width F in inches from
    F(i)=(W_t(i)*P(i))/(K_v(i)*Y*sig_p*1000);% usage : sig_p has units of (kpsi)
    if(F(i)>3*p(i) & F(i)<5*p(i)),
        F
        P
        p
        W_t
        V
        K_v
        % Addendum a
        a=1/P
        % Dedendum b
        b=1.25/P
        % Whole Height h
        h=a+b
        % tooth thickness
        thickness=p/2
        break;
```

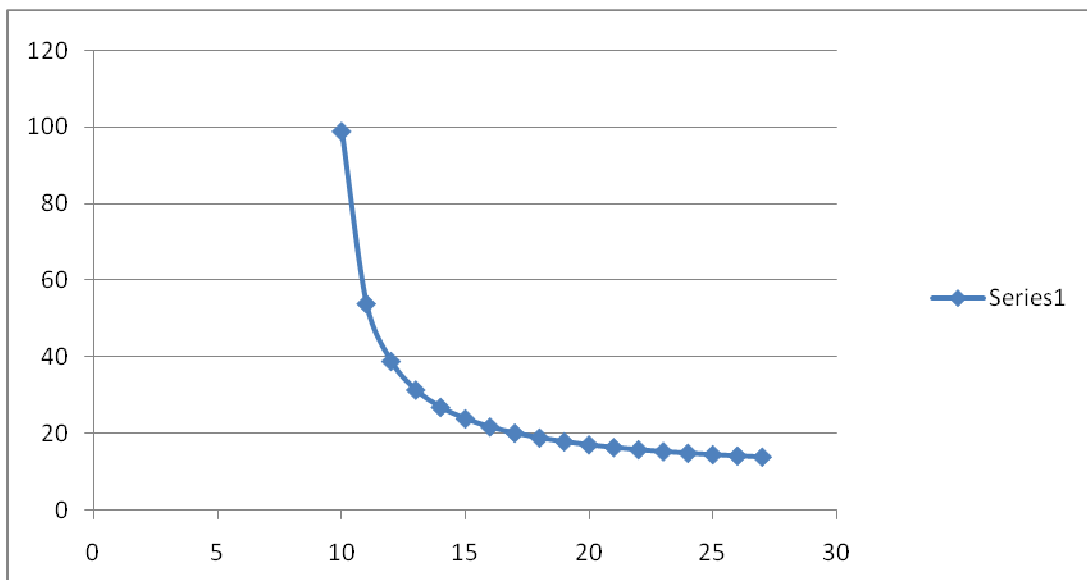
```
end;  
end;
```

## APPENDIX B

### P-CVT ANALYSIS

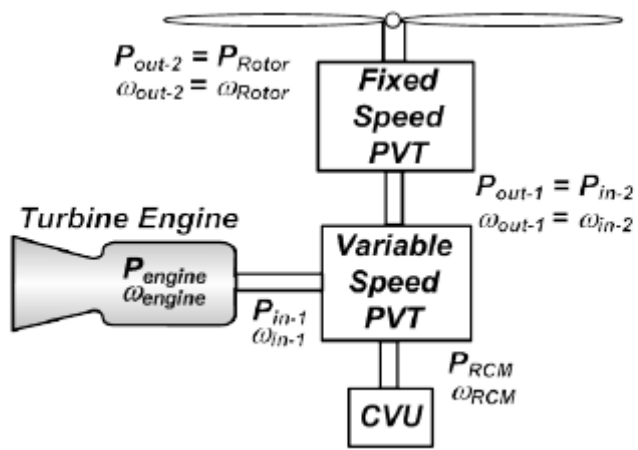
#### PVT ANALYSIS

**OBJECTIVE : TO REPLACE FIRST AND SECOND STAGE PLANETARY GEAR SYSTEM OF THE JHL WITH A SPLIT TORQUE TYPE P-CVT**



A Graph of Npout vs. NR





from paper by Saribay and et al

Design Analysis of Pericyclic Variable-Speed Transmission System  
for a 600 HP Class Unmanned  
Rotorcraft

Tensile Stress

Face Gears

$$s_t = [63000 * P * K_o * N_{gear} * K_s * K_m * K_T * K_R * c / k] / [2 * w * R_{gear}^2 * K_v * F * J * K_L]$$

P= power transmitted

Ko = application factor

Ngear = Number of teeth in gear

ks = size factor

km = load distribution factor

KR = Reliability factor

k=split torque factor

c = ratio of the tooth meshing

w = RPM of gear

Kv = Dynamic factor

Rgear = pitch radius of gear

F = Facewidth

J = Geometry Factor

KT = Temperature Factor

KL = Life factor

Power (hp)	8773		N	0.95
Ko	1	Power source uniform		
NR	28			
NPR	30			
NOOUT	56			
NPOUT	57			
Ks	1			
Km	1.3			
KR	0.7			
c/k	0.1			
JNR	0.33			
JNPR	0.33			
JNOUT	0.33			
JNPOUT	0.33			
F	1.8	INCHES		
KT	1	TEMP < 250 DEGREES FAHRENHEIT		
KL	1			
wRCR	0	for fixed ratio - PVT		
win	1151.6			
wout	115			
KvNR	1			
KvNPR	1			
KvNOUT	1			
KvNPOUT	1			

PVT (FIXED RATIO) ANALYSIS

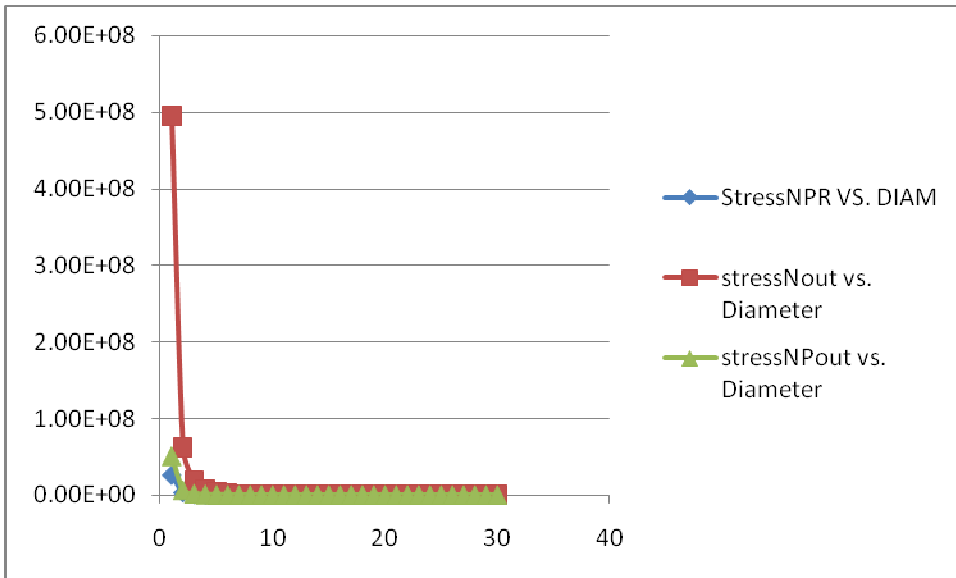
Facewidth	DiamNpR	Tensile stress	DiamNout	Tensile Stress	DiamNpout	TensileStress
7.50E-02	1	2.65E+07	1	4.95E+08	1	5.03E+07
1.50E-01	2	3.31E+06	2	6.18E+07	2	6.29E+06
2.25E-01	3	9.80E+05	3	1.83E+07	3	1.86E+06
3.00E-01	4	4.14E+05	4	7.73E+06	4	7.86E+05
3.75E-01	5	2.12E+05	5	3.96E+06	5	4.02E+05
4.50E-01	6	1.23E+05	6	2.29E+06	6	2.33E+05
5.25E-01	7	7.72E+04	7	1.44E+06	7	1.47E+05
6.00E-01	8	5.17E+04	8	9.66E+05	8	9.82E+04
6.75E-01	9	3.63E+04	9	6.79E+05	9	6.90E+04
7.50E-01	10	2.65E+04	10	4.95E+05	10	5.03E+04
8.25E-01	11	1.99E+04	11	3.72E+05	11	3.78E+04
9.00E-01	12	1.53E+04	12	2.86E+05	12	2.91E+04
9.75E-01	13	1.20E+04	13	2.25E+05	13	2.29E+04
1.05E+00	14	9.65E+03	14	1.80E+05	14	1.83E+04
1.13E+00	15	7.84E+03	15	1.47E+05	15	1.49E+04
1.20E+00	16	6.46E+03	16	1.21E+05	16	1.23E+04
1.28E+00	17	5.39E+03	17	1.01E+05	17	1.02E+04
1.35E+00	18	4.54E+03	18	8.48E+04	18	8.62E+03
1.43E+00	19	3.86E+03	19	7.21E+04	19	7.33E+03
1.50E+00	20	3.31E+03	20	6.18E+04	20	6.29E+03
1.58E+00	21	2.86E+03	21	5.34E+04	21	5.43E+03
1.65E+00	22	2.49E+03	22	4.65E+04	22	4.72E+03
1.73E+00	23	2.18E+03	23	4.07E+04	23	4.13E+03
1.80E+00	24	1.91E+03	24	3.58E+04	24	3.64E+03
1.88E+00	25	1.69E+03	25	3.17E+04	25	3.22E+03
1.95E+00	26	1.51E+03	26	2.82E+04	26	2.86E+03
2.03E+00	27	1.34E+03	27	2.51E+04	27	2.56E+03
2.10E+00	28	1.21E+03	28	2.25E+04	28	2.29E+03
2.18E+00	29	1.09E+03	29	2.03E+04	29	2.06E+03
2.25E+00	30	9.80E+02	30	1.83E+04	30	1.86E+03

material : VASCOJET 2000

DENSITY 0.28 lb/cu in

Bending Tensile stress 200,000 psi at room temp and 226,000 psi at 950 degrees fahrenheit

Objective of the stress analysis is to calculate a range of diameters  
that would give stresses below the allowable bending stress of the material  
The facewidth of the gear should be approximately 15% of the gear radius



From the graph the Highest stress occurs on the output rotor

Diameter chosen 24  
inches

Weight of PVT Gearbox = 911.55 lbs

## PCVT ANALYSIS

### OVERALL RATIO

20

50% rotor speed change desired

A variable system for the JHL whose high speed is 115 RPM  
and low speed is 57.5 RPM

Therefore reaction member is actuated from 0 to 60.44 Rpm  
The split torque type P-CVT will consist of 50% variable speed  
P-CVT cascaded in series with a fixed ratio PVT

Power (hp)	8773	N	0.95
Ko	1	Power source uniform	
NR	28		
NPR	30		
NOOUT	56		
NPOUT	57		
Ks	1		
Km	1.3		
KR	0.7		
c/k	0.1		
JNR	0.33		
JNPR	0.33		
JNOUT	0.33		
JNPOUT	0.33		
F	1.8	INCHES	
KT	1	TEMP < 250 DEGREES FAHRENHEIT	
KL	1		
wRCR	60.44		
win	1151.6		
wout	57.5		
KvNR	1		
KvNPR	1		
KvNOOUT	1		
KvNPOUT	1		

P-CVT

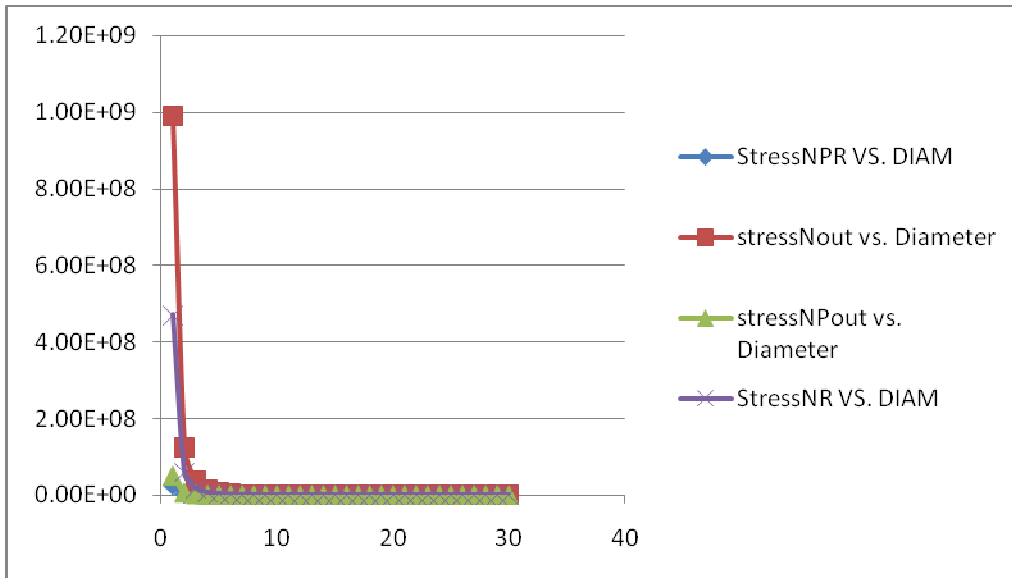
Facewidth	DiamNpR	Tensile stress	DiamNout	Tensile Stress	DiamNpout	TensileStress	DiamNR	Tensile Stress
7.50E-02	1	2.65E+07	1	9.90E+08	1	5.03E+07	1	4.71E+08
1.50E-01	2	3.31E+06	2	1.24E+08	2	6.29E+06	2	5.88E+07
2.25E-01	3	9.80E+05	3	3.67E+07	3	1.86E+06	3	1.74E+07
3.00E-01	4	4.14E+05	4	1.55E+07	4	7.86E+05	4	7.35E+06
3.75E-01	5	2.12E+05	5	7.92E+06	5	4.02E+05	5	3.77E+06
4.50E-01	6	1.23E+05	6	4.58E+06	6	2.33E+05	6	2.18E+06
5.25E-01	7	7.72E+04	7	2.89E+06	7	1.47E+05	7	1.37E+06
6.00E-01	8	5.17E+04	8	1.93E+06	8	9.82E+04	8	9.19E+05
6.75E-01	9	3.63E+04	9	1.36E+06	9	6.90E+04	9	6.46E+05
7.50E-01	10	2.65E+04	10	9.90E+05	10	5.03E+04	10	4.71E+05
8.25E-01	11	1.99E+04	11	7.43E+05	11	3.78E+04	11	3.54E+05
9.00E-01	12	1.53E+04	12	5.73E+05	12	2.91E+04	12	2.72E+05
9.75E-01	13	1.20E+04	13	4.50E+05	13	2.29E+04	13	2.14E+05
1.05E+00	14	9.65E+03	14	3.61E+05	14	1.83E+04	14	1.72E+05
1.13E+00	15	7.84E+03	15	2.93E+05	15	1.49E+04	15	1.39E+05
1.20E+00	16	6.46E+03	16	2.42E+05	16	1.23E+04	16	1.15E+05
1.28E+00	17	5.39E+03	17	2.01E+05	17	1.02E+04	17	9.58E+04
1.35E+00	18	4.54E+03	18	1.70E+05	18	8.62E+03	18	8.07E+04
1.43E+00	19	3.86E+03	19	1.44E+05	19	7.33E+03	19	6.86E+04
1.50E+00	20	3.31E+03	20	1.24E+05	20	6.29E+03	20	5.88E+04
1.58E+00	21	2.86E+03	21	1.07E+05	21	5.43E+03	21	5.08E+04
1.65E+00	22	2.49E+03	22	9.29E+04	22	4.72E+03	22	4.42E+04
1.73E+00	23	2.18E+03	23	8.13E+04	23	4.13E+03	23	3.87E+04
1.80E+00	24	1.91E+03	24	7.16E+04	24	3.64E+03	24	3.41E+04
1.88E+00	25	1.69E+03	25	6.33E+04	25	3.22E+03	25	3.01E+04
1.95E+00	26	1.51E+03	26	5.63E+04	26	2.86E+03	26	2.68E+04
2.03E+00	27	1.34E+03	27	5.03E+04	27	2.56E+03	27	2.39E+04
2.10E+00	28	1.21E+03	28	4.51E+04	28	2.29E+03	28	2.14E+04
2.18E+00	29	1.09E+03	29	4.06E+04	29	2.06E+03	29	1.93E+04
2.25E+00	30	9.80E+02	30	3.67E+04	30	1.86E+03	30	1.74E+04

material : VASCOJET 2000

DENSITY 0.28 lb/cu in

Bending Tensile stress 200,000 psi at room temp and 226,000 psi at 950 degrees fahrenheit

Objective of the stress analysis is to calculate a range of diameters that would give stresses below the allowable bending stress of the material  
The facewidth of the gear should be approximately 15% of the gear radius



From the graph the Highest stress occurs on the output rotor

Diameter chosen 24 inches

Weight of P-CVT Gearbox = 911.55 lbs

SUMMARY      for split torque type P-CVT  
Total Gearbox weight = 1823 lbs

Total Shaft weight at 50% RPM REDUCTION IS 5,000 lbs

Total Shaft Weight = 5000 lbs

Total Gearbox Weight for the split torque type P-CVT = 1823 lbs      (P-CVT 50% PLUS PVT FIXED RATIO)  
Housing Weight = 144.5 lbs (steel fabricated truss like structure)      FOR P-CVT

Bearings      FOR P-CVT

Center Support Cylindrical = 333 lbs

Thrust ball = 70 lbs

Nutator roller support = 232 lbs      Nutator also known as PMC

Reaction control rotor and shaft support = 145 lbs

Input Pinion and Bearings = 35 lbs

Bearings FOR PVT

Center Support Cylindrical = 333 lbs

Thrust ball = 70 lbs

Nutator roller support = 232 lbs      Nutator also known as PMC

Reaction control rotor and shaft support = 145 lbs

Input Pinion and Bearings = 35 lbs

Housing Weight = 144.5 lbs (steel fabricated truss like structure) For PVT

Total Split torque type P-CVT weight = 8742 lbs      (50% P-CVT PLUS PVT FIXED RATIO)

JHL transmission weight = 15,203 lbs  
(planetary drive system )

JHL transmission weight = 14,750 lbs  
(split torque drive system)

% Weight reduction achieved over planetary drive system = 42.5%

% Weight reduction achieved over split torque drive system = 40.7%













```

wpof,,0.050000
CYL4,0,0,0, ,12, ,1 ! Second gear
/VIEW,1,1,1,1
/ANG,1
/REP,FAST
wpof,,0.050000
CYL4,0,0,0, ,12, ,1 ! third gear
! next step was to select all the volumes for meshing
! mesh analysis was done using the mesh tool
SMRT,6
SMRT,OFF
MSHAPE,1,3D
MSHKEY,0
!*
CM,_Y,VOLU
VSEL, , , 5
CM,_Y1,VOLU
CHKMSH,'VOLU'

```

```

CMSEL,S,_Y
!*
! VMESH,_Y1
!*
CMDELE,_Y
CMDELE,_Y1
CMDELE,_Y2
!*
SMRT,6
SMRT,3
CM,_Y,VOLU
VSEL, , , , 5
CM,_Y1,VOLU
CHKMSH,'VOLU'
CMSEL,S,_Y
!*
VMESH,_Y1
!*
CMDELE,_Y
CMDELE,_Y1
CMDELE,_Y2

```

!Creating the contact elements between the gears

!creating the first contact surface: between the PMC & the reaction Control rotor

```

/COM, CONTACT PAIR CREATION - START
CM,_NODECM,NODE
CM,_ELEMCM,ELEM
CM,_KPCM,KP
CM,_LINECM,LINE
CM,_AREACM,AREA
CM,_VOLUCM,VOLU
/GSAV,cwz,gsav,,temp
MP,MU,1,
MAT,1
R,3
REAL,3
ET,2,170
ET,3,174
KEYOPT,3,9,0
KEYOPT,3,10,2
R,3,
RMORE,

```

```

RMORE,,0
RMORE,0
! Generate the target surface
ASEL,S,,27
CM,_TARGET,AREA
TYPE,2
NSLA,S,1
ESLN,S,0
ESLL,U
ESEL,U,ENAME,,188,189
ESURF
CMSEL,S,_ELEMCM
! Generate the contact surface
ASEL,S,,27
CM,_CONTACT,AREA
TYPE,3
NSLA,S,1
ESLN,S,0
ESURF
ALLSEL
ESEL,ALL
ESEL,S,TYPE,,2
ESEL,A,TYPE,,3
ESEL,R,REAL,,3
/PSYMB,ESYS,1
/PNUM,TYPE,1
/NUM,1
EPLOT
ESEL,ALL
ESEL,S,TYPE,,2
ESEL,A,TYPE,,3
ESEL,R,REAL,,3
CMSEL,A,_NODECM
CMDEL,_NODECM
CMSEL,A,_ELEMCM
CMDEL,_ELEMCM
CMSEL,S,_KPCM
CMDEL,_KPCM
CMSEL,S,_LINECM
CMDEL,_LINECM
CMSEL,S,_AREACM
CMDEL,_AREACM
CMSEL,S,_VOLUCM
CMDEL,_VOLUCM
/GRES,cwz,gsav
CMDEL,_TARGET

```

```

CMDEL,_CONTACT
/COM, CONTACT PAIR CREATION - END
/AUTO,1
/REP,FAST
APLOT
/ZOOM,1,RECT,0.467046,0.709929,0.752578,0.523759
!*
!*

```

!creating the Second contact surface: between the output rotor & the PMC

```

/COM, CONTACT PAIR CREATION - START
CM,_NODECM,NODE
CM,_ELEMCM,ELEM
CM,_KPCM,KP
CM,_LINECM,LINE
CM,_AREACM,AREA
CM,_VOLUCM,VOLU
/GSAV,cwz,gsav,,temp
MP,MU,1,0
MAT,1
R,4
REAL,4
ET,4,170
ET,5,174
KEYOPT,5,9,0
KEYOPT,5,10,2
R,4,
RMORE,
RMORE,,0
RMORE,0
! Generate the target surface
ASEL,S,,23
CM,_TARGET,AREA
TYPE,4
NSLA,S,1
ESLN,S,0
ESLL,U
ESEL,U,ENAME,,188,189
ESURF
CMSEL,S,_ELEMCM
! Generate the contact surface
ASEL,S,,23
CM,_CONTACT,AREA
TYPE,5
NSLA,S,1

```

```

ESLN,S,0
ESURF
ALLSEL
ESEL,ALL
ESEL,S,TYPE,,4
ESEL,A,TYPE,,5
ESEL,R,REAL,,4
/PSYMB,ESYS,1
/PNUM,TYPE,1
/NUM,1
EPLOT
ESEL,ALL
ESEL,S,TYPE,,4
ESEL,A,TYPE,,5
ESEL,R,REAL,,4
CMSEL,A,_NODECM
CMDEL,_NODECM
CMSEL,A,_ELEMCM
CMDEL,_ELEMCM
CMSEL,S,_KPCM
CMDEL,_KPCM
CMSEL,S,_LINECM
CMDEL,_LINECM
CMSEL,S,_AREACM
CMDEL,_AREACM
CMSEL,S,_VOLUCM
CMDEL,_VOLUCM
/GRES,cwz,gsav
CMDEL,_TARGET
CMDEL,_CONTACT
/COM, CONTACT PAIR CREATION - END

```

!Applying the displacements & force (torque to gears) boundary conditions

```

/SOL
FLST,2,9,1,ORDE,9
FITEM,2,8
FITEM,2,57
FITEM,2,-58
FITEM,2,5953
FITEM,2,-5954
FITEM,2,5956
FITEM,2,-5957
FITEM,2,5960
FITEM,2,10149

```

```

!*
/GO
D,P51X, ,0, , , ,ALL, , , , ,
FLST,2,7,1,ORDE,7
FITEM,2,1
FITEM,2,37
FITEM,2,42
FITEM,2,5651
FITEM,2,5656
FITEM,2,-5657
FITEM,2,5660
!*
/GO
D,P51X, ,0, , , ,ALL, , , , ,
/ZOOM,1,RECT,0.447183,0.727305,0.735198,0.501418
APLOT
FLST,2,1,1,ORDE,1
FITEM,2,6778
!*
/GO
F,P51X,FX,10000
FLST,2,1,1,ORDE,1
FITEM,2,3368
!*
/GO
F,P51X,FX,-10000
FLST,2,1,1,ORDE,1
FITEM,2,3999
!*
/GO
F,P51X,FX,10000
/AUTO,1
/REP,FAST
/ZOOM,1,RECT,0.442217,-0.578369,0.745130,-0.712411
FLST,2,1,1,ORDE,1
FITEM,2,6625
!*
/GO
F,P51X,FX,-10000
FLST,2,1,1,ORDE,1
FITEM,2,5031
!*
/GO
F,P51X,FX,10000
FLST,2,1,1,ORDE,1
FITEM,2,4268

```

```
!*  
/GO  
F,P51X,FX,-10000
```

```
!Solving the model
```

```
/STATUS,SOLU  
SOLVE  
FINISH  
/POST1
```

**APPENDIX D**

**MATHEMATICAL ANALYSIS OF THE P-CVT**

**ALL OF THE MATERIAL OBTAINED FROM:**

**NUTATING MECHANICAL TRANSMISSION(MAROTH DRIVE PRINCIPLE)**

**RAYMOND J. DRAGO, A. J. LEMANSKI**

**BOEING VERTOL COMPANY**

**PHILADELPHIA, PA**

**JAN 1974**

### LIST OF SYMBOLS

$A_{35}^i$	Rotation of the $X_A, Y_A, Z_A$ system about the $X_A$ axis in the $Y_A, Z_A$ plane
AF	Distance defined in calculation of cam tooth root tensile stress (Figure A18)
$A_{ijCA}$	The angle between points i and j, where i and j may be an integer from 1 through 9, with the apex at the mechanism focus
$a_{CAi}$	The distance from load line to the intersection point of a tooth centerline with its critical section, measured perpendicular to the load line in the tooth mean plane
$a_{OCA}$	A nutator roller dimension (defined in Figures A19 and A20)
$B_{KLCA}$	Backlash of cam teeth
$b_{CAi}$	Contact bandwidth between tooth and roller
$b_{OCA}$	A nutator roller dimension (defined in Figures A19 and A20)
C	Rated dynamic capacity of a rolling element bearing
$C_{OCA}$	A nutator roller dimension (defined in Figures A19 and A20)
$C_{PCA}$	Angular pitch of the nutator rollers
$C_{TCA}$	Contact duration
c	Minimum axial clearance required between nutators in a double nutator unit
D	Total distance normal to nutator centerline required for each center support bearing
$D_A$	Total axial distance along the NMT centerline required for each center support bearing
$D_{BM}$	Maximum center support bearing mean diameter

$D_{\max CA}$	Total axial distance along NMT centerline inherently available on cam side of nutator for spreading center support bearings
DN	A factor which measures bearing operating speed
$D_{SACT}$	Actual shaft diameter
$D_{SMAX}$	Maximum shaft diameter possible for a specified support bearing ID
d	Diameter of rolling element of a cylindrical roller bearing
$d_{CA}$	Diameter of the rolling elements used to support a nutator roller on either the rotor or stator side of the nutator
$d_{CAi}$	Distance between the point of load application and the critical section of a cam tooth, measured parallel to tooth centerline
$d_{CCA}$	Axial clearance available within the center region of a cam
$d_{OCA}$	A nutator roller dimension (defined in Figures A19 and A20)
$d_{SCA}$	Axial clearance on either rotor or stator side of nutator required for the nutator structure and rollers as they sweep through angles $\sigma$ and $\nu$
$E_{CA}, E_{RCA}$	Elastic moduli for cam tooth and roller, respectively
$e_{CAi}$	One half the tooth thickness at its critical section
$F_{ast}$	Torsional shear stress allowable
FE	Distance defined in calculation of tooth root tensile stress (Figure A18)
$F_e$	Bending stress endurance limit
$F_{FRCA}$	Friction force required to prevent skidding of nutator roller
$F_{MAXCA}$	Maximum instantaneous load in the assumed roller load distribution

$F_{mc}$	Dynamic balancing force generated by a rotating nutator balance weight
$F_{NCAi}$	Normal load acting on the $i^{th}$ cam tooth, or normal load on a roller at $i^{th}$ contact point
$F_{NFRCA}$	Normal roller load required to prevent skidding of nutator roller
$F_{RCAi}$	The radial component of the normal load $F_{NCAi}$ acting on the $i^{th}$ cam tooth
$F_{su}$	Ultimate torsional shear stress limit
$F_{TCAi}$	The thrust component of the normal load $F_{NCAi}$ acting on the $i^{th}$ cam tooth
$F_{TNXCA}$ , $F_{TNYCA}$ , $F_{TNZCA}$	Net forces on the nutator
$F_{TXCA}$ , $F_{TYCA}$ , $F_{TZCA}$	Net loads on a cam due to the summation of the loads on all the cam teeth
$F_X$	Radial load at nutator center support bearing required to react the nutator driving loads
$F_{XCAi}$ , $F_{YCAi}$ , $F_{ZCAi}$	The X, Y, Z components, respectively, of the normal load $F_{NCAi}$ acting on the $i^{th}$ cam tooth
$f$	Coefficient of friction between nutator roller and cam tooth
$f_b$	Bending stress
$f_{cCA}$	Minimum radial clearance between nutator center support bearing and cam support structure
$f_{st}$	Torsional stress
$g$	Acceleration due to gravity
$h_{CA}$	Radial distance from mechanism centerline to point of intersection of cam tooth and cam support structure
$ID$	Inner diameter
$IL_{ACA}$	Integer component of $L_{ACA}$

$I_S$	Moment of inertia of nutator support shaft
$I_{XA}, I_{YA}, I_{ZA}$	Elements of nutator moment of inertia matrix $[I_N]$
$I_{XN}, I_{YN}, I_{ZN}$	Elements of nutator moment of inertia matrix $[I]_{XYZ}$
$[I_N]$	Moment of inertia matrix of the nutator in the $X_A, Y_A, Z_A$ coordinate system
$[I]_{XYZ}$	Moment of inertia of the nutator as a function of time in the X, Y, Z coordinate system
$J_{RCA}$	Polar moment of inertia of nutator roller
$J_{XYA}, J_{XZA},$ $J_{YXA}, J_{YZA},$ $J_{ZXA}, J_{ZYA}$	Elements of nutator moment of inertia $[I_N]$
$J_{XYN}, J_{XZN},$ $J_{YXN}, J_{YZN},$ $J_{ZX}, J_{ZY}$	Elements of nutator moment of inertia $[I]_{XYZ}$
$K'$	A factor, based on the tooth/roller contact duration, used to adjust the frequency of the sinusoidal load function for the nutator roller
$K_b, K_{st}$	Stress concentration factors for shaft bending and torsion, respectively
$L$	Life (B-10) of a cylindrical roller bearing
$L_{ACA}$	Contact ratio
$L_m$	Distance from mechanism focus to center of mass of a nutator balancing weight measured along the mechanism axis
$l$	Length of the rolling element of a cylindrical roller bearing
$l_{CA}$	Length of a nutator roller on either the rotor or stator side of the nutator
$l'_{CA}$	Length of roller/tooth contact
$M$	Overturning moment applied to nutator center support bearing and shaft

$M_C$	Mass of cylindrical hole through center of nutator roller
$M_C$	Mass of a nutator balance weight
$M_F$	Material factor for cylindrical roller bearing
$M_F$	Mass of solid frustum of a cone
$M_G$	Reduction ratio
$M_{GF}$	Fixed reduction ratio
$M_{GV}$	Variable reduction ratio
$M_{mc}$	Moment generated by a rotating nutator balance weight
$M_{mcX}, M_{mcY}, M_{mcZ}$	Components of the moment $M_{mc}$ generated by the synchronous nutator balance weight system
$M_{TNXCA}, M_{TNYCA}$	Net overturning moments about $X_0$ and $Y_0$ axes, respectively, acting on the nutator
$M_{TXCA}, M_{TYCA}$	Net overturning moments about the $X_0$ and $Y_0$ axes, respectively, acting on a cam
$M_{XN}, M_{YN}, M_{ZN}$	Moments due to nutator unbalance
$M_{1CAi}, M_{2CAi}$	Reaction moments which must be exerted by the nutator structure to restrain the roller at its outer and inner ends, respectively
$M_{OCAi}$	Maximum moment exerted on loaded portion of nutator roller shaft
$N_{CA}$	Number of teeth on cam
$N'_{CA}$	Number of teeth on cam <u>not</u> under consideration (e.g., if considering rotor $N'_{CA} = N_S$ and if considering stator $N'_{CA} = N_R$ )
$N_{NCA}$	Number of rollers on cam side of nutator
$\omega_{NCA}$	Angular velocity of nutator
$n_1$	Input speed
OD	Outer diameter

$P$	Angular velocity of stator expressed as a fraction of input speed
$P_m$	Cubic mean radial load applied to a bearing
$R'$	Radial load at nutator center support bearing required to react the overturning moments
$R_b$	Ratio of actual to allowable bending stress
$R_{BCCA}$	Basic spherical radius on rotor or stator side
$R_{BCCA}^i$	Radius perpendicular to mechanism axis
$R_{BO}$	Outer radius of nutator center support bearing
$R_{CAi}$	Radius to the load point, measured perpendicular to the shaft centerline
$R_{FCA}$	Cam tooth fillet radius
$R_m$	Radius from mechanism axis to center of mass of nutator balancing weight
$RPM_{Rel}$	Rotational speed of bearing outer race relative to inner race
$R_{so}$	Outside radius of nutator support shaft
$R_{si}$	Inside radius of nutator support shaft
$R_{st}$	Ratio of actual to allowable torsional stress
$R_T$	Total radial load on nutator center support bearing
$R_{1CAi}, R_{2CAi}$	Reaction forces which must be exerted by the nutator structure to restrain the roller at its outer and inner ends, respectively
$r_{CA}$	Nutator roller mean outside radius at $R_{BCCA}$
$r'_{CA}$	Nutator roller effective radius of curvature
$r_{ICA}$	Outside radius of nutator roller at end nearest mechanism outer diameter
$r_{OCA}$	Outside radius of nutator roller at end nearest mechanism centerline
$r_{IN}$	Radius of hole through center of nutator roller

$r_{SCA}$	Radius of nutator roller support shaft (cam follower mounting only)
$S_{bCAi}$	Stress in nutator roller at point at which maximum moment ( $M_{OCAi}$ ) is exerted
$S_{CCAi}$	Maximum compressive stress between tooth and roller at $i^{th}$ point
$S_{FF}$	Nutator roller skidding force factor
$S_{OCA}$	Amount by which nutator roller support structure extends outward past the greatest diameter of the roller
$S_{TCAi}$	Maximum bending stress at the fillet of a cam tooth
$T_{CA}$	Total torque on a cam
$T_{FRCA}$	Friction torque required to prevent skidding of a nutator roller
$T_{TCA}$	Theoretical cam tooth tip thickness
$V_C$	Volume of cylindrical hole through center of nutator roller
$V_F$	Volume of solid frustum of a cone
$V_{PCA/CA}$	Linear velocity of a point on the centerline of a nutator roller with respect to a cam
$V_{XPCA/CA}$ , $V_{YPCA/CA}$ , $V_{ZPCA/CA}$	Components of $V_{PCA/CA}$
$W$	Width of a nutator center support bearing
$w$	Spread distance between centerline of the nutator and the mid-width plane of a nutator center support bearing
$X, Y, Z$	Rectangular coordinate system fixed to nutator and with origin at mechanism focus
$X_{HPCCA}$ , $Z_{HPCCA}$	Coordinates of mean tooth profile at initial point of tooth/roller contact (i.e., start of active profile)

$X_{LPCCA}, Z_{LPCCA}$	Coordinates of mean tooth profile at final point of tooth/roller contact (i.e., end of active profile)
$X_0, Y_0, Z_0$	Coordinate system with $Z_0$ axis lying along mechanism axis, $X_0$ axis horizontal, and $Y_0$ axis vertical (Figure A16)
$X_{PCA}, Y_{PCA}, Z_{PCA}$	Coordinates of a point on the centerline of a nutator roller with respect to nutator null plane
$X_{PCA/CA}, Y_{PCA/CA}, Z_{PCA/CA}$	Coordinates of a point on the centerline of nutator roller relative to cam (i.e., pitch path)
$X_{PF/CAi}, Y_{PF/CAi}, Z_{PF/CAi}$	Coordinates of $i^{th}$ point on a cam tooth profile
$X_{TCA}, Y_{TCA}, Z_{TCA}$	Coordinates of the tangent line to the pitch path
$\gamma$	Minimum installation clearance required between shaft outer radius and bearing bore radius
$\gamma_{SCAi}$	Nutator roller deflection at point at which maximum moment is exerted
$Z_{SCAi}$	Depth of maximum subsurface shear stress
$\alpha_{CA}$	Angular pitch of cam teeth
$\alpha_{BKL}$	Angular backlash
$\alpha_{PFCAi}$	Angle between line $a_{CAi}$ and the cam tooth centerline
$\alpha_{ROL}$	Included roller half-angle
$\alpha_{RCA/CL}$	Angular acceleration of nutator roller about its own centerline
$\alpha_{TCA}$	Angular cam tooth tip thickness
$\cos(\alpha_{CLCA}), \cos(\beta_{CLCA}), \cos(\gamma_{CLCA})$	Direction cosines of a line from the mechanism focus to a point on the centerline of a nutator roller

$\cos (\alpha_{PCA/CA}),$ $\cos (\beta_{PCA/CA}),$ $\cos (\gamma_{PCA/CA})$	Direction cosines of a line tangent to the pitch path
$\alpha'_{PCA/CA}$ $\beta'_{PCA/CA}$ $\gamma'_{PCA/CA}$	Derivatives of the coordinates of the pitch path
$\cos (\alpha_{PFCA}),$ $\cos (\beta_{PFCA}),$ $\cos (\gamma_{PFCA})$	Direction cosines of a line joining a point on a cam tooth profile and the pitch path (i.e., the direction cosines of the normal tooth load vector)
$\beta_{CAi}$	Angle between cam tooth fillet tangent line and the load line
$\gamma_{CA}$	Angle between path of nutator roller centerline and the plane of the nutator
$\gamma_{ROL/CA}$	Nutator roller taper angle
$[\gamma]$	Matrix of direction cosines of rotated position
$[\gamma]'$	Transpose of $[\gamma]$
$[\gamma_A]$	Matrix of direction cosines of the X, Y, Z coordinate system with respect to the $X_A, Y_B, Z_B$ coordinate system, after rotation through angle $A_{35}'$ about the X axis
$[\gamma_A]'$	Transpose of $[\gamma_A]$
$[\gamma_B]$	Matrix of direction cosines of the X, Y, Z coordinate system with respect to the $X_A, Y_B, Z_B$ system, after rotation through angle $\tau_{CA}$ about the Y axis
$[\gamma_B]'$	Transpose of $[\gamma_B]$
$[\gamma]_C$	Equal to $[\gamma_B] [\gamma_A]$ , matrix of direction cosines after rotation thru $A_{35}'$ and $\tau_{CA}$
$[\gamma]_C'$	Transpose of $[\gamma]_C$ , equal to $[\gamma_A]' [\gamma_B]'$
$\Delta_{CA}$	Cam tooth undercut
$\zeta_{SCAi}$	Maximum subsurface shear stress of tooth/roller

$\theta_{CA/N}$	Relative angle of rotation between cam and nutator
$\theta_{PCA}$	Angle between tooth centerline and tangent line to tooth fillet
$\theta_{PF/PPCA}$	The angle between the line defined by a point on the pitch path and the corresponding point on the tooth profile, and the tangent line to the pitch path at the point of interest.
$\theta_{PF/PVCA}$	The angle between the line defined by a point on the pitch path and the corresponding point on the tooth profile, and the radius vector from the mechanism focus to the point on the pitch path
$\theta_S$	Angular rotation of the stator cam
$\theta_{1CAi}, \theta_{2CAi}$	Slope of nutator roller across its support bearings
$\mu_{CA}, \mu_{RCA}$	Poisson's ratio for cam tooth and roller, respectively
$\nu$	Nutation half-angle
$\rho_{CAi}$	Cam tooth profile curvature radius at $i^{th}$ point
$\sigma_{CA}$	Nutator roller centerline coning angle on either rotor or stator side
$T_C$	Output torque of mechanism
$\tau_{CA}$	Rotation in the $XZ$ plane of the $X_A, Y_B, Z_B$ coordinate system about the $Y$ axis
$\omega_C, \omega_{C/G}$	Angular velocity of input (relative to ground)
$\omega_{CA}, \omega_{CA/G}$	Angular velocity of cam (relative to ground)
$\omega_{C/CA}$	Angular velocity of input relative to cam
$\omega_{CA/C}$	Angular velocity of cam relative to input
$\omega_{CA/N}$	Angular velocity of cam relative to nutator
$\omega_{N/C}$	Angular velocity of nutator relative to input

$\omega_{N/CA}$	Angular velocity of nutator relative to cam
$\omega_{N/G}$	Angular velocity of nutator relative to ground
$\omega_{NCA}$	Input angle at which roller/tooth contact begins
$\omega_0$	Input shaft turning angle
$\omega_{O_i}$	The $i^{\text{th}}$ point in the sinusoidal load distribution cycle applied to the nutator roller
$\omega'_{O_i}$	The angular distance from the start of tooth/roller contact to the $i^{\text{th}}$ point in the load cycle
$\omega_{RCA/CL}$	Angular velocity of nutator roller about its own centerline
$\omega_{XCA}$	Input angle at which tooth/roller contact ends
$\omega_{XN}, \omega_{YN}, \omega_{ZN}$	Components of the nutator angular velocity
$\omega_{XN/S}, \omega_{YN/S}, \omega_{ZN/S}$	Components of the nutator angular velocity with respect to the stator

#### Subscripts

CA	General term referring to cam, where the cam may be either rotor (CA = R) or stator (CA = S)
N	Refers to nutator
R	Refers to rotor
S	Refers to stator

## DETAILED DERIVATION OF NUTATING MECHANICAL TRANSMISSION

### MECHANISM SPEED RATIO AND COMPONENT SPEEDS

At this point, it will be advantageous to develop the equation for the reduction ratio of the mechanism. As in conventional gearing, the speed ratios between the various members of the nutating mechanical transmission are dependent upon the relative angular spacing of their teeth (i.e.: rotor and stator cam teeth and nutator rollers).

Considering the schematic diagram shown in Figure A1, we see that

$$\omega_{S/C} = \omega_{N/C} \left( \frac{N_{NS}}{N_S} \right) \quad (A1)$$

$$\omega_{R/C} = \omega_{N/C} \left( \frac{N_{NR}}{N_R} \right) \quad (A2)$$

Solving Equations (A1) and (A2) simultaneously yields

$$\omega_{R/C} \left( \frac{N_{NS}}{N_S} \right) - \omega_{S/C} \left( \frac{N_{NR}}{N_R} \right) = 0 \quad (A3)$$

But

$$\omega_{R/C} = \omega_R - \omega_C \quad (A4)$$

$$\omega_{S/C} = \omega_S - \omega_C \quad (A5)$$

Substituting Equations (A4) and (A5) into Equation (A3) yields

$$\omega_R \left( \frac{N_{NS}}{N_S} \right) - \omega_C \left[ \left( \frac{N_{NS}}{N_S} \right) - \left( \frac{N_{NR}}{N_R} \right) \right] - \omega_S \left( \frac{N_{NR}}{N_R} \right) = 0 \quad (A6)$$

Solving for the rotor speed we have

$$\omega_R = \omega_C \left[ 1 - \frac{N_{NR} N_S}{N_R N_{NS}} \right] + \omega_S \left[ \frac{N_{NR} N_S}{N_R N_{NS}} \right] \quad (A7)$$

Simplifying

$$\omega_R = \omega_C - \left[ \frac{N_{NR} N_S}{N_R N_{NS}} \right] (\omega_C - \omega_S) \quad (A8)$$

Some interesting observations may be made from Equation (A7).

If the stator is fixed, the reduction ratio of the mechanism is found by

$$M_{GF} = \frac{N_R N_{NS}}{N_R N_{NS} - N_{NR} N_S} \left[ \omega_{S/G} = 0 \right] \quad (A9)$$

where

$\omega_R$  = rotor speed

$\omega_C$  = input speed

$N_R$  = number of rotor teeth

$N_{NR}$  = number of nutator rollers on the rotor side

$N_{NS}$  = number of nutator rollers on the stator side

$N_S$  = number of stator teeth

$M_{GF}$  = fixed reduction ratio

If the stator is allowed to rotate at a controlled rate, we note that since

$$\frac{N_{NR} N_S}{N_R N_{NS}} = 1 - \frac{1}{M_{GF}} \quad (A10)$$

$$\omega_R = \omega_C / M_{GF} + \omega_S \left( \frac{M_{GF} - 1}{M_{GF}} \right) \quad (A11)$$

If the stator speed is expressed as a fraction,  $P$ , of the input speed,  $\omega_C$ , then

$$\omega_R = \omega_C / M_{GF} + P \omega_C \left( \frac{M_{GF} - 1}{M_{GF}} \right) \quad (A12)$$

We may note that the rotor speed is zero if

$$0 = \omega_C \left( \frac{1}{M_{GF}} \right) + P \omega_C \left( \frac{M_{GF} - 1}{M_{GF}} \right) \quad (A13)$$

$$P = - \left( \frac{1}{M_{GF} - 1} \right) \text{ (for } \omega_R = 0 \text{)} \quad (A14)$$

Similarly, the variable reduction ratio may be expressed by

$$M_{GV} = \frac{M_{GF}}{1 + P (M_{GF} - 1)} \quad (A15)$$

In subsequent calculations, it will be necessary to use the relative angular velocities of the major components.

We will first derive the angular velocity of the nutator with respect to the rotor.

$$\omega_{R/G} = \omega_{R/N} + \omega_{N/G} \quad (A16)$$

$$\omega_{N/C} = \omega_{N/G} - \omega_{C/G} \quad (A17)$$

But from Equation (A1) we have

$$\omega_{N/C} = \omega_{S/C} \left( \frac{N_S}{N_{NS}} \right) \quad (A18)$$

So Equation (A17) becomes

$$\omega_{N/G} = \omega_{S/C} \left( \frac{N_S}{N_{NS}} \right) + \omega_{C/G} \quad (A19)$$

Substituting Equations (A19) and (A7) into equation (A16) yields

$$\begin{aligned} \omega_{C/G} \left[ 1 - \frac{N_{NR} N_S}{N_R N_{NS}} \right] + \omega_{S/G} \left[ \frac{N_{NR} N_S}{N_R N_{NS}} \right] &= \omega_{R/N} \\ + \omega_{S/C} \left( \frac{N_S}{N_{NS}} \right) + \omega_{C/G} & \end{aligned} \quad (A20)$$

Simplifying

$$\omega_{S/G} \left( \frac{N_{NR} N_S}{N_R N_{NS}} \right) - \omega_{C/G} \left( \frac{N_{NR} N_S}{N_R N_{NS}} \right) = \omega_{R/N} + \omega_{S/C} \left( \frac{N_S}{N_{NS}} \right) \quad (A21)$$

Noting that

$$\omega_{S/C} = -\omega_{C/S} = \omega_{S/G} - \omega_{C/G} \quad (A22)$$

And substituting Equation (A22) into (A7) Equation (A21) gives

$$\begin{aligned} \omega_{S/G} \left( \frac{N_{NR} N_S}{N_R N_{NS}} \right) - \omega_{C/G} \left( \frac{N_{NR} N_S}{N_R N_{NS}} \right) &= \omega_{R/N} - \omega_{C/G} \left( \frac{N_S}{N_{NS}} \right) \\ + \omega_{S/G} \left( \frac{N_S}{N_{NS}} \right) & \end{aligned} \quad (A23)$$

Combining terms yields

$$\omega_{C/G} \left[ \frac{N_S}{N_{NS}} - \frac{N_{NR} N_S}{N_R N_{NS}} \right] + \omega_{S/G} \left[ \frac{N_{NR} N_S}{N_R N_{NS}} - \frac{N_S}{N_{NS}} \right] = \omega_{R/N} \quad (A24)$$

Equation (A24) is the angular velocity of some point on the rotor with respect to some point on the nutator. The angular velocity of the nutator with respect to the rotor is the negative of this quantity, so

$$\omega_{N/R} = \omega_{C/G} \left( \frac{N_{NR} N_S - N_S N_R}{N_R N_{NS}} \right) + \omega_{S/G} \left( \frac{N_S N_R - N_S N_{NR}}{N_R N_{NS}} \right) \quad (A25)$$

Simplifying Equation (A25) yields

$$\omega_{N/R} = \left( \frac{N_{NR} N_S - N_S N_R}{N_R N_{NS}} \right) \left( \omega_{C/G} - \omega_{S/G} \right) \quad (A26)$$

Equation (A26) is valid for any tooth number combinations and for any member fixed; however, some interesting observations may be made by applying some restrictions:

$$\begin{aligned} \omega_{N/R} = \omega_{C/G} \left( \frac{N_{NR} N_S - N_S N_R}{N_R N_{NS}} \right) \quad (\omega_{S/G} = 0) \\ \text{(Stator fixed)} \end{aligned} \quad (A27)$$

Further, if the number of teeth on both sides of the nutator are the same,

$$\omega_{N/R} = \omega_{C/G} \left( \frac{N_S}{N_R} - \frac{N_S}{N_N} \right) \quad \begin{matrix} (\omega_{S/G} = 0) \\ (N_{NS} = N_{NR} = N_N) \end{matrix} \quad (A28)$$

and finally, if the number of teeth on the stator and the nutator are identical,

$$\omega_{N/R} = \omega_{C/G} \left( \frac{N_N - N_R}{N_R} \right) \quad \begin{matrix} (\omega_{S/G} = 0) \\ (N_{NS} = N_{NR} = N_N = N_S) \end{matrix} \quad (A29)$$

Similar reasoning may be used to derive the angular velocity of the nutator with respect to the stator.

Equation (A7) may be solved to yield the stator speed

$$\omega_{S/G} = \omega_{R/G} \left( \frac{N_R N_{NS}}{N_{NR} N_S} \right) - \omega_{C/G} \left( \frac{N_R N_{NS} - N_{NR} N_S}{N_{NR} N_S} \right) \quad (A30)$$

Noting that

$$\omega_{N/C} = \omega_{N/G} - \omega_{C/G} \quad (A31)$$

and from Equation (A2)

$$\omega_{N/C} = \omega_{R/C} \left( \frac{N_R}{N_{NR}} \right) \quad (A32)$$

also

$$\omega_{S/G} = \omega_{S/N} + \omega_{N/G} \quad (A33)$$

therefore,

$$\omega_{N/G} = \omega_{R/C} \left( \frac{N_R}{N_{NR}} \right) + \omega_{C/G} \quad (A34)$$

Substituting Equations (A34) and (A30) into Equation (A33) yields

$$\omega_{R/G} \left( \frac{N_R N_{NS}}{N_{NR} N_S} \right) - \omega_{C/G} \left( \frac{N_R N_{NS} - N_{NR} N_S}{N_{NR} N_S} \right) = \omega_{S/N} + \omega_{R/C} \left( \frac{N_R}{N_{NR}} \right) + \omega_{C/G} \quad (A35)$$

simplifying

$$\omega_{R/G} \left( \frac{N_R N_{NS}}{N_{NR} N_S} \right) - \omega_{C/G} \left( \frac{N_R N_{NS}}{N_{NR} N_S} \right) = \omega_{S/N} + \omega_{R/C} \left( \frac{N_R}{N_{NR}} \right) \quad (A36)$$

We note that

$$\omega_{R/C} = -\omega_{C/R} = \omega_{R/G} - \omega_{C/G} \quad (A37)$$

Substituting Equation (A37) into Equation (A36) gives

$$\omega_{R/G} \left( \frac{N_R N_{NS}}{N_{NR} N_S} \right) - \omega_{C/G} \left( \frac{N_R N_{NS}}{N_{NR} N_S} \right) = \omega_{S/N} - \omega_{C/G} \left( \frac{N_R}{N_{NR}} \right) + \omega_{R/G} \left( \frac{N_R}{N_{NR}} \right) \quad (A38)$$

Combining terms yields

$$\omega_{S/N} = \omega_{C/G} \left[ \frac{N_R}{N_{NR}} - \frac{N_R N_{NS}}{N_{NR} N_S} \right] + \omega_{R/G} \left[ \frac{N_R N_{NS}}{N_{NR} N_S} - \frac{N_R}{N_{NR}} \right] \quad (A39)$$

Equation (A38) may be written

$$\omega_{N/S} = \omega_{C/G} \left[ \frac{N_R N_{NS} - N_R N_S}{N_{NR} N_S} \right] + \omega_{R/G} \left[ \frac{N_R N_S - N_R N_{NS}}{N_{NR} N_S} \right] \quad (A40)$$

Simplifying yields

$$\omega_{N/S} = \left[ \frac{N_{NS} N_R - N_R N_S}{N_S N_{NR}} \right] \left( \omega_{C/G} - \omega_{R/G} \right) \quad (A41)$$

Equations (A41) and (A25) are quite similar in form, which points out the basic similarity of the rotor and stator. Substituting Equation (A8) into Equation (A41) gives

$$\omega_{N/S} = \left[ \frac{N_{NS} N_R - N_R N_S}{N_S N_{NR}} \right] \left[ \omega_{C/G} - \omega_{C/G} + \left( \frac{N_{NR} N_S}{N_R N_{NS}} \right) (\omega_{C/G} - \omega_{S/G}) \right] \quad (A42)$$

which simplifies to

$$\omega_{N/S} = \left[ \frac{N_{NS} N_R - N_R N_S}{N_R N_{NS}} \right] (\omega_{C/G} - \omega_{S/G}) \quad (A43)$$

and ultimately

$$\omega_{N/S} = \left[ \frac{N_{NS} - N_S}{N_{NS}} \right] (\omega_{C/G} - \omega_{S/G}) \quad (A44)$$

Equation (A44) is valid in the most general case. Some restrictions will prove interesting.

If the stator is fixed,

$$\omega_{N/S} = \left[ \frac{N_{NS} - N_S}{N_{NS}} \right] \omega_{C/G} ; (\omega_{S/G} = 0) \quad (A45)$$

If the number of teeth on the stator and the stator side of the nutator are equal,

$$\omega_{N/S} = 0 ; (N_{NS} = N_S) \quad (A46)$$

If we now consider Equations (A26) and (A43) we may write a general expression for the angular velocity of the nutator with respect to either the rotor or stator:

$$\omega_{N/CA} = \left[ \frac{N_{NCA} N'_{CA} - N_S N_R}{N_R N_{NS}} \right] (\omega_{C/G} - \omega_{S/G}) \quad (A47)$$

where  $N_{NCA}$  = number of rollers on cam side of nutator

$N'_{CA}$  = number of teeth on the cam (rotor or stator) not under consideration (NOTE: If rotor is under consideration,  $N'_{CA} = N_S$  and if stator is under consideration,  $N'_{CA} = N_R$ )

$\omega_{C/G}$  = Input speed

At this point it is convenient to derive the equations for the velocities of all the major components.

The angular velocity of the rotor with respect to the reference frame, in the most general case is given by Equation (A8)

$$\omega_R = \omega_C - \begin{bmatrix} N_{NR} & N_S \\ N_R & N_{NS} \end{bmatrix} \begin{bmatrix} \omega_C \\ \omega_S \end{bmatrix} \quad (\text{A8})$$

where  $\omega_C$  = input speed

$\omega_R$  = rotor speed

$\omega_S$  = stator speed

The angular velocity of the nutator with respect to the reference frame is found considering Equation (A19) by

$$\omega_{N/G} = \omega_{S/C} \left( \frac{N_S}{N_{NS}} \right) + \omega_{C/G} \quad (\text{A19})$$

$$\omega_{S/C} = \omega_{S/G} - \omega_{C/G} \quad (\text{A48})$$

Substituting Equation (A48) into Equation (A19) yields

$$\omega_{N/G} = (\omega_{S/G} - \omega_{C/G}) \left( \frac{N_S}{N_{NS}} \right) + \omega_{C/G} \quad (\text{A49})$$

But if we express the stator speed as a fraction P of the input speed,

$$\omega_{N/G} = \omega_{C/G} \left( \frac{(P-1) N_S}{N_{NS}} + 1 \right) \quad (\text{A50})$$

From Equation (A50) we can see that if the stator is stationary, that is if  $\omega_{S/G} = 0$  and  $P = 0$ , the nutator speed is

$$\omega_{N/G} = \omega_{C/G} \left( \frac{N_{NS} - N_S}{N_{NS}} \right); \quad (\omega_{S/G} = 0) \quad (\text{A51})$$

If the number of teeth on the stator and the stator side of the nutator are the same, Equation (A50) becomes

$$\omega_{N/G} = \omega_{C/G} [P]; (N_{NS} = N_S) \quad (A52)$$

Obviously if the stator is also stationary, from equation (A52) we can see that the nutator does not rotate

$$\begin{aligned} \omega_{N/G} &= 0 & N_{NS} &= N_S \\ & & & \& \\ & & \omega_{S/G} &= 0 \end{aligned} \quad (A53)$$

In all cases, the nutator undergoes an oscillatory motion due to it's "Lemniscular" motion.

The angular velocity of the nutator with respect to the input shaft is required to calculate the life of the nutator support bearing. It is given by

$$\omega_{N/C} = \omega_{N/G} - \omega_{C/G} \quad (A54)$$

substituting Equation (A49) into Equation (A54) yields

$$\omega_{N/C} = (\omega_{S/G} - \omega_{C/G}) \left( \frac{N_S}{N_{NS}} \right) + \omega_{C/G} - \omega_{C/G} \quad (A55)$$

Simplifying

$$\omega_{N/C} = (\omega_{S/G} - \omega_{C/G}) \left( \frac{N_S}{N_{NS}} \right) \quad (A56)$$

Again expressing the stator speed as a fraction of the input

$$\omega_{N/C} = \omega_{C/G} (P-1) \left( \frac{N_S}{N_{NS}} \right) \quad (A57)$$

If the stator is stationary,

$$\omega_{N/C} = -\omega_{C/G} \left( \frac{N_S}{N_{NS}} \right); (\omega_{S/G} = 0) \quad (A58)$$

If the number of teeth on the stator and stator side of the nutator are the same,

$$\omega_{N/C} = \omega_{C/G} (P-1); (N_S = N_{NS}) \quad (A59)$$

finally if  $\omega_{S/G} = 0$  and  $N_S = N_{NS}$

$$\omega_{N/C} = -\omega_{C/G} \quad \begin{matrix} (N_S = N_{NS}) \\ (\omega_{S/G} = 0) \end{matrix} \quad (A60)$$

## REFERENCES

- [1] AMCP 706-201: Engineering Design Handbook. Helicopter Engineering. Part One -PreliminaryDesign. Headquarters, U.S. Army Material Command. 1974.
- [2] Brown, Gerald V., Kascak, Ebihara, Johnson, Choi.: High Power Density Motors for Aeropropulsion. NASA Glenn Research center. Cleveland, Ohio. December 2005.
- [3] Schmidt, A.H.: A Simplified Method for Calculating the Weight of AircraftTransmission Drive Shafting. The Boeing Company. Philadelphia, Pennsylvania. May 13, 1968.
- [4] Stepniewski, W.Z., Shinn, W.A.: A Comparative Study of Soviet vs. Western Helicopters. Ames Research Center. Moffett Field, California. 1983.
- [5] Lemanski, A.J., Saribay, B.Z., Elmoznino, J.M.: Conceptual Design of Pericyclic Non-Traction Continuously Variable Speed Transmissions: Rotorcraft Applications. AHS 62<sup>nd</sup> Annual Forum. Phoenix, Arizona. May 9, 2006.
- [6] Bellocchio,A.: Drive System Design Methodology for a Single Main Rotor Heavy Lift Helicopter. 2005.
- [7] Belanger, P., Berry, A., Pasco, Y., St-Amant, Y., Rajan, S.: Active Structural Acoustic Control of A Bell 407 Transmission Noise: AHS 62<sup>nd</sup> Annual Forum. Phoenix, Arizona. May 9-11, 2006.
- [8] Kish, Jules.: Vertical Lift Drive System Concept Studies Variable Speed/ Two-speed Transmissions, US ARMY RESEARCH LABORATORY. 2002.
- [9] Mishke, Shigley : Mechanical Engineering Design. 1989.

- [10] Mucino, V., Smith, J., Cowan, B., Kmicikiewicz, M.: A Continuously Variable Power Split Transmission for Automotive Applications: SAE. 1997.
- [11] Long, T., Wohl, R., Mucino, V., Smith, J.: A Model for a Planetary- CVT Mechanism: Analysis and Synthesis: SAE. 1993.
- [12] Singh, T., Nair, S.: A Mathematical Review and Comparison of Continuously Variable Transmissions: SAE. 1992.
- [13] Mahoney, J., Bai, S., Maguire, Joel.: Ratio Changing the Continuously Variable Transmission: SAE. 2004.
- [14] Kluger, M., Fussner, R.: An Overview of Current CVT Mechanisms, Forces and Efficiencies: SAE. 1997.
- [15] Madrigal, J., Benitez, F.: A Continuous Variable Transmission Based on Epicyclic Gears: SAE. 2002.
- [16] Maten, J., Anderson, B.: Continuously Variable Transmission (CVT): SAE. 2006.
- [17] Krantz, T.: Dynamics of a split torque helicopter transmission: U.S. Army Research Laboratory. 1994.
- [18] Lemanski, A., Saribay, Z., Smith, E.: Compact Pericyclic Continuously Variable Speed Transmission Systems: Design Features and High-Reduction Variable Speed Case Studies: AHS 63<sup>rd</sup> Annual Forum, Virginia Beach, Virginia. May 1-3, 2007.
- [19] Handschuh, R. Stevens, M.: Concepts for Variable/Multi-Speed Rotorcraft Drive System: AHS 64<sup>th</sup> Annual Forum, Montreal, Canada. April 29- May 1, 2008.
- [20] Saribay, Z., Design Analysis of Pericyclic Variable-Speed Transmission System, AHS, 2009.

- [21] Hoffmann, F., Berthe, A., Maier, R., Janker, P., Hermle, F.: Helicopter Interior Noise Reduction by Using Active Gearbox Struts: 12<sup>th</sup> AIAA Aeroacoustics Conference, Cambridge, MA. May 8-10, 2006.
- [22] Naval Postgraduate School Helicopter Design Team, CH-83 CONDOR, March 2003.
- [23] David J. Smith, “Reliability Maintainability and Risk”, Butterworth-Heinemann, MA. 2005.
- [24] “FAR Part 29 – Airworthiness standards: Transport Category Rotorcraft.”, Federal aviation Agency,  
[http://www.flightsimaviation.com/data/FARS/part\\_29.html](http://www.flightsimaviation.com/data/FARS/part_29.html)
- [25] Drago, R., Lemanski, A.: Nutating Mechanical Transmission: Boeing Vertol, Philadelphia, PA. Jan 1974.
- [26] Korzun, A.: Fabricated Helicopter Transmission Housing Analysis: Army Air Mob Mobility Research and Development Laboratory, Jan 1975.
- [27] Aeronautical Design Standard Handbook “Rotorcraft and Aircraft Qualification Handbook”,  
<http://www.redstone.army.mil/amrdec/sepd/tdmd/Documents/ADS51HDBK.pdf>
- [28] Krantz, T., Kish, J.: Advanced Rotorcraft Transmission (ART) Program Summary: 28<sup>th</sup> Joint Propulsion Conference and Exhibit cosponsored by AIAA, SAE, ASME, and ASEE, Nashville, TN. July 6-8, 1992.
- [29] Handschuh, R.: Propulsion Study Details & Risk Reduction Plans: Heavy-Lift Rotorcraft Systems Investigation Review, Aug 10-11, 2005.